WASM: Minerals, Energy and Chemical Engineering

Influence of Clay on Mineral Processing Techniques

Lahiru Rasanga Basnayaka

This thesis is presented for the Degree of

Doctor of Philosophy

of

Curtin University

October 2018

Declaration

To the best of my knowledge and belief this thesis contains no material previously published by any other person except where due acknowledgement has been made

This thesis contains no material which has been accepted for the award of any other degree or diploma in any university

Signature: Lahiru Basnayaka.....

Date: 29/10/18

Acknowledgement

It would not have been possible to achieve this thesis without all the support I received throughout the PhD programme. First of all I must thank Curtin University for the financial support given through CIPRS/MEME scholarship. Also I must convey my sincere gratitude to my supervisors, Associate Professor Nimal Subasinghe and Dr. Boris Albijanic for their guidance, patience, technical support, understanding, and most importantly, their friendship during my PhD studies at Curtin University. This would not be possible without their contribution.

I must convey my gratitude to the teaching staff of WASM for their valuable advices and support. Last but not the least, I must express my sincere thanks to the WASM laboratory technical staff for their assistance and support. Also, I would like to thank all my colleagues in the PhD office to helping me out in the road to the PhD thesis.

I would like to dedicate this thesis to my beloved wife, Chamila Nishshanka for always being by my side giving me the confidence to complete this thesis and having faith on me. Also I would like to thank my parents and for laying the initial foundation and giving me unconditional support so that I could come this far. In addition I must thank my friend Ushan de Zoysa for all his help.

Abstract

Due to the depletion of higher grade ores, there is an increasing demand to process lower grade clay bearing ores in the future. It is widely accepted in the mineral industry that the presence of clay adversely affects the efficiency of most mineral processing operations. These include most widely used beneficiation techniques encompassing size reduction, classification and separation and dewatering processes that involve differential movement of particles within the equipment concerned. However, the extents and mechanisms by which different clays affect such processes have not yet been adequately understood. This research program was aimed at addressing these issues with regard to selected widely affected processes, namely, flotation, enhanced gravity concentration and filtration.

The influence of clays on these processes differs according to the type of clay present owing to their differences in their structure and characteristic features. Thus, two clays with distinctly different charateristics, namely, kaolin and bentonite, which are the most commonly encountered in Australia were selected for the study. The outcomes of the study are summarized below.

Influence of kaolin and bentonite clays on the flotation performance was studied in terms of of a pyritic gold ore as such ores are commonly associated with clays in the Australian context. The experimental conditions used were similar to those encountered in industrial practice. Within the range of experimental conditions tested, flotation recovery and the kinetics were significantly affected in the presence of bentonite in comparison to those of kaolin. clay, especially due to addition of bentonite. Slurry rheology in the presence of bentonite clay was observed to be more altered than that of kaolin clay and was associated with the decrease in pyrite recovery. Addition of Ca^{2+} ions to the processed water improved the flotation recovery of pyritic gold ore by diluting the adverse effects of bentonite clay. More precisely, Ca^{2+} ions reduce the swelling capacity of bentonite clays thus minimizing the rheological influence. Flotation performance characteristics such as the ultimate recovery showed a strong correlation with the rheological parameters such as flow index and consistency index. Moreover, the influence of clays on the froth stability was studied in the context

of maximum froth height and froth half-life using the same ore where both clays showed reduced froth stability.

In this study influence of kaolin and bentonite clays on enhanced gravity separation which is widely used to recover fine liberated gold. Particularly, the study was focused on the performance of a Knelson concentrator that processed an artificial mixture of magnetite and quartz to mimic a pyritic gold ore. While it was anticipated that the rheological properties of the processed slurry would be affected by the presence of clay, the testwork showed that neither bentonite nor kaolin significantly affected the separation of magnetite from a quartz matrix within the range of experimental conditions tested. Even though presence of bentonite increased the yield stress and the apparent viscosity of the feed slurry, dilution of the slurry with fluidization water minimized the viscous effect. However, fluidization water rate and the feed size distribution significantly influenced the separation of the magnetite. The separation efficiency of the Knelson depends on whether the particle bed formed in the Knelson concentrator be in packed bed or fluidized bed state. Identifying the transitional operating conditions for the given commodity can improve the performance of the Knelson concentrator.

The third major study was focused on investigating the influence of clays on the filtration performance as it could be a bottle neck in industrial practices. The presence of clays resulted in decreasing the rate of filtration and increasing the final moisture content of the filter cake, especially in the case of bentonite clay. Bentonite clay showed the most detrimental effects on the filtration in comparison to kaolin, since it increased the specific cake resistance, filter medium resistance and the moisture content dramatically as a result of extensive swelling due to hydration. Addition of Ca^{2+} ions decreased the effects of filter cake resistance, filter medium resistance and the moisture content due to bentonite.

It was also revealed that filtration efficiency of fine particles can be improved by the addition of adequate amount of hydrophobic reagent. Walls of the flow channels become hydrophobic due to adsorption of hydrophobic reagents on the particle surfaces thereby reducing the resistance to flow and increasing the rate of filtration more specifically in fine particle slurries. The increase in the resulting filtration rates has been explained using a capillary filtration model and by superimposing a slip

velocity at the surface of the particle surfaces in the bed. The addition of hydrophobic reagents improved the filtration performance of kaolin clay containing ore while bentonite containing ore was not affected by the addition of hydrophobic reagents.

The results obtained from this study indicate that the presence of clay in a processed ore can inhibit the flotation and filtration performance eventhough it did not show significant influence on enhanced gravity separation. It was evident effect of the clays on the processing may vary according to the present clay type since bentonite clays showed more detrimental effects on both flotation and filtration over kaolin clay. Addition of Ca^{2+} ions reduced the adverse effects of bentonite clay on flotation and filtration. The addition of hydrophobic reagent improved filtration performance of fine particles. Moreover, hydrophobic reagent improved the filtration of kaolin containing ore but not bentonite containing ore. It can be concluded that existence of clay gives rise to adverse effects but remedial measures would depend on the type of clay present.

Table of contents

List of Figures

List of tables

List of symbols

τ	Shear stress
μ	Viscosity, Dynamic viscosity
γ	Shear rate
τ_b	Yield stress
μ_{pl}	Plastic viscosity
K	Consistency index
n	Flow index
R	Flotation recovery, Effective radius of capillary
R_∞	Infinite flotation recovery
k	Flotation rate constant
t	Time
$F(k)$	Distribution function of kinetic rate constants of mineral particles
k_{max}	Maximum flotation rate constant in rectangular model
k_{slow}	Sow floating rate constant in kelsal model
k_{fast}	Fast floating rate constant in kelsal model
$\emptyset$	Fast floating fraction in kelsal model
R	Coefficient of correlation
F_c	Centrifugal force
F_d	Drag force
F_b	Bagnold force
r	Radius of the trajectory of particles in Knrlson concentrator
m_s	Submerged weight of the particle
ω	Angular velocity of a particle in Knelson concentrator
C_d	Drag coefficient
A	Cross sectional area
ρ_f	Fluid density
ρ_p	Particle density
V_f	Fluidization water flow velocity
d	Particle diameter
λ	Linear concentration of particles
X	Performance criterion
X^*	Transitional performance criterion
L	Length of capillary
ΔP	Pressure drop
b	Slip length
Q	Volume flow rate
V	Filtrate Volume
w	Volume of solids deposited by the passage of a unit volume of filtrate
ε	Porosity
ΔP_c	Pressure drop across the filter cake
ΔP_m	Pressure drop across the filter medium
r_m	Filter medium resistance
r_c	Filter cake resistance
M	Mass of filter cake
ρ_{solid}	Density of solids

List of Abbreviations

ANOVA	(Analysis of Variance)
$CaCl_2$	(Calcium Chloride)
$CuSO_4$	(Copper Sulphate)
DAH	(Dodecyl Amine Hydrochloride)
FODD	(First order model with the Dieac delta)
IEP	(Iso Electric Point)
PAX	(Potassium Amyl Xanthate)
MIBC	(Methyl Isobutyl Carbinol)
SEM	(Scanning Electron Microscopy)
XRD	(X-Ray Diffraction)

Chapter 1 Introduction

1.1 Background

Mining and mineral processing industry is considered as one of the major contributors to the economy of Australia, since 10% of the gross domestic product is accounted for by the mining and mineral processing industry. In the context of mineral and metal production, Australia is the leading producer of bauxite, ilmenite, iron, rutile and zircon and the second largest producer of gold, lead, lithium, manganese and zinc (Jaques et al, 2002).

Mineral deposits are naturally occurring accumulations of minerals with economic value. Such deposits are called ore bodies when the extraction and the processing of the deposit is economically viable. Mineral deposits in Australia are differentially distributed attributing to the geological formation that formed them (Jaireth and Huston, 2010). Therefore, deposits of a particular mineral are accumulated in certain geological provinces. As an example, 80% of gold deposits in Australia are of organic origin and majority of them are located in Yilgarn Craton in Western Australia. Also, most of the iron ore deposits are located in the Pilbara Craton. These deposits generally contain clays particularly in lower grade deposits.

Clay minerals can be formed in various geological settings. In the deposits with igneous origin such as copper and gold deposits, clay minerals can be formed due to both hydrothermal alteration and weathering of volcanoclastic sediment pile. Also, clay minerals are readily available in deposits of sedimentary origin, formed by erosion, deposition (titenium and phosphorous), and by diagenetic processes (coal, oil and gas) (Grafe et al, 2017).

Clay minerals are hydrated phyllosilicates which can be associated with valuable mineral deposits as an accessory mineral (Chen and Peng, 2018). There is a general belief among metallurgists who process these clay-containing ore deposits that they present additional difficulties due to the presence of clay minerals. However, in the future processing of clay containing mineral deposits will be inevitable with the depletion of high-grade deposits. The occurrence of clays in ore bodies have been

reported as having adverse effects on mineral processing techniques such as crushing, grinding, flotation, and filtration etc. (Connelly, 2011). However, the extent to which and mechanisms by which these processes are adversely affected have not been studied adequately.

Influence of clays on the flotation process which is considered the primary process for processing base metal and refractory gold ores is of particular interest. Many studies have confirmed that clay minerals inhibit the flotation performance (Tao et al., 2010; Connelly, 2011; Patra et al., 2010; Vasudevan et al., 2010; Jorjani et al., 2011; Bakker et al., 2009; Shabalala et al., 2011). The literature states that clay minerals can affect flotation performance in numerous ways. Clay mineral particles may adhere onto the valuable mineral surfaces preventing the collector adsorption (Tao et al., 2010). Also clay minerals may adsorb the flotation reagents on to their surfaces damping the flotation process (Connelly, 2011). Entrainment of fine particles of clay in to the concentrate is another adverse effect of clay which results in the reducing the grade of the recovery (Patra et al., 2010; Vasudevan et al., 2010; Jorjani et al., 2011). Furthermore, the presence of clays reported to have altered the hydrodynamics in the flotation cell while modifying the rheological characteristics of the flotation slurry (Bakker et al., 2009; Shabalala et al., 2011). Therefore, the change in hydrodynamics in the flotation cell may also inhibit the flotation performance. Some researchers have shown that increased slurry viscosity and yield stress reduce the flotation recovery (Zang and Peng, 2015a; Bakker et al., 2009; Shabalala et al., 2011).

In addition, other processes also could be affected by the presence of clay minerals. Sticky nature of clays makes clay containing ore difficult to be crushed and transported since the clays can stick to conveyors, idlers and screens (Connelly, 2011). Higher viscosity incurred due to clay minerals obstruct the movement in the grinding media in grinding mills (Tangsathitkulchai, 2003). Sensitivity of the gravity concentration may be effected by clay as the increased viscosity reduces the settling rates of the particles. Unique properties of the clay minerals such as anisotropic particle shape, swelling properties and network structures may affect the filtration efficiency (Aksu et al, 2015). It should be noted that extent of the influence of clay minerals on mineral processing may vary according to the available clay type. Different clay types have distinctive properties due to the differences in layer structure and the mineralogy. Therefore, two distinctive clay types commonly encountered in Australian mineral

deposits have been used in this study, namely, kaolin and bentonite. The study is mainly focused on investigating the influence of kaolin and bentonite clays on the most widely used processes of flotation, filtration and centrifugal concentration.

1.2 Objectives

Occurrence of clay minerals as an impurity in the mineral deposits is a common phenomenon, especially in the deposits close to the surface. It is known that these minerals inhibit the performance of mineral processing techniques. The main objective of this thesis is to identify the adverse effects of commonly encountered clays on flotation, gravity separation and filtration techniques and investigate the remedial measures to mitigate the adverse effects of clays. Knelson concentrator was selected as the gravity separation technique to be studied in the research as it is widely applied enhanced gravity separation technique in the gold processing industry to extract finely liberated gold. Kaolin and bentonite were selected for the experimental work as they are commonly encountered clay types with distinct properties and structure. Additionally, it is expected from this thesis to distinguish, understand, and quantify the mechanism behind the adverse effects caused by clay minerals on the above-mentioned processes. Findings of this thesis might be useful for plant operators to address the issues in processing clay containing ores. The sub-objectives of the thesis are.

- To critically review the literature relevant to influence of clay minerals on the processing of minerals.
- To quantify and identify the effects of clay minerals on flotation of refractory gold ore.
- Assess the changes in rheological properties of the flotation slurries due to the presence of bentonite and kaolin clays.
- Assess the adsorption of clay on valuable mineral particles in various pulps with different chemical composition.
- Correlate the flotation performance and the rheological parameters of the slurry

- Identify and quantify the influence of kaolin and bentonite clays on gravity separation using Knelson concentrator.
- Evaluate the effect of slurry rheology on the performance of Knelson concentrator.
- Investigate the influence of kaolin and bentonite clays on the filtration of a refractory gold ore.
- Investigate the effect of hydrophobicity on the filtration performance.
- Quantify the filtration performance using filtration models.

1.3 Thesis overview

This thesis is sub divided into seven chapters. A general briefing of the content of each chapter is given below

Chapter 1 Background and the objectives of the study is provided in this chapter.

Chapter 2 This chapter critically discusses the available literature on the influence of clay minerals on the mineral processing. Initially the genesis, structure and the classification of the clay minerals, relevant to this study is discussed, followed by their differences in characteristics and the challenges encountered in the mineral processing industry due to the presence of clay. Then the influence of clay minerals on the flotation is critically discussed based on the available literature. The discussion includes the influence of clays on both pulp and froth phases. Subsequently, the influence of clay minerals on gravity separation and the filtration is thoroughly discussed using available literature.

Chapter 3 The chapter describes the materials and reagents used in this research project. Also, all the experimental procedures and the analytical techniques are discussed in the chapter.

Chapter 4 This chapter discuss the influence of kaolin and bentonite clays on the flotation of a pyritic gold ore. Used experimental models and the results are given and the flotation results are described using flotation kinetic models. Experimental results have been analysed statistically using MINITAB software. Effects of clays on experimental results are measured and explained in terms of slurry rheological measurements, zeta potential measurements, and the settling test results. Furthermore, the effects of kaolin and bentonite clays on the froth stability is also discussed. Some

parts of this chapter were also published in the Applied Clay Science journal and the proceedings of Mill Operators Conference 2016.

1. Basnayaka, L., Subasinghe, N., Albijanic, B., 2017. Influence of clays on the slurry rheology and flotation of a pyritic gold ore. Appl. Clay Sci. 136, 230–238.
2. Basnayaka, L., Subasinghe, N., Albijanic, B., 2016. Effect of Clay Rheology on Flotation of a Refractory Gold Ore. Proceedings of Mill Operators Conference 2016.

Chapter 5 In this chapter, the influence of kaolin and bentonite clays on the performance of a Knelson concentrator which is the widely used enhanced gravity separator in recovering fine gold, is discussed. Experimental results were analysed statistically using MINITAB software. Experiments were conducted on artificial mixtures of magnetite, quartz and clay. Results were analysed based on the performance curves developed using sizing data of concentrate.

Chapter 6 This chapter discusses the influence of kaolin and bentonite clays on the filtration of a pyritic gold ore. Moreover, effect of hydrophobicity on clay containing and non-clay containing ore which enhances the filtration rates is also discussed. Filtration experiment results were quantified using a filtration model compatible with both slip and non-slip boundary conditions. Results were statistically analysed using MINITAB software. Some parts of this chapter have been published in the Applied Clay Science journal and under review with the journal Powder Technology.

1. Basnayaka, L., Subasinghe, N., Albijanic, B., 2018. Influence of clays on fine particle filtration. Appl. Clay Sci. 136, 230–238.

Chapter 7 This chapter describes the conclusions drawn from this work and makes recommendation for further research and implementation.

Chapter 2 Literature review

2.0 Introduction

The main focus of this chapter is to review the studies on the influence of commonly encountered clays on the mineral processing industry and their mineralogical characteristics. In this chapter, an effort has been taken to review the available literature on clay mineral structure, classification, and the effect of clay on mineral processing, particularly in flotation, gravity separation and filtration. Even though a considerable amount of literature is available to explain the influence of clay minerals on mineral processing industry, proper quantification of the effects and the underlying mechanisms are not available. Also, a very limited number of literature is available on filtration and gravity separation.

2.1 Clay minerals and classification

2.1.1 Origin of clay minerals

Clay minerals are generally classified as hydrated phyllosilicates. The origin of clay minerals takes place due to processes such as chemical decomposition, physical disaggregation, and hydrothermal alteration of metamorphic and igneous rocks. Metamorphic and igneous rocks are subjected to disaggregation in the weathering process attributing to the change in physical and chemical environment, while clay minerals are formed resulting in the diagenesis (Konata, 1992). Krekeler (2004) described six processes that contribute to the formation of clay minerals namely (1) crystallization from solution, equivalent to authigenesis or neoformation; (2) replacement by clay minerals; (3) weathering of silicate mineral sand rocks (not clay minerals); (4) weathering of other clay minerals; (5) diagenesis, reconstitution, and ion exchange; and (6) hydrothermal alteration of minerals and rocks.

2.1.2 Mineralogy and structure of clay minerals

The basic building block of clay minerals comprises of silica tetrahedron sheets (“T” sheets) and alumina octahedron sheets (“O” sheets) (Bergaya et al, 2006). One tetrahedron comprises of a cation bonded to four oxygen atoms where three oxygen atoms are shared with other tetrahedrons. The shared basal oxygen atoms are arranged to form a two-dimensional lattice with hexagonally shaped cavities while remaining epical oxygen exist on the same side of the lattice as given in Fig.2-1. Si^{4+}, Al^{3+}, Fe^{3+} are the most common tetrahedron cations present in clay tetrahedron sheets.

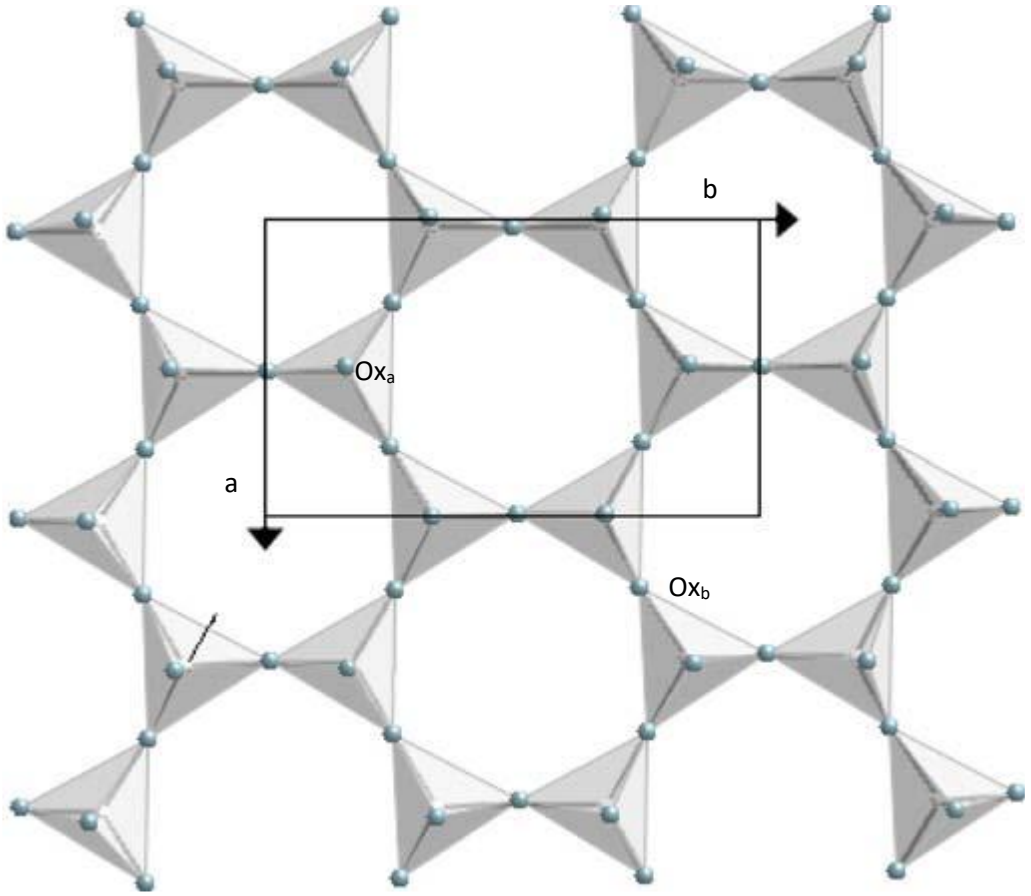

Figure 2-1**.** Atomic arrangement of a tetrahedron:Ox$_a$, apical oxygen atoms; Ox$_b$, basal oxygen atoms. a and b refer to unit cell parameters. (Adapted from (Brigatti et al, 2013))

Octahedron comprises of a cation bonded to either to O^{-2} or OH^{-} ions in six-fold coordination (Bergaya et al, 2006). These octahedrons are interconnected to form a lattice by sharing six vertices. Depending on the valency of the central cation octahedron layers are categorized as dioctahedral or trioctahedral. If the octahedron layer is dioctahedral valency of the central cation is three and if the octahedron layer is trioctahedral valency of the central cation is two. The topology of the octahedron layer is given in Fig.2-2. Al^{3+}, Fe^{3+}, Mg^{2+}, Fe^{2+} are the most common octahedron cations present in clay octahedron sheets.

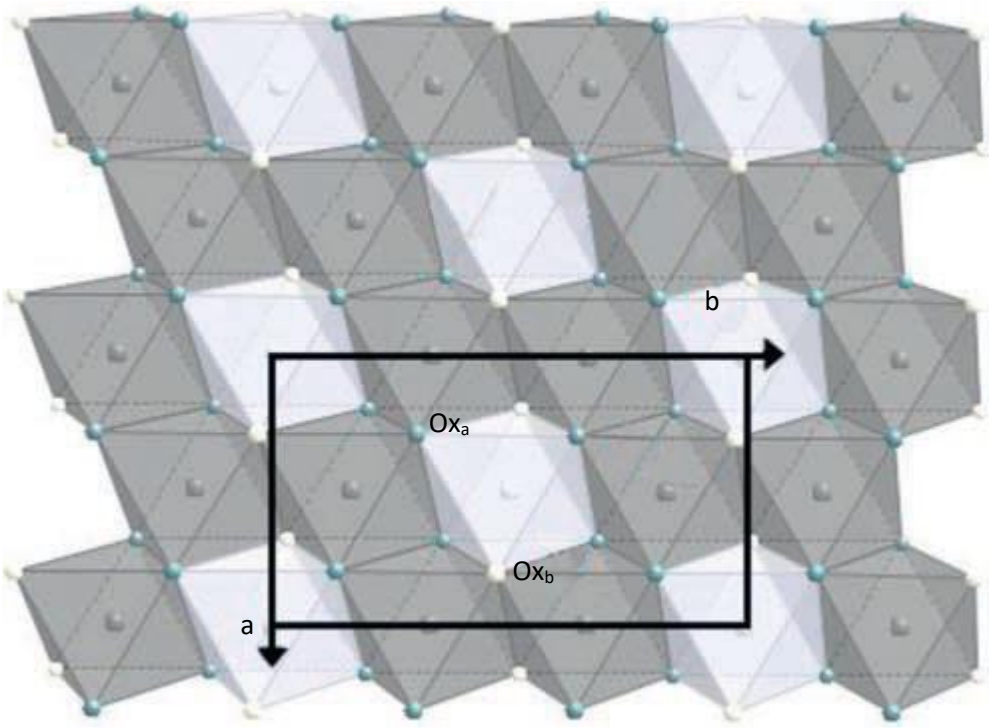

Figure 2-2. Atomic arrangement of octahedron: Ox_a, apical oxygen atoms; Ox_b, Octahedral anions. a and b refer to unit cell parameters. (Adapted from (Brigatti et al, 2013))

Tetrahedron sheets and octahedron sheets are bonded with each other to form clay layers by sharing epical oxygen ions in the tetrahedron sheet. Various compilations of "T" and "O" sheets result in the formation of different types of clay minerals with similar structure and different physical and chemical properties. However, most of the clay minerals have either 1:1 "T" to "O" (eg. kaolinite) or 2:1 "T" to "O" layer arrangement (eg. smectite) where one "T" sheet is combined with one "O" sheet in 1:1 structure and one "O" sheet is sandwiched between two "T" sheets in 2:1 structure as seen in Figure 2-3. A clay particle is formed as a result of stacking of clay layers where clay layers are bonded with van der Waals bonds with each other.

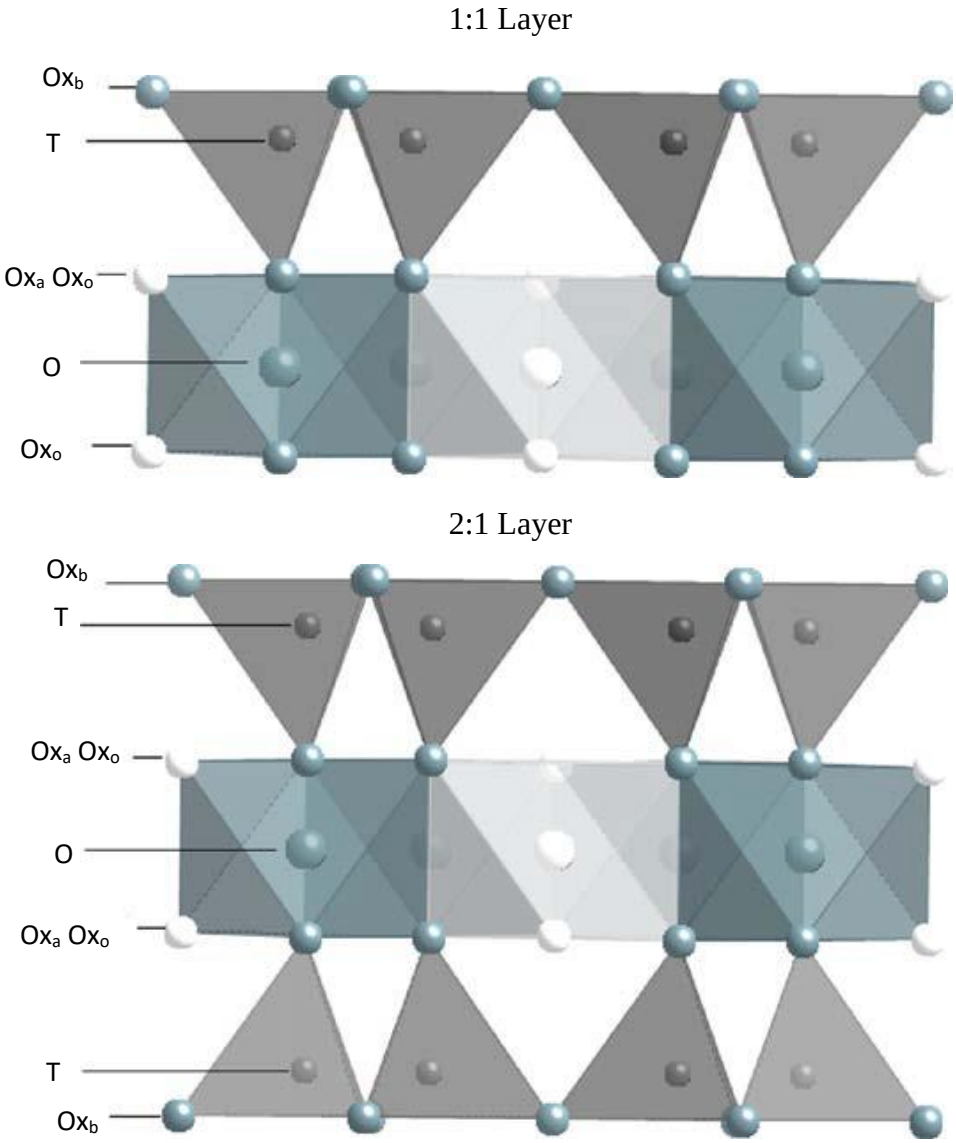

Figure 2-3**.** Models of 1:1 and in 2:1 layer structures. Ox_b, basal oxygen atoms; T, tetrahedral cations; O, octahedral cations; Ox_a, apical oxygen atoms; Ox_o, octahedral anions (OH, F, Cl). (Adapted from (Brigatti et al, 2013))

2.1.3 Classification of clay minerals

Different types of clay classifications and definitions can be found in the literature (Dixon and Weed, 1989; Hurlbut and Sharp, 1998). The classification given below is adapted from Deer et al (1992) in which clay minerals are classified according to the sheet arrangement of clay layers, interlayer bonding, and the interlayer cations. Therefore, clay minerals can be classified as kaolin, Illites, Smectite, and vermiculite (swelling clays). Figure 2-4 shows the structural differences in classified clays.

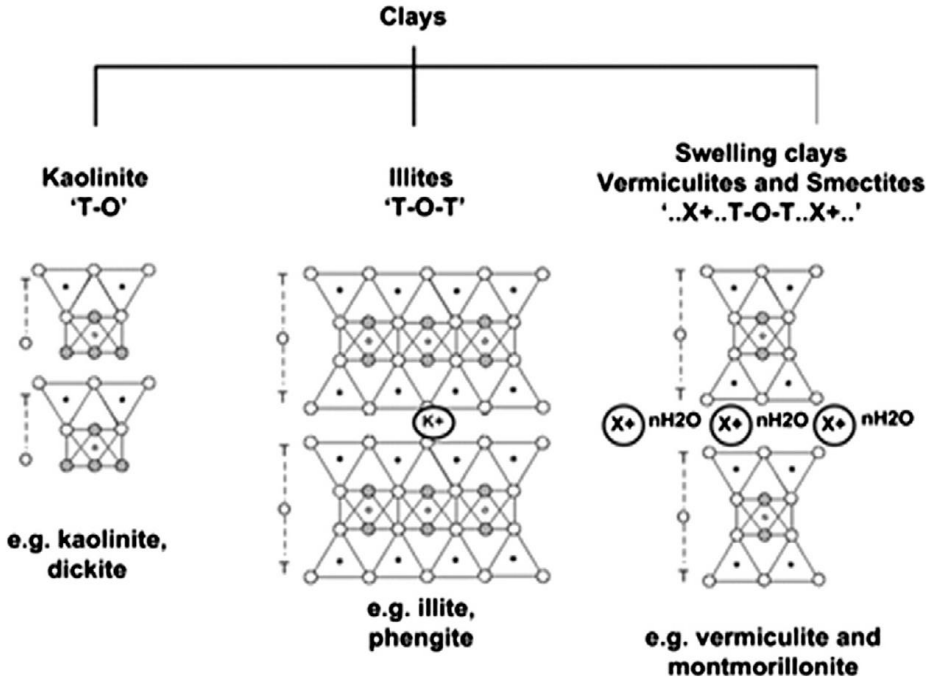

Figure 2-4**.** Classification of clay minerals (Deer et al, 1992)

Kaolinite type clays are 1:1 layer structured non-swelling clays. Clay layers of kaolinite type clays are bonded with strong hydrogen bonds, thus water molecules are unable to penetrate through interlayers of clay particles. Illites are 2:1 layer structured non -swelling clays with anhydrous K^+ ions as interlayer cations. K^+ ions in the interlayers tightly bound the clay layers so that water molecules are unable to penetrate into interlayers to cause swelling (Cheng and Peng, 2018). Smectite and vermiculites are 2:1 layer structured swelling clays with hydrated interlayer cations. Smectite clays such as montmorillonite have higher swelling capacity over vermiculites clay as a result of lower layer charge of smectite clay (Brigatti et al, 2013; Brindley and Brown, 1980; Laird, 2006).

2.1.4 Surface characteristics of clay minerals

Clay particles are anisotropic particles with platy morphology. Therefore, clay particles typically have faces with a larger surface area and narrow thickness. Clay mineral faces carry pH-independent negative charges resulting to the isomorphous substitution. Isomorphous substitution is characterized as the substitution of cations in the clay layers with lower valency cations (substitution of Si^{4+} with Al^{3+} in tetrahedron

sheets and substitution of Al^{3+} with Mg^{2+} or Fe^{2+} in octahedron sheets) (Swartzen-Allen and Matijevic, 1974; Johnson et al., 2000).

By contrast, given that edges of clay mineral particles have the broken bonds, edges can carry either positive or negative charge depending on the pH values. More specifically, clay particle edges carry a positive charge in acidic pH values. Nevertheless, the overall surface charge of clay mineral particles is negative, particularly at pulp pH values encountered in a flotation cell.

As a result of anisotropic surface charges, clay particles exhibit different modes of aggregations: face to face (F-F), edge to edge (E-E), edge to face (E-F), particularly in acidic pH region (Rand and Melton, 1977). Different modes of aggregations are given in Figure 2-5.

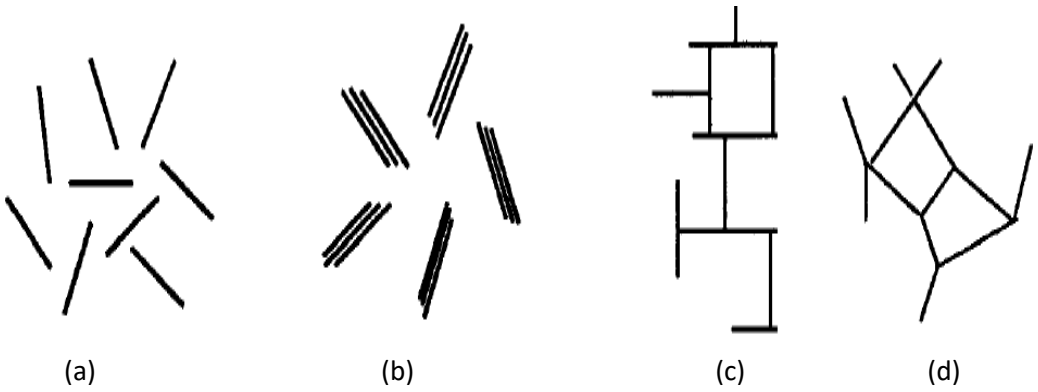

Figure 2-5. Modes of aggregation in clay particles, (a) dispersed, (b) F-F, (c)E-F,(d)E-E (adopted from (Luckham and Rossi, 1999))

2.2 Rheology of clay containing slurries

Wet processing of ores is a common practice in the mineral processing industry. Rheological behaviour of slurries may have a significant influence on the mineral processing operations because the flow of the slurry depends on the rheological principles which are briefly discussed in section 2.2.1.

2.2.1 Rheological models

Slurry rheology can be expressed as the flow characteristics and the deformation of a slurry when subjected to a shear stress. Rheological behaviour of a slurry is illustrated as the relationship between applied shear stress and the shear rate. If the slurry is Newtonian, there exist a linear relationship between shear stress and the shear rate where the gradient of the line is defined as the slurry viscosity *(μ)*. The behaviour of a Newtonian slurry can be described by the Eq.2-1.

$$\tau = \mu\gamma \tag{2-1}$$

where, τ is the applied shear stress, μ is the slurry viscosity, and the γ is the shear rate. The linear relationship given above indicate that the Newtonian slurries have constant viscosity at any shear rate (King, 2002).

When the slurries contain colloidal or microscopic particles the relationship between shear rate and shear stress become non-linear showing non-Newtonian slurry properties (King, 2002). Also, at elevated pulp densities the behaviour of slurries become non-Newtonian, particularly in the slurries containing fine particles. Shear stress and shear rate relationships of Newtonian and non-Newtonian slurries are shown in Figure 2-6. As seen in Figure 2-6 complex rheological models are used to describe the behaviour of the non-Newtonian slurries.

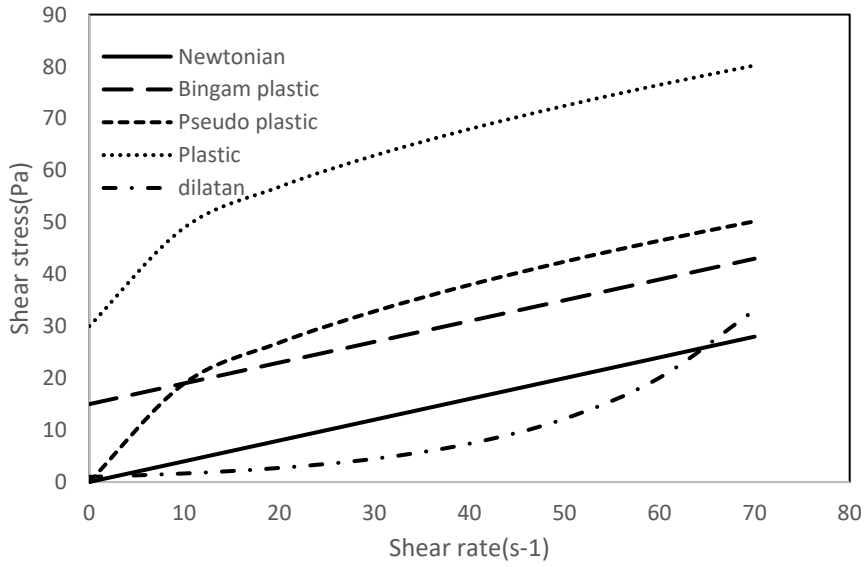

Figure.2-6 Rheological representations of Newtonian and non-Newtonian slurries (King, 2002).

Yield stress and the apparent viscosity are the properties used to quantify the flow characteristics of the non-Newtonian slurries in the rheological studies. Yield stress is the shear stress value at zero shear rate as given by the curve. Furthermore, yield stress can be expressed as the minimum shear stress required for a slurry to deform. The apparent viscosity of a Non- Newtonian slurry is the ratio of the applied shear stress to the resulting shear rate at the point of measurement. Also, the plastic viscosity of non-Newtonian slurries is represented by the gradient of the shear rate vs shear stress curve. A graphical representation of the apparent viscosity, plastic viscosity, and the yield stress for a Bingham plastic slurry is given in the Figure 2-7. Yield stresses and apparent viscosities of slurries can be determined using an appropriate rheometer.

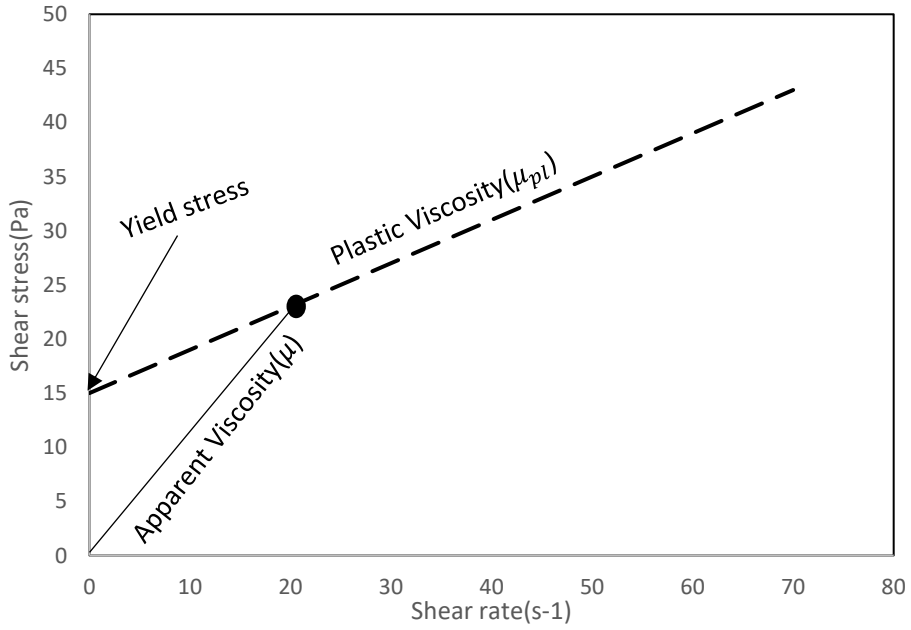

Figure.2-7 Rheological parameters (King, 2002).

Mathematical models are used in rheological studies to estimate the yield stress due to the difficulties in measuring shear stress at very low shear rates (Farrokhpay, 2012). Therefore, the model curve is extrapolated to estimate the yield stress. Non-Newtonian mineral slurries often behave as either Bingham plastic slurries or pseudo- plastic slurries and can be expressed by the mathematical models given in Eq.2-2 and Eq.2-3 respectively (Hunter, 2001; Malkin and Isayev, 2006; He and Forssberg, 2007).

$$\tau = \tau_b + \mu_{pl}\gamma \tag{2-2}$$

Where, τ_b is the yield stress, μ_{pl} is the plastic viscosity

$$\tau = K\gamma^n \tag{2-3}$$

Where *K* is the consistency index and *n* is the flow index. In the power law, *n* indicate the behaviour of slurry viscosity with the shear rate. Slurry is Newtonian when *n=1* , psudo-plastic (shear thinning) when *n<1,* and dilatant (shear thickning) when *n>1. K* is an indicator of slurry viscosity. The higher the *K* values, the slurry is more viscous.

The discussed rheological models are applied to the time-independent slurries. However, there are slurries which show different apparent viscosity values with the time for a particular shear rate. The most common type of time dependent slurries is the thixotropic slurry in which apparent viscosity decreases with the time for a particular shear rate (Hunter, 2001). The behaviour of a thixotropic slurry is shown in Figure 2-8.

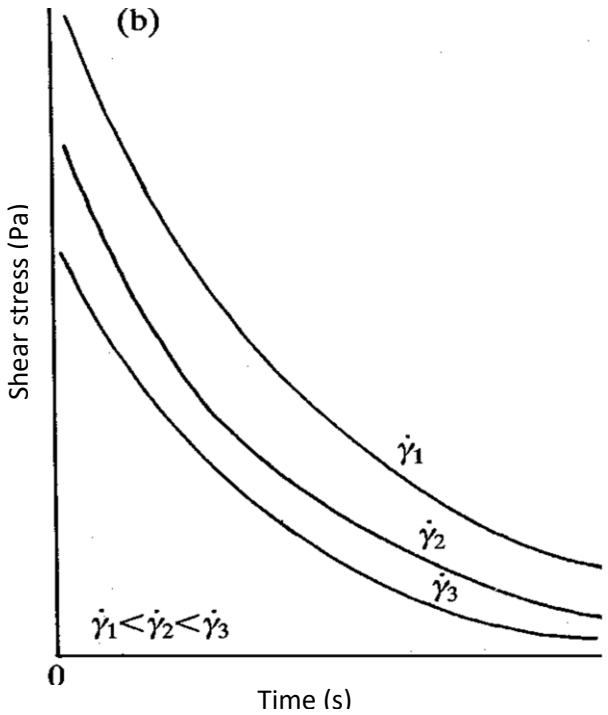

Figure 2-8. The behaviour of thixotropic slurries (Hunter, 2001).

2.2.1 Effects of clay on slurry rheology

As discussed earlier slurry rheology is the branch of physics which convey the deformation and the movement of the slurry. In most of the mineral processing techniques ore is processed in the form of slurries, thus slurry rheology has a paramount importance in mineral processing (Ndlovu et al, 2013).

However, the slurry rheology is controlled by the properties of mineral particles such as morphology, surface charges, swelling capacity, concentration and mode of aggregation etc. Clay minerals have the potential to modify the rheological properties of slurries arising from their anisotropic shape and the charge heterogeneity (Mueller et al., 2010). The presence of clay results in increasing apparent viscosity and the yield stress. However, the degree of alteration to rheological properties may vary according to the present clay type (Zang and Peng, 2015). It has been reported that swelling smectite clays like montmorillonite have more influence on the slurry rheology than that of non-swelling clays (Ndlovu et al, 2013).

Attributing to the anisotropic shape and surface charges, clay particles tend to aggregate in three different orientations: Edge-edge, edge-face, and face-face, particularly in acidic pH values (Rand and Melton, 1977). Edge-edge and edge-face aggregation of clay mineral particles may create a voluminous structure which may also result in higher viscosities and yield stresses of clay slurries (Swartzen-Allen and Matijevic, 1974; Luckham and Rossi, 1999). Face-face aggregation of clay mineral particles has a thicker flaky structure, preventing the increase in viscosity and yield stress of clay mineral particles.

2.3 Challenges in mineral processing environment due to presence of clay

The presence of clay in an ore body have been known to be detrimental in most of the metallurgical processes such as crushing, grinding, flotation, and leaching etc. It has been reported that the presence of clay reduces the efficiency in crushing and grinding, transportation of slurries/ore, and flotation and leaching etc (Connelly, 2011). Influence of clay minerals on flotation is a vastly discussed topic and is of particular interest. It is well known that the presence of clay minerals in flotation slurry inhibit the flotation performance. It must be noted that flotation is a physicochemical process

and clay minerals are also able to influence both physically and chemically. Attributing to the physicochemical nature of clay, clay minerals have numerous effects on flotation, (i) coating on both valuable mineral surfaces and air bubbles (Tao et al., 2010), (ii) consumption of flotation reagents (Connelly, 2011), (iii) entrainment of clay particles to the concentrate in both roughing and scavenging stages (Patra et al., 2010; Vasudevan et al., 2010; Jorjani et al., 2011) (iv) increasing pulp apparent viscosity and the yield stress (Bakker et al., 2009; Shabalala et al., 2011), (v) Either increasing or decreasing froth stability (Dippenaar, 1988; Bulatovic, 2007; Farrokhpay, 2011). It must be noted that the extent of the above-mentioned effects may vary depending on the available clay type. Despite the effect of clay minerals on flotation believed to be results of anisotropic shape and charge, complex rheological effects and large surface area the exact underlying mechanism of these effects are not properly identified. Also, the increase in viscosity changes the hydrodynamics in the flotation cell in a way that it requires more power to maintain the agitation of the slurry (Bakker et al., 2009). It is evident that rheological modifications incurred due to the presence of clay increase the power requirement in flotation.

Apart from flotation, other metallurgical operations such as crushing, grinding, gravity separation, filtration and, leaching may also be adversely affected by the presence of clay. Crushing efficiency of a clay containing ore is significantly reduced since the ore sticks to the liners and blinds the openings of crushers (Connelly, 2011). Because of the higher viscosities incurred by clay minerals, grinding mills need to be operated at significantly low slurry densities which hinders the grinding efficiency and throughput rates (Tangsathitkulchai, 2003). It must be noted that the effect of viscosity on grinding efficiency is more pronounced in the regime of ultrafine grinding (Shi and Napier-Munn, 2002). Due to the sticky nature of clays, chunks of clayey ore stick on to the conveyers and blind the screens making transportation more difficult. Furthermore, the presence of clay causes difficulties in the pumping of processed slurry due to increase in viscosity which results in lower throughput rates exacerbating the plant performance (Connelly, 2011). The efficiency of the gravity separation devices may also be influenced due to the increased viscosity of clay (Wills and Napier-Munn, 2006). Percolation of pregnant solutions during heap leaching is restricted due to the voluminous structures formed in clay-containg ores (Connelly, 2011; Tremolada et al., 2010). Also, clayey ores can cause preg-robbing. Low settling rates of clay containing

ores could result in overflowing water with high solid content in thickener tanks which would contaminate the downstream processes such as solvent extraction (Connelly, 2011). Furthermore, clayey ores cause difficulties in pumping the underflow of thickener tanks due to the elevated viscosity (Mpofu et al, 2004). The increase in apparent viscosity and yield stress hinders the flowability of the processed slurry which results in pumping difficulties. Moreover, clay minerals substantially reduce the filtration efficiency by decreasing the rate of filtration, particularly in the presence of smectite-type clays (Benna et al, 2000).

In this thesis, the influence of the commonly encountered clays on the flotation, gravity separation and, filtration processes have been investigated. Even though the effects of clays on flotation is well documented the underlying mechanisms are not well understood. Therefore, the influence of clays on the flotation of a pyritic gold ore was investigated in the thesis. The influence of clays on Knelson gravity concentrator was also investigated since Knelson concentrators are commonly applied in the mineral processing industry. Finally, the influence of clays on the filtration performance of a pyritic gold ore was also investigated. Filtration and gravity separation processes were selected in this thesis because the influence of clays on those processes has been rarely investigated adequately and the presence of clays has the potential to adversely affect these processes.

2.4 Influence of clay minerals on flotation

2.4.1 Flotation process

Flotation is a technique used to separate valuable from gangue minerals. This technique was introduced at the beginning of the 20th century in order to enable the processing of low grade and complex ore bodies (Wills and Napier-Munn, 2006). Flotation is a physicochemical mineral processing technique used to beneficiate valuable minerals from gangue. The basic process of flotation is to preferentially attach the valuable mineral particles to the air bubbles and then carry them to the top of a flotation cell. Most often pulps are chemically conditioned to enhance the floatability of the valuable minerals. The process of flotation involves sub-processes such as bubble-particle attachment, bubble-particle detachment, entrainment, and slime coating and etc (Wills and Napier-Munn, 2006). Despite the flotation process has not

been completely understood, number of authors have comprehensively discussed the underlying mechanism (Sutherland and Wark, 1955; Glembotskii et al., 1972; King, 1982; Leja, 1982; Ives, 1984; Jones and Woodcock, 1984; Schulze, 1984; Fuerstenau et al, 1985).

In flotation, differences in the ability of mineral particles to physically adhere on to air bubbles are utilized to separate valuable minerals from an agitated pulp. It must be noted that the more hydrophobic the particle surfaces are, more susceptible they are to adhere on to air bubbles. Chemical reagents (i.e collectors, activators) are applied in flotation to selectively induce hydrophobicity on to the particle surfaces of the valuable commodity in the slurry so that those particles are more vulnerable to report to the concentrate. The schematic diagram of a conventional flotation is shown in Figure 2-9.

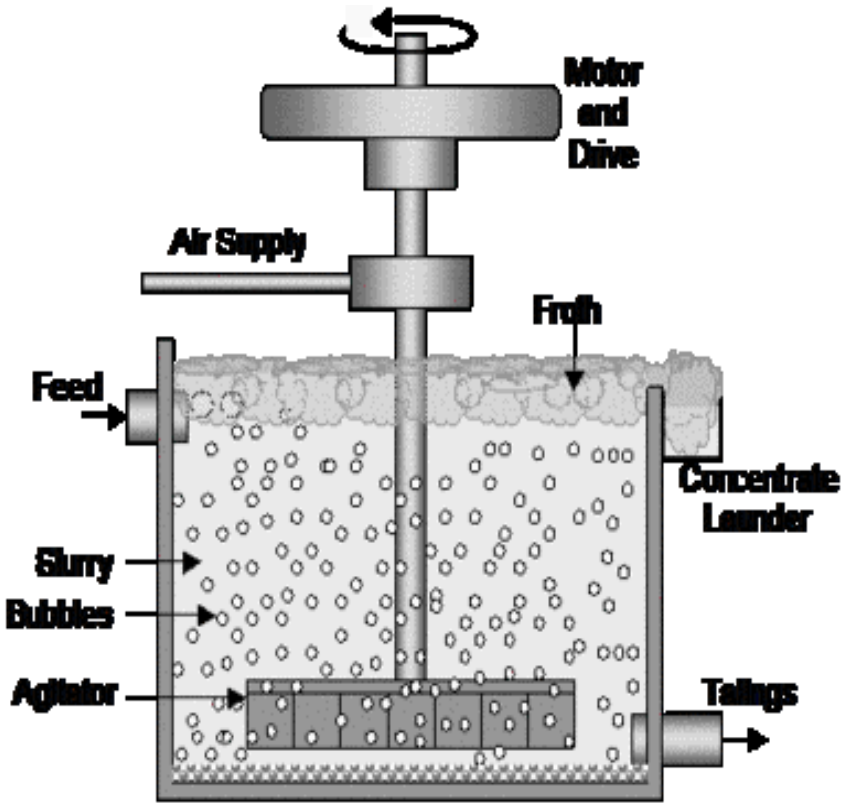

Figure 2-9**.** Schematic diagram of a flotation cell (Wills and Napier-Munn, 2006).

2.4.2. Flotation models

Kinetics of the flotation process is either modelled using micro or macro scale models. In micro scale models, sub process such as collision, attachment, and detachment are incorporated to model the flotation process, in which measurement and evaluation of sub-processes can be extremely challenging (Polat and Chander, 2000). Therefore, macro scale phenomenological kinetic models are often applied to model flotation process (Polat and Chander, 2000). Even though the order of the flotation process is quite debatable (Tomlinson and Fleming, 1965; Harris and Chakravarti, 1970), first order kinetic models are applied to describe flotation processes in most instances. Flotation is a process in which the rate of flotation depends on the floatability of the designated material, concentration, and operating variables

First order kinetic models have been used to describe the batch flotation test data under normal operating conditions (Dowling et al., 1985; Rastogi and Aplan, 1985). First order flotation models have been developed with different distributions of flotation rate constants to mathematically represent the recovery of the mineral during flotation. The general equation for the first order flotation models with different distributions of *k* is given in Eq.2-4.

$$R = R_\infty \int_0^\infty (1 - e^{-kt}) F(k) dk \quad \text{(Polat and Chander, 2000)} \qquad (2\text{-}4)$$

where *R* is the flotation recovery at time *t*, R_∞ is the infinite flotation recovery, *k* is the kinetic flotation rate constant and *F(k)* is the distribution function of kinetic rate constants of mineral particles. Most common fist order flotation models with different functions for flotation rate constant are illustrated in the Table 2-1.

Table 2-1. A summary of common first order flotation models (From (Polat and Chander, 2000))

	F(k)	Kinetic parameters	Model
First order model with the Dirac delta function(FODD) (Lynch et al., 1981)	d(k - k_B)	k_b – average rate constant	$R = R_\infty(1 - e^{-k_b t})$
Rectangular model (Klimpel, 1980)	$\frac{1}{k_{max}}$, $0 \leq k \leq k_{max}$	$k_{\max}$ – fastest floating rate constant	$R = R_\infty(1 - \frac{(1 - e^{-k_{max}t})}{k_{max}})$
Kelsall model (Kelsall, 1961)	$\emptyset\delta(k - k_{fast}) + (1 - \emptyset)\delta(k - k_{slow})$	k_{slow} – slow floating rate constant k_{fast} – Fast floating rate constant	$R = \emptyset(1 - e^{-k_{fast}t}) + (1 - \emptyset)(1 - e^{-k_{slow}t})$

In the FODD model, it is assumed that all the particles have constant flotation rate constant and the model is applied in the flotation work more often due to the simplicity of the model. Also, in the Kelsal model, it is assumed that the particles comprise of both fast floating or slow floating particles whose flotation rate contents are k_{fast} and k_{slow} respectively. The rectangular model was derived assuming that rate constants of the particles are distributed in a rectangular distribution from 0 to $k_{max.}$ In both the FODD and rectangular models, R_∞ is used as a model parameter and it is the ultimate flotation recovery of floatable materials which represents the maximum flotation recovery for the infinite flotation time. However, neither of these models can be highlighted as the best representation of the flotation process. For example, Dowling et al. (1985), by analysing 13 flotation models using statistical model discrimination observed that the rectangular model better represent most flotation process. Kelly and Carlson. (1991) illustrated the drawbacks of statistical model discrimination and observed that the Kelsal model shows the best fitting for flotation data over the rectangular model. It must be noted that the best fitting flotation model may vary according to the various flotation conditions and the degree of mineral exposure of mineral particles (Dowling et al, 1985). The rectangular model was applied in the present study given in the chapter 4 of this thesis, as that model described the observed data adequately

2.4.3 Modification of pulp rheology

Rheological measurements provide an indirect assessment of the degree of particle-particle aggregations and interactions of particles in a slurry (Farrokhpay, 2012). Most unit operations rely on the differential movement of mineral and gangue particles. Clay mineral particles have unique properties such as very fine particle size, anisotropic surface charges, and shape, swelling capacity, the formation of voluminous structures which may result in modifying the rheological properties of the processed slurry (Ndlovu et al, 2014).

The intrusion of clay in certain concentrations results in slurries exhibiting non-Newtonian behaviour which attributes to modify the hydrodynamics within a flotation cell (Bakker et al, 2010). Increase in yield stresses and apparent viscosities adversely affects various flotation sub-processes such as gas dispersion, bubble coalesce and gas holdup (Shabalala et al. 2011). Furthermore, the increase in rheological properties reduces the mobility of bubbles and particles which reduces the susceptibility of bubble-particle collision and attachment, impeding the flotation performance. (Bakker et al. 2009).

Modification of hydrodynamics in flotation cell may vary according to the clay type present as different clay types have distinctive properties. Multiple studies have confirmed swelling smectite clays significantly alter the slurry rheology where even 5% of solids can significantly reduce the flotation performance (Zang and Peng, 2015a; Zang and Peng, 2015b; Cruz et al, 2015c;). Non-swelling clays like kaolinite cause modifications to the slurry rheology above 10% of solid concentration. Figure 2-10 shows how different the effect of bentonite and kaolin on the apparent viscosity of a slurry. Smectites like montmorillonite become a gelatinous sludge when hydrated due to osmotic and crystalline swelling where a clay particle can swell by more than twenty times of its original size (Luckham and Rossi, 1999). Kaolin-type clays affect the slurry rheology due to very fine particle size and also due to the different modes of particle aggregations explained in the section 2.1.4.

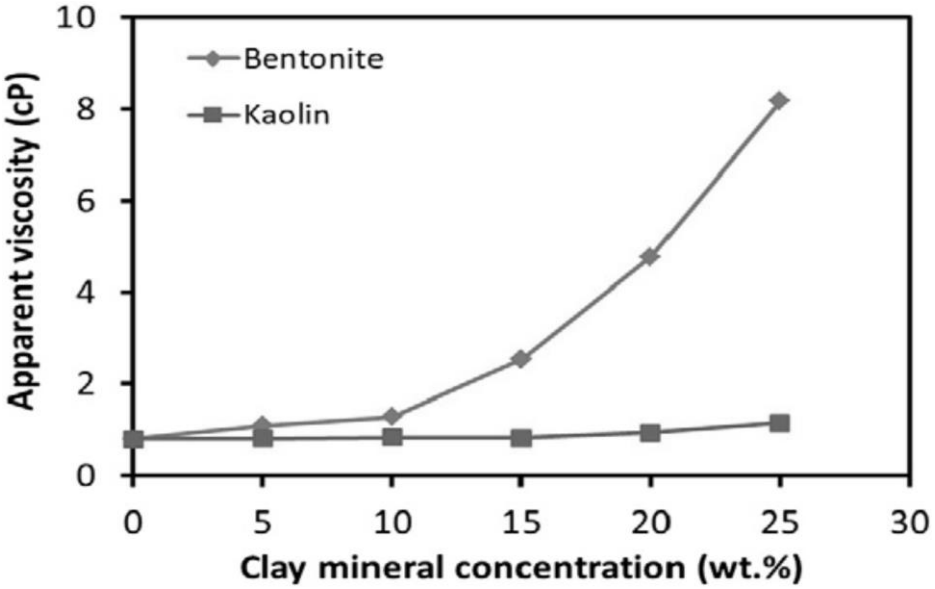

Figure 2-10. Apparent viscosity as a function of clay mineral concentration in Telfer clean ore at a shear rate of 100 s−1 (Wang et al, 2015b).

2.4.4 Slime coating on valuable mineral surfaces

Particles tend to coat with each other due to the electrostatic attraction between particles when they carry opposite surface charges. Clay mineral particles exhibit anisotropic surface charge properties where clay particle faces (basal planes) carry a pH independent negative charge due to isomorphous substitution and edges with pH-dependent charge (Schoonheydt and Johnston, 2006). However, most clay particles have net negative charge, more specifically in the pH values used in flotation. When surface of the valuable mineral is positively charged clay particles have the potential to coat the mineral surface restricting the reagent adsorption thus inhibiting the bubble-particle attachment.

Multiple studies have revealed that flotation performance of galena, coal, and bitumen flotation was hindered due to slime coating of clays (Arnold and Aplan, 1986a; Quast et al, 2008; Tao et al, 2010). The surface charge of sulfide minerals (pyrite, chalcopyrite) is usually negative, therefore the surface coating of negatively charged clay particles is not possible (Chen and Peng, 2018). However, sulfide surfaces become positively charged when oxidized, therefore clay particles could electrostatically adhere on to the sulfide surfaces. Peng and Zhao (2011) observed that chalcocite flotation was significantly hindered due to slime coating of bentonite

particles since chalcocite particle surfaces become positively charged in the grinding stage due to oxidization. The zeta-potential measurements shown in Figure 2-11 confirms that chalcocite particles become negatively charged after grinding. To the contrast, chalcopyrite doesn't get oxidized to the level of chalcocite as seen in Figure 2-11, therefore the coating of bentonite on chalcopyrite particles may not occur on chalcopyrite particles in the pH values where flotation is conducted. Zhao and Peng (2014) observed that kaolinite clays also coated on oxidized chalcocite reducing the chalcocite recovery.

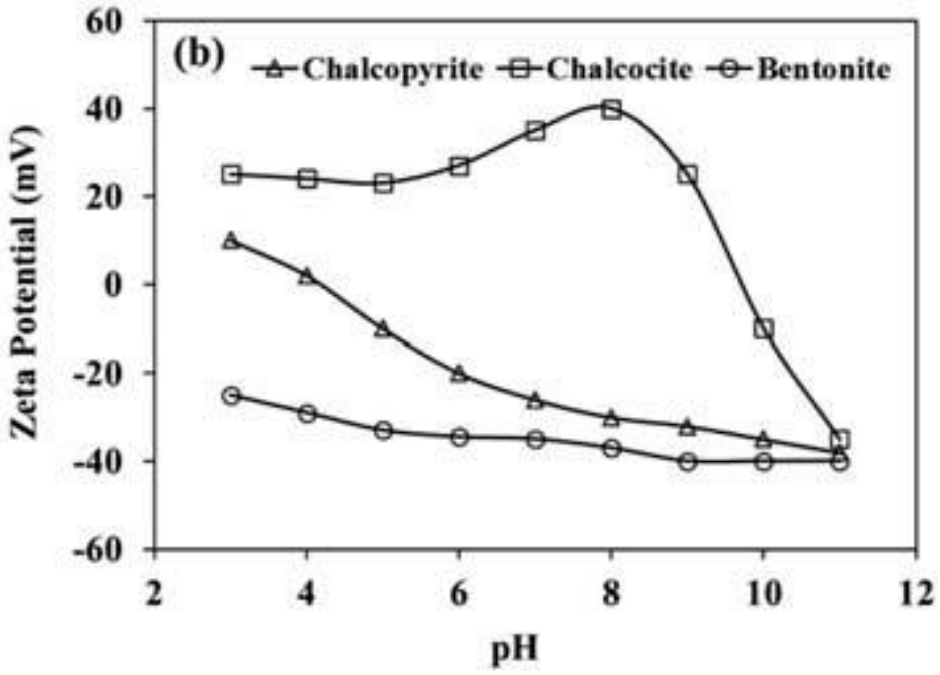

Figure 2-11. Zetpotential of chalcopyrite and chalcocite after grinding and zetapotential of bentonite (Peng and Zhao, 2011)

The surface charge of the particles heavily depends on the pH value of the suspension. As discussed earlier edges of the clay particles become positively charged in acidic pH values and may coat on the negatively charged sulfide mineral surfaces which would hinder the flotation recovery. Also if the pH is below the isoelectric point (IEP) of the sulfide mineral clay particles would coat on to the surfaces owing to the negative charge of clay basal planes (Chen and Peng, 2018). It must be noted that slime coating may occur in the pH range between IEP of clay particle edges and the sulfide mineral.

It was observed, flotation recovery of galena was decreased significantly due to the coating of bentonite particles at pH 5 when compared with pH 10 (Chen et al, 2017a).

2.4.5 Clay entrainment in flotation froths

Entrainment is another mechanism that allows materials to report to the froth phase apart from the true flotation. In the entrainment process, particles are transferred to the bottom of the froth column in the form of suspended particles in the water trapped between bubbles and then transferred to the concentrate (Gaudin 1957; Wang et al. 2015a). Both valuable and gangue minerals are subjected to entrainment where gangue entrainment results in lowering the grade. Entrainment is a physical process that does not involve particle selectivity. Properties such as water recovery, particle shape, particle size, pulp density, gas flow rate, rheology and the froth structure are the determinant factors of the degree of entrainment (Savassi et al. 1998, Wang et al. 2015a).

Entrainment of clay particles into the concentrate can mainly be attributed to the very fine particle size. It must be noted that particles less than 30 microns have significant potential to be entrained (Smith and Warren, 1989). Size of clay mineral particles normally range between 2-10 microns, therefore the entrainment of clay minerals is inevitable. Furthermore, some recent studies have revealed that clay network structures further enhance the clay entrainment (Cruz et al. 2015b, 2015c; Zhang et al. 2015c).

Zhang et al (2015c) observed that the presence of kaolin clay significantly reduced the grade of copper and gold flotation. The authors also concluded that this observation is mainly due to the entrainment of kaolin particles and the network structures formed with kaolin particles might have further enhanced the kaolin entrainment. Kaolin particles are more susceptible to entrain into froth attributing to the low density of voluminous honeycomb structure formed owing to E-E and E-F aggregations (Chen and Peng, 2018). Despite bentonite clay exhibits more detrimental effects on flotation recovery than kaolinite, bentonite shows less effect in the context of entrainment (Zhang and Peng 2015a; Zhang et al. 2015b).

2.4.6 Influence of clays on the stability of froth

The behaviour of froth has a substantial importance in flotation performance. Froth needs to be adequately stable for optimum flotation performance (Farrokhpay, 2011). If the bubbles in the froth are unstable they rupture before the collection of froth which results in dropping the collected material into the pulp again. If the froth is overly stable, difficulties may arise when handling and transporting the froth. Also, overly stable froth may result in increasing the entrainment reducing the grade of the concentrate.

Study of froth behaviour can be quite complex since multiple factors such as pH value, drainage, amount of solids in the froth and the frother concentration have a significant influence on froth stability (Farrokpay, 2011, Aktas et al, 2008). Available literature provides two methods to measure froth stability, (1) measuring the height of the froth column at the dynamic equilibrium of froth forming and decaying, (2) measuring the rate of decaying of froth.

Effect of clay on the froth phase is not well defined as literature provides contradictory results. It has been reported that clay minerals would increase or decrease the froth stability. The decrease in froth stability in the presence of clay minerals might be caused due to adsorption of frother onto the clay mineral surfaces (Miller et al, 1983). The entrainment of clay aggregates increases the present solids in the froth which could increase the stability of the froth column. Wang et al. (2015b) observed that froth was more stable in the vicinity of kaolin clay and froth stability decreased with the addition of bentonite clay. It can be argued that decrease in froth stability when pulp contains bentonite is due to the increased apparent viscosity which results in poor dispersion of bubbles. In the case of kaolin, the entrainment of kaolin particles might have increased the froth stability. To the contrast, Farrokhpay et al (2016) reported that both kaolin and bentonite resulted in increasing the froth stability. However, both clay types reported having bubble size reduced in the froth as seen in Figure 2-12. Since there are contradictory observations on the effect of clay on froth stability, further comprehensive studies need to be conducted to verify the effects.

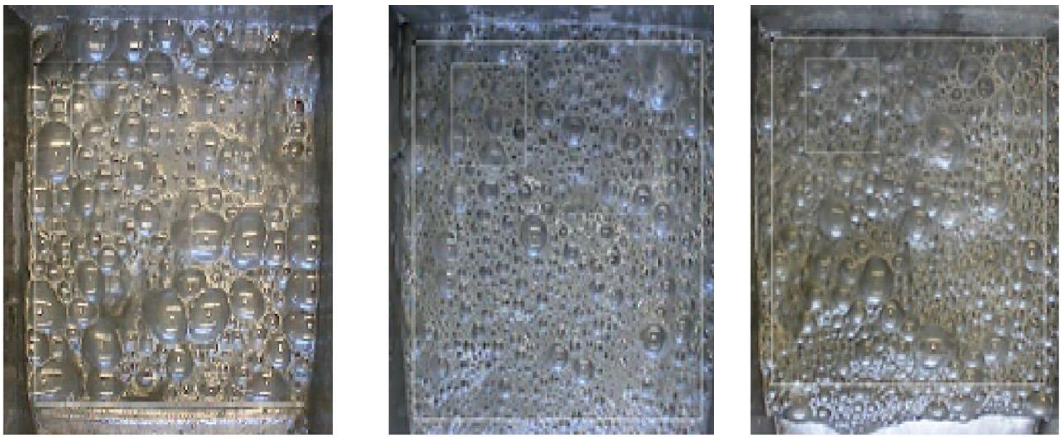

(a) (b) (c)

Figure 2-12. Effect of clays on bubble size, (a) 0% clay (b) 15% bentonite (C) 20% kaolin (Farrokhpay et al, 2016)

2.4.7 Mitigation of adverse effects of clay on flotation

Researchers have investigated the remedial measures to mitigate the adverse effects of clay in flotation. Slime coating, modification of pulp rheology and entrainment are the well-known adverse effects which lead to poor flotation performance.

Coated clay particles need to be removed from valuable mineral for better flotation performance where coated clay particles can be separated either mechanically or chemically. Available references provide three techniques to mechanically remove coated clay particles namely, 1) High-intensity agitation, 2) Use of de-sliming hydro cyclone, 3) Ultrasonic vibration. Flotation performance of coal was improved due to the high-intensity agitation in the conditioning stage of the pulp in the presence of kaolin clay (Yu et al, 2017a, 2017b). Moreover, the authors observed that the clay coating was further increased if the agitation does not reach a critical value.

It is a common practice to use hydrocyclones to remove clay particles from clay containing ore prior to the flotation. Oats et al (2010) claim that clay particles, coated the valuable minerals also get removed attributing to the high shear environment. Ultrasonic treatment is another physical method for removal of slime. Celik et al

(1998) observed a significant increase in the flotation of boron minerals after de-sliming using a hydrocyclone; boron minerals were heavily coated with clay minerals.

Slime coating occurs as a result of electrostatic attraction between clay particles and the valuable mineral particles. Addition of chemical dispersants can impose repulsive forces between clay and other mineral particles thus restrict the coating of clay particles. Addition of lignosulfonate, anionic dispersant improved the coal flotation from clay containing ore (Liu and Peng, 2015). Wei et al (2013) reported that lignosulfonate was effective in improving flotation of clay containing copper-gold ore too. In addition to the inorganic dispersants such as lignosulfonate, low molecular weight polyaminoaldehyde polymer may reduce slime coating since the polymer acts as a clay binder (Tao et al, 2010).

As discussed earlier increased apparent viscosity and the yield due to the presence of clay inhibit the flotation performance. Addition of inorganic dispersants may reduce the slurry viscosity of clay containing slurry by dispersing the clay particles in clay aggregate structures. Papo et al. (2002) observed that addition of sodium polyphosphate dispersant significantly reduced the slurry viscosity of a kaolin suspension. Furthermore, Goh et al (2011) observed a significant decrease in viscosity of bentonite suspension due to the addition of polyphosphate dispersant, especially at higher pH values. Moreover, the presence of electrolytes reported having improved the flotation performance of clay containing slurry by altering the slurry rheology (Cruz et al, 2015a, 2015c). Also, there are commercially available biopolymers which are used as clay dispersants in the flotation. Pionera group states that gold recovery can be increased by 5% by the addition of PIONERA F-100 biopolymer to the flotation circuits

Entrainment of fine clay particles is mainly attributed to the fine particle size and the low-density voluminous structures. Aggregation of clay particles in a dense particle structure may result in reducing the entrainment. Addition of polymer flocculants has the potential to aggregate clay particles in a dense structure. Entrainment of kaolin particles was reduced quite significantly due to aggregation of particles with the addition of high molecular weight polyethylene oxide flocculent (Liu and Peng, 2014).

2.5 Influence of clay minerals on gravity separation

Gravity concentrator devices utilize the difference in density in feed materials to separate valuable minerals. In modern-day plants, centrifugal gravity concentrators such as Knelson and Falcon concentrators are used because of their low environmental impact, low installation and operational costs. The most common application of Knelson or Falcon concentrator is in gold processing industry since it has the ability to recover 96% of free liberated gold coarser than 30µm (Silva, 1986).

Influence of clays on gravity separation techniques is not studied extensively. Nevertheless, modification of slurry rheology in the presence of clay could inhibit the efficiency of the gravity separation as settling rates of particles get reduced in a high viscous environment. Increase in apparent viscosity decreases the settling rates of particles adversely affecting the sensitivity of gravity concentration devices such as jigs, tables, and spirals (Wills and Napier-Munn, 2006). Moreover, some studies have reported that centrifugal gravity concentrators can be used to de-slime clay-containing ore. Clay minerals are a less dense material which can be separated from dense materials when subjected to high shear rates and agitation in centrifugal gravity concentrators (Lyubomir et al, 1993).

Nowadays, Knelson concentrator is widely used in processing plants particularly in the gold mining industry. There are two methods available in the literature to evaluate the performance of Knelson concentrator, one is the GRG (Gravity Recoverable Gold) test proposed by Laplante et al (2000), and another method is using performance curves and performance criterion proposed by Coulter and Subasinghe (2004).

Influence of commonly encountered clays on the Knelson concentrator was studied in this thesis and the results are reported in chapter 5. The test results were evaluated using the performance curve method.

2.6 Influence of clay minerals on dewatering

2.6.1 *Influence of clay minerals on thickening*

Thickening is a commonly applied dewatering method to separate water from solids. Thickening utilizes gravitational sedimentation of particles to dewater a slurry in a cylindrical tank in which the thickened slurry is the underflow and the clarified liquid overflows from the peripheral launder (Wills and Napier-Munn, 2006). Also, a thickener tank consists of one or two radial arms with blades, designed to rake the solids towards the central outlet at the bottom of the thickener. Furthermore, flocculants are used in thickening processes to enhance the settling of particles.

Faster settling behaviour of solids is favourable for the better performance of the thickening process. However, the presence of clay minerals in the tailing slurries of hydrometallurgical processes has the potential to reduce the efficiency of the thickening process attributing to the lower settling rates of clay particles (Mpofu et al, 2004; McFarlane et al, 2005, Harris et al, 2018; Liu et al, 2018). Lower settling rates of clay minerals can be attributed to their fine particle size, anisotropic particle shape, and low density which would result in very low terminal velocities of solids. Moreover, it has been reported that smectite type clays are detrimental due to the swelling of clay particles; the reason is that swelled smectite clays have very low settling rates and also increase the viscosity of thickener underflow causing pumping difficulties (Mpofu et al, 2005). Also, low settling rates of clay containing ores could result in overflowing water with high solid content in a thickener tank and thus solids would contaminate the downstream processes such as solvent extraction (Connelly, 2011).

Even though polymer flocculants are added to flocculate the slow settling particles, they may be inefficient in the presence of clay minerals, particularly smectite clays such as montmorillonite (Addai-Mensah et al, 2007). Mpofu et al (2005) showed that the addition of polyacrylamide-acrylate copolymer (PAM) together with adequate concentrations of hydrolysable metal ions (Ca^{2+}, Mn^{2+}) improved the dewatering behaviour of the smectite clay. Furthermore, the addition of non-ionic polyethylene oxide flocculant improved the dewatering of smectite clays (Addai-Mensah et al, 2007). Electroosmotic dewatering also improved the dewatering behaviour of clay containing slurries (Harris et al, 2018)

2.6.2 Influence of clay minerals on filtration

Filtration is a commonly used dewatering technique in the mineral processing industry. Precisely, in filtration, a pressure difference is applied to a slurry through a filter medium (i.e. filter cloth) so that solids retain in the system. The presence of very fine particles inhibits the filtration rate as it reduces the porosity and the permeability of the build-up filter cake resulting in low filterability (Besra et al, 1999). Low filterability reduces the throughput rates of large-scale mineral processing operations like the iron ore industry. Also, the amount of moisture retained in the filter cake has utmost importance, especially in the context of transportation and storage. High retained moisture increases the transportation cost as well as results in collapsing of tailing dams (De Kretser and Boger, 1992).

Presence of even small amount of clay minerals has the potential to exacerbate the reduction of filtration rate significantly due to unique properties of clay minerals such as anisotropic shape, very fine particle size and swelling characteristics. However, the literature lacks the information on the effect of clay minerals on the filtration performance. It has been reported that the size, shape and particle network structure of clay minerals substantially effect on the filtration performance. Influence of different types of clay on filtration may vary since different clay types have unique properties of their own. Non-swelling kaolin type clays cause difficulties in filtration by reducing the permeability, only if available in high solid concentrations in the filtered slurry. Kaolin clay inhibits the filtration performance especially due to the very fine particle size where very fine particle size reduces the effective flow diameter (Aksu et al, 2015). In addition, the presence of small amount of bentonite clay results in inhibiting the filtration performance, more specifically increasing the retained moisture and reducing the rate of filtration. These effects are mainly attributed to the swelling of bentonite particles where clay particles are swelled more than twenty times of its original size due to hydration (Aksu et al, 2015)

Adverse effects caused by the presence of fine particles on filtration performance can be mitigated by the addition of filtering aids such as surfactants and flocculants (Sastry et al, 1999). Amarante et al (2002) reported that addition of polyacrylamide flocculant increased the filtration rate and reduced the moisture content in filtering iron containing ore. Poly-acryl amide polymer causes bentonite clay particles to

agglomerate thus increases the rate of filtration (Hocini et al., 2017). Furthermore, Hung et al (2017) reported that the addition of cationic hydrophobic reagents increased the filtration of kaolin clay. Kaolin clay particles surfaces become hydrophobic since kaolin particles have a net negative charge which forms electrostatic bonding with cationic hydrophobic molecules. Therefore, water is repelled from the hydrophobic clay surfaces resulting in higher filtration rate (Hung et al, 2017).

This study includes a chapter which discusses the effect of kaolin and bentonite clay on the filtration performance of the refractory gold ore.

2.7 Influence of clays on comminution

As discussed in section 2.3, the presence of clay minerals in ore bodies decrease the efficiencies in crushing and grinding circuits. Connelly (2011) states that crushing efficiency of a clay-containing ore is significantly reduced as the ore would stick to the crusher plates and the liners while blinding the opening of crushers. One of the common applications to avoid the difficulties in crushing clay-containing ores might be to directly place ores into the grinding stage (Connelly, 2011).

In regard to grinding, there is a very limited literature on the effect of clays on the grinding performance (Grafe et al, 2017). However, the influence of slurry rheology on the grinding is well documented. It is evident that the presence of clay minerals modifies the slurry rheology by increasing apparent viscosity and the yield stress. The increase in yield stress in the ground slurry increases the power consumption and hinders the particle breakage rate (Grafe et al, 2017). Because of the higher viscosities incurred by clay minerals, grinding mills need to be operated at significantly low slurry densities which reduce the grinding efficiency and throughput rates (Tangsathitkulchai, 2003). It must be noted that the effect of viscosity on grinding efficiency is more pronounced during ultrafine grinding (Shi and Napier-Munn, 2002).

The adverse effect of elevated yield stresses and apparent viscosities on milling processes could be addressed by the addition of the suitable grinding aids (Wang and Forssberg, 1995; Klimpel, 1999; Somasundran et al, 1988). Water soluble low molecular weight polymers are commonly used as viscosity modifiers in grinding (He et al, 2004). Some of the used grinding aids are given in Table 2-2. Moreover, the

application of PIONERA biopolymer as a viscosity modifier in grinding has been reported to have potential in improving the grinding efficiency (Lauten et al, 2014).

Table 2-2. Commonly used grinding aids (Klimpel, 1999)

Polyacrylic Acid	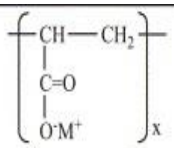	Polyvinyl Amine	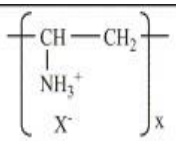
Polymethacrylic Acid	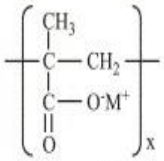	Polyvinyl Alcohol	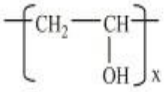
		Polyacrylamide	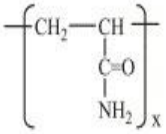
Polyphosphoric Acid	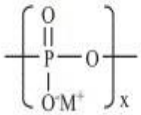		
		Polyethylene Oxide	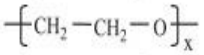
Polystyrene Sulfonic Acid	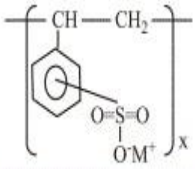	Copolymer of Acrylamide and Acrylic Acid	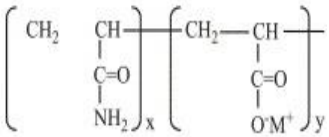

2.8 Concluding remarks

This literature review confirms that most of the studies related to the effect of clays on mineral processing are focused on flotation. It is evident from the literature that the modification of the pulp rheology and the slime coating are the most dominant adverse effect caused by the clays in flotation. However, the effect may differ with the available clay type. Even though, the mechanisms behind these effects are established to a certain extent, proposed solutions do not properly address the adverse effects of clay, especially in the context of swelling type clays which modifie the slurry rheological properties significantly. Therefore, more studies need to be conducted to identify the possible solutions to minimise the adverse effects of clay on mineral processing. In this thesis, effects of two distinct clay types, kaolin and bentonite were studied in flotation of pyritic gold ore and solutions for adverse effects were discussed and thus new solutions have been introduced.

In the context of filtration, clay minerals cause the decrease in the rate of filtration and increase in the retained moisture. More research needs to be conducted in this area.

The literature on the effect of clays on gravity separation is also very limited. However, the change in slurry viscosity was reported to have effects on some gravity equipment.

Chapter 3 Materials and Methods

3.0 Materials

A gold pyritic ore (Western Australia, Kalgoorlie) was used for the flotation, froth stability and filtration experiments. For all the experiments, ore was first crushed to -2.36 mm size using a laboratory jaw crusher. For flotation and the froth stability experiments crushed ore was dry ground using a laboratory rod mill to obtain 80% passing 150 µm particle size. For filtration experiments, the crushed ore was ground using also the rod mill followed by using a pulveriser to achieve five different particle sizes. Mineral composition of the used gold ore is given in Table 3-1.

Table 3-1. Mineral composition of the pyritic gold ore (%)

Dolomite	Albite	Pyrite	Quartz	Non- crystalline material
19.7	43	3	25.1	9.1

The kaolin and sodium bentonite clay samples were purchased from Sibelco group, Australia. The clay content of the samples was above 80% w/w which was confirmed by the XRD analysis. The XRD spectrum of kaolin and bentonite clays are given in the Figure 3-1. The particle size distributions of both clay types are given in Figure 3-2. It is evident from the size distribution curves that both clay types have P_{80} around 10µm

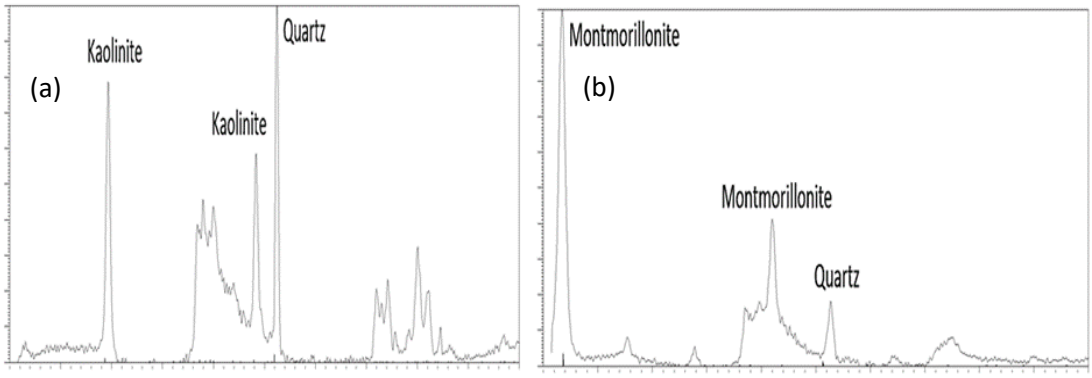

Figure 3-1. XRD spectrums of (a) kaolin and (b) bentonite clay

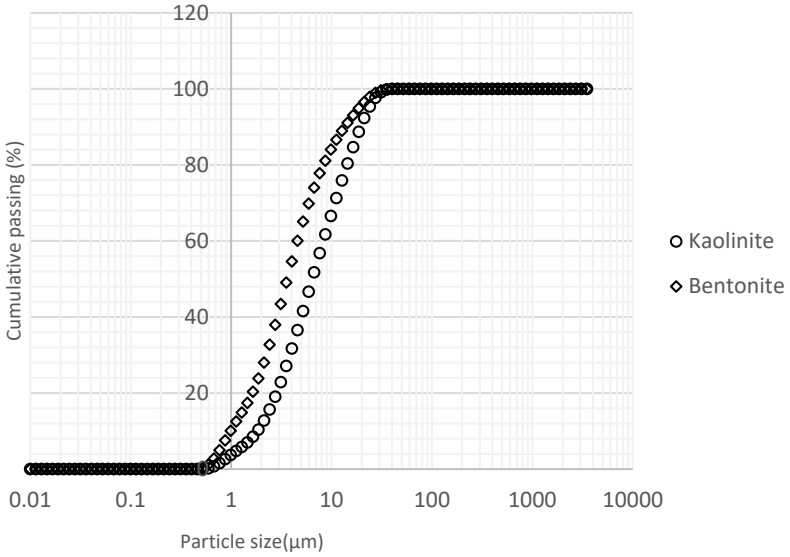

Figure 3-2. Particle size distribution of kaolin and bentonite clays

The quartz samples from Western Australian mines was obtained for gravity separation tests using a Knelson concentrator. Initially, quartz was crushed to achieve -2.36 mm particle size and dry ground using the rod mill followed by the pulveriser. Then the ground material was wet sieved to obtain required particle sizes.

Magnetite from Western Australian mines was obtained for the gravity separation tests using the Knelson concentrator. Initially, magnetite ore was crushed to achieve -2.36 mm particle size and dry ground using the rod mill followed by the pulveriser. Then, magnetite was separated from the ore using a magnetic separator. Separated magnetite was wet sieved to acquire the required size fractions.

3.1 Flotation experiments

The flotation tests were performed on the artificially mixed slurries of gold ore and one of the clays (kaolin or bentonite) at a certain solid ratio. A 3L Leeds flotation cell with a vaned impeller was used for the experiments. A factorial experimental design was used to plan the flotation experiments. The experiments were designed mainly to evaluate the effects of the clay concentration and the clay type (kaolin and bentonite) on flotation performance. Clay type, clay concentration, air rate, pulp pH, and the dispersant (polyacrylate based dispersant (Cytec Cyquest 3223)) concentration were

the operation variables considered in designing the experiments. Additionally, the flotation experiments also were conducted substituting the dispersant with Ca^{2+} which is known to affect the swelling properties of clays (Assemi et al., 2015; Cruz et al., 2015). It should be noted that the dispersant or Ca^{2+} ions were mixed in the deionized water before adding the clay-containing ore. The ore and clay mixtures were prepared separately and introduced into the agitating flotation cell, and the slurry level was adjusted by adding deionized water with 18.2 MΩ cm to achieve 30 %w/w. The slurry was well stirred for 15 min at 1500 rpm after the addition of dispersant or $CaCl_2$.

Flotation experiments were conducted under the similar reagent conditions to that used in operating gold plants in Western Australia, treating gold-bearing pyritic ores. More precisely, the pulp was conditioned with the analytical grade reagents: $CuSO_4$ activator (40 g/t), PAX collector (40 g/t), and MIBC (10 g/ton). The flotation concentrates were collected after 15, 30, 60, 120, and 240 s. The impeller speed was kept at 800 rpm, and NaOH and HCl were used for adjusting the pulp pH.

3.2 Froth stability experiments

Froth stability tests were conducted to evaluate the effects of clay on the stability of the froth phase. A froth column given in Figure 3-3 was used for conducting the experiments. The froth column was 50 cm long and had a cross-section of 25 cm^2. A porous sparger was fixed to the bottom of the column for uniformly diffused air supply. Air supply was connected to the sparger through an air flow meter. The experiments were performed on the artificially mixed slurries of the pyritic gold ore and one of the clays (kaolin or bentonite) with 30 % slurry density. Clay type, clay concentration, and Ca^{2+} concentration were the operational variables used in the experiments. In each experiment, the 500ml slurry was conditioned with the activator ($CuSO_4$), the collector (PAX), and the frother (MIBC) and Ca^{2+} ions. Air was turned on after slurry being introduced into the column. Then the increase in the froth level was measured until the froth reaches equilibrium height. Then the air was turned off and the height of the decaying froth was measured with time. The maximum froth height and the half-life time for decaying of the froth phase were used as the indicators of the froth stability. The air rate was maintained at 5 l/min in all the experiments

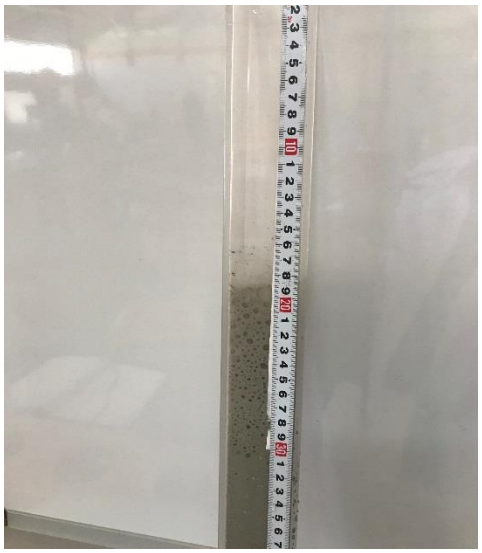

Figure 3-3. Froth column

3.3 Settling experiments

The settling tests were performed on the pure kaolin and bentonite slurries in the presence and absence of Ca^{2+} ions to investigate the rheological influence of clay minerals in the flotation experiments. Also, the settling behaviour was used to understand the swelling capacity of the clay slurries. In each experiment, 5% w/w clay slurry was transferred to the 100 mL graduated cylinder after adjusting slurry pH to 9. The slurries were mixed vigorously, and then the settling behaviour of the slurries was observed after 20 min by recording the solid-liquid interface.

3.4 Gravity concentration experiments with Knelson concentrator

The gravity separation experiments were conducted to evaluate the effect of clay on the separation of magnetite from quartz using the Knelson concentrator. The artificially mixed slurries of quartz, magnetite and clay having a slurry density of 40% and 5% magnetite were introduced to the Knelson concentrator at a solid rate of 200 g/min. The experiments were performed for two different particle sizes i.e. -100 μm and +100-300 μm. Particle size, clay concentration and the fluidization water rate were the operating variables considered in formulating the experimental design. An image of laboratory Knelson concentrator is given in Figure 3-4.

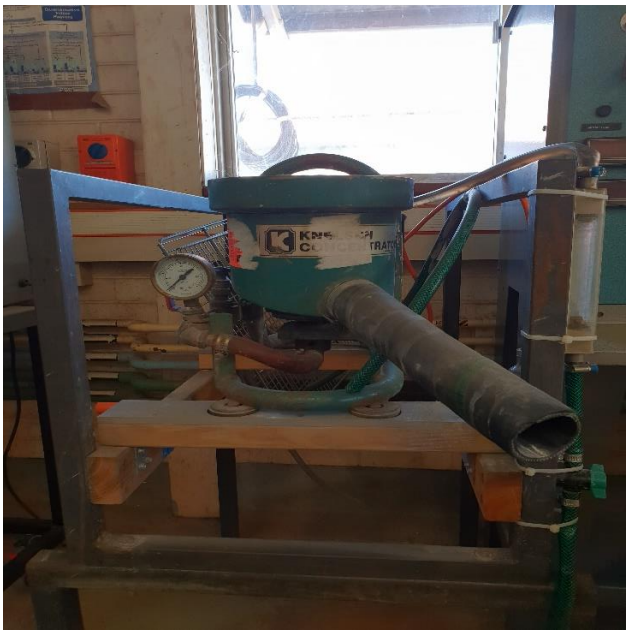

Figure 3-4. The laboratory Knelson concentrator.

3.5 Filtration experiments

The pressure filtration experiments were conducted on the artificially mixed slurries of pyritic gold ore and one of the clays (kaolin or bentonite) in order to identify the effects of bentonite and kaolin clays on filtration. The experiments were performed using a 20 cm diameter cylindrical pressure filter. The slurries were filtered at a constant pressure of 500 kPa and the volume of the filtrate was measured with time for each experiment.

The vacuum filtration experiments were conducted to identify the effects of hydrophobic reagents (dodecyl ammine hydrochloride) on the filtration of pyritic gold ore in the absence and presence of bentonite and kaolin. The experiments were performed using a constant vacuum pressure of 71 kPa. All the filtration experiments were conducted using Whatman grade 3 qualitative filter papers with a pore size of 6 μm becuase the slurries contained very fine particles.

3.6 Rheological measurements

The viscometer (LV1 Brookfield, USA) was used to measure the slurry rheological properties. The apparatus called ULA adapter was attached to the viscometer for analysing slurries with low viscosity while small sample adapter was used for measuring highly viscous slurries. In the flotation experiments, the rheological properties of the flotation pulp were measured to identify the effect of clay minerals in the flotation pulp. 16 mL sample was withdrawn from the agitating flotation cell after conditioning with flotation reagents using a syringe. Then the extracted slurry was introduced into the viscometer, and rheograms were generated at the shear rates from 0 to 122 s^{-1}. The rheological properties of pure clay slurries were measured in the presence and absence of Ca^{2+} ions i.e. $CaCl_2$. All rheological measurements were conducted at 20 ± 2 °C.

Similarly, rheological measurements of feed and processed slurries of gravity experiments, conducted using Knelson concentrator were measured. It must be noted that in order to measure the rheological properties of processed slurries, Slurry was artificially prepared considering the dilution caused by the fluidizing water. Image of the viscometer and the used spindles are given in Figure 3-5

Figure 3-5. Brookfield LV1 viscometer

3.7 Zeta potential measurements

The zeta potential measurements were carried out using a Zetasizer (Malvern Nano Z, UK). Initially, the zeta potentials of the pure pyrite particles and the mixture of pyrite with kaolin or bentonite were determined in the presence and the absence of Ca^{2+} ions. 0.05 g of pure pyrite and clay samples were mixed for 5 min with the deionized water. The experiments were performed in the absence and presence of Ca^{2+} ions. The coarse particles were allowed to settle down, and the supernatant solution containing fine particles was used for the zeta potential measurements which were repeated 4 times, and the mean value was used for further analysis.

Similarly, the zeta potential measurements of pure bentonite, kaolinite and gold ore particles were measured in the presence of DAH (dodecyl ammine hydrochloride) to investigate the coating of DAH molecules on the particles in the filtration experiments. The zetasizer, used in the experiments, is given in Figure 3-6

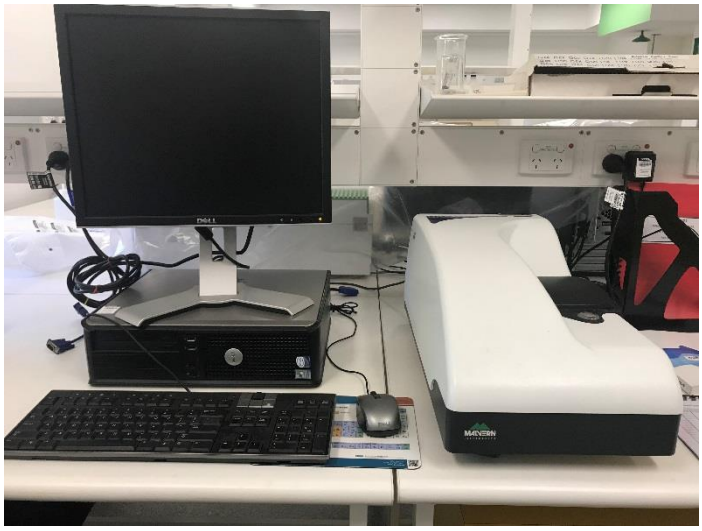

Figure 3-6. Malvern Nano Z, UK Zetasizer

3.8 XRD methodology

XRD technique was performed using a diffractometer Olympus with radiation Co-Kα in the range between 5 and 55° (2θ). The mineralogical composition of the ore was determined by the quantitative XRD analysis which is illustrated in Table 3-1. The composition of clays also was analysed using the XRD analysis. X-Powder software package was used to analyse the diffractograms. It should be noted that the glycol saturation method (Inoue et al., 1989) was used for the preparation of clay samples.

When air dried method was used with clay, the peaks in the diffractograms were difficult to identify probably due to the sticky nature of clays. The glycol saturation method eliminated the noise and significant peaks were visible in the diffractograms. The XRD results showed that kaolin clay contained 87% kaolinite and 13% quartz whereas bentonite had 82.9 % montmorillonite and 17.1% quartz.

3.9 Scanning electron microscopic (SEM) analysis

The SEM instrument, used in this study, is ZEISS NEON 40EsB FIBSEM. The NEON is dual beam focussed ion beam scanning electron microscope (FIBSEM) comprised of a field emission gun and a liquid metal Ga^+ ion source. This instrument is capable of capturing high resolution images using a precision ion beam using either secondary electrons or back scattered electrons. Additionally, instrument is capable of analysing the elemental composition of a sample using energy dispersive X-ray Spectroscopy (EDX). The SEM analysis was performed on the filter cake surface after the filtration. More specifically, two samples of a filter cake containing 5% (w/w) bentonite and 10% kaolin were analysed to identify the effects of clays on the microstructure of the filter cakes.

Chapter 4 Influence of clays on flotation performance

4.0 Introduction

Processing of low-grade ores will have to be considered in the future with the depletion of high-grade ores. In most instances particularly in Australia, low-grade ores may contain clays as an impurity. Processing of clay containing ores can be extremely challenging as the processing system needs to be altered and modified to suit the processing of clay-containing ores (Connelly, 2011). It is well known that the presence of clay minerals hinders the performance of most mineral processing techniques such as flotation, filtration, and gravity separation etc. However, effects of clays on such processes have not been adequately quantified. Moreover, the effect of clay varies according to the available clay type due to the differences in the clay structure and the mineralogy. Therefore, it is of paramount importance for plant operators to understand the negative effect of clays on mineral processing and to propose new solutions.

Influence of clays on the flotation performance is of particular interest. It has been reported that the presence of clay minerals in mineral slurries inhibits the flotation performance. Clay minerals may have different effects on flotation processes such as (i) coating of valuable mineral surfaces and air bubbles with clay particles (Tao et al., 2010), (ii) increased consumption of flotation reagents (Connelly, 2011), (iii) entrainment of clay particles to flotation concentrates in both roughing and scavenging stages (Patra et al., 2010; Vasudevan et al., 2010; Jorjani et al., 2011) (iv) increasing pulp viscosity (Bakker et al., 2009; Shabalala et al., 2011), (v) increasing or decreasing froth stability (Dippenaar, 1988; Bulatovic, 2007; Farrokhpay, 2011). It must be noted that the extent of these effects may vary depending on the available clay type. Despite the effect of clay minerals have been attributed to their structure and composition, underlying mechanisms of these interactions have not been adequately identified.

In this chapter, the influence of commonly encountered clay types (bentonite and kaolin) on the flotation of pyritic refractory gold ore was investigated particularly in the context of pulp rheology and the surface coating of the clay minerals. The influence of

these clays on the froth stability was also investigated. Relationship between flotation performance and pulp rheology has also been proposed.

4.1 Experiments

Initially, batch flotation experiments were conducted according to a half factorial design as shown in Tables 4-1 and 4-4. Rheological properties of the flotation slurries were measured in every flotation experiment prior to the introduction of air. Also, zeta potential measurements and settling tests were conducted to better understand the results of the flotation experiments. Froth stability experiments were performed to investigate the influence of clays on the froth stability according to the experimental design shown in Table 4-12. The experimental procedures are further explained in Chapter 3.

4.2 Relevant process models

4.2.1 Flotation models

Flotation process is modelled using various types of models and their particulars are discussed with more details in the literature review in section *2.4.2*. Several first-order flotation models are available in the literature, which differ in their assumptions about the distribution of flotation rate constants of the particles. The most common assumptions are a) particles having constant rate constant b) particles that float at two different rates (fast and slow), and c) particles having a rectangular distribution of rate constants ranging from 0 to k_{max}. Of these models, the rectangular distribution model with two model parameters, proposed by Klimpel (1980), has been reported to be more versatile and fit the performance under a wide range of flotation conditions. In this work, this model was used to quantify the batch flotation performance. It is given by:

$$R = R_{\infty}\left(1 - \frac{(1 - e^{-k_{\max} t})}{k_{\max} t}\right) \tag{4-1}$$

where k_{max} is the maximum flotation rate constant and R_{∞} is the recovery at infinite time. The variation of flotation performance due to the presence of clays was monitored by these two model parameters.

4.2.2 Rheological models

Rheology of a slurry is represented by the relationship between shear stress and shear rate (King, 2002). Rheological behaviour of a slurry varies depending on the different attributes of the solids suspended in the slurry such as particle size, particle density, particle shape and colloidal behaviour. Therefore, different models are used to describe the shear rate vs shear stress relationship. The rheological models applied in this study are:-

Newtonian model: $\tau = \mu\gamma$ (4-2)

Bingham model: $\tau = \tau_b + \mu_{pl}\gamma$ (4-3)

Power law model: $\tau = K\gamma^n$ (4-4)

Where τ is the shear stress, γ represents the shear rate (generally taken as the velocity gradient), μ is the Newtonian viscosity, τ_b represents the yield stress, μ_{pl} is the plastic viscosity, *K* and *n* are the consistency index and the flow index, respectively. Graphical representations of the applied rheological models are given in Figure 4-1

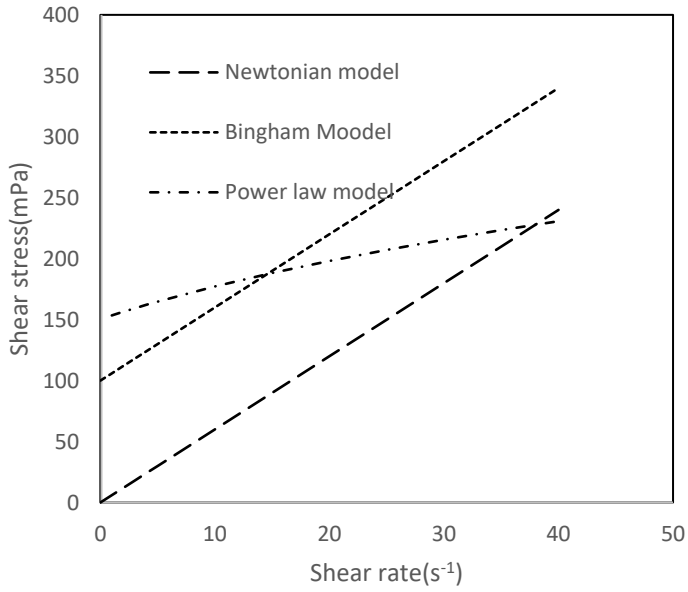

Figure 4-1. Graphical representation of applied rheological models

4.2 Results and discussion

4.2.1 Flotation experiments

The flotation experiments were performed to investigate the influence of kaolin and bentonite on the flotation of pyrite from the pyritic gold ore. The experimental variables were clay type (type 1 is kaolin or type 2 is bentonite), clay concentration, pulp pH, air rate and dispersant concentration. The flotation results are given in Table 4-1. The flotation model parameters k_{max} and R_∞, discussed in section *2.4.2* (see Eq.4-1) were obtained by curve fitting for each experiment. Sample model fitting for three selected experiments are given in Figure 4-2. Also, the coefficient of correlation (R) between experimental flotation recovery and the calculated values using Eq. 4-1 is given in Table 4-1. It is evident that the calculated flotation recovery values have significant correlation to the experimental values as coefficient of correlation is 0.99 for each experiment. Therefore, it justifies using R_∞ *and* k_{max} to represent flotation results of the experiments since both parameters are used for calculated points.

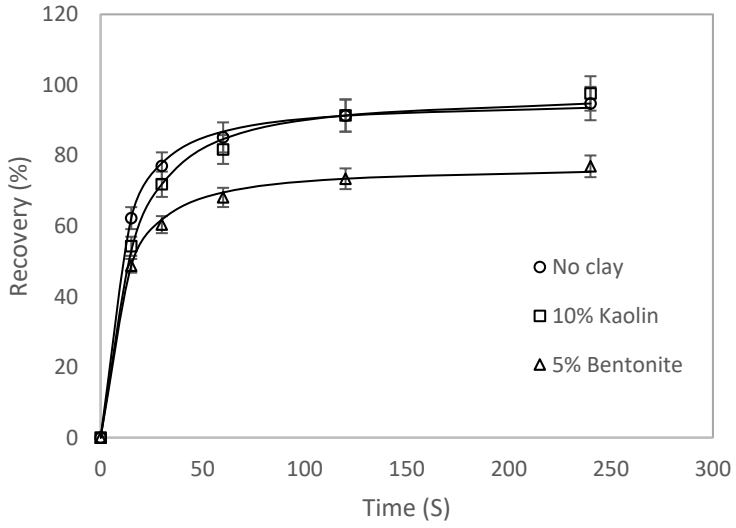

Figure 4-2. Example fitting of flotation model (Eq. 4-1) to three selected flotation experiments

It should be noted that oxides like quartz and feldspar are not floatable with xanthate.

Table 4-1. Flotation performance in the presence of polyacrylate dispersant, CuSO4 activator (40 g/t), PAX collector (40 g/t), and MIBC (10 g/ton).

Test	Clay type	Clay conc. (%)	pH	Air rate (L/min)	Dispersant (g/t)	R_∞ (%)	k_{max} (s^{-1})	R
1	1	0	7	5	0	98.58	13.71	0.99
2	1	10	7	5	200	100.00	3.37	0.99
3	1	0	9	5	200	95.78	10.61	0.99
4	1	10	9	5	0	98.09	7.27	0.99
5	1	0	7	10	200	96.42	11.36	0.99
6	1	10	7	10	0	96.94	6.70	0.99
7	1	0	9	10	0	97.04	16.37	0.99
8	1	10	9	10	200	98.15	17.78	0.99
9	2	0	7	5	0	98.59	13.72	0.99
10	2	5	7	5	200	81.79	4.14	0.99
11	2	0	9	5	200	95.78	10.61	0.99
12	2	5	9	5	0	77.31	9.91	0.99
13	2	0	7	10	200	96.42	11.36	0.99
14	2	5	7	10	0	83.83	5.73	0.99
15	2	0	9	10	0	97.04	16.37	0.99
16	2	5	9	10	200	87.06	10.53	0.99

The ANOVA analysis was performed on the model parameters (k_{max} and R_∞) using MINITAB statistical software in order to identify the significant variables on the flotation performance. The significance of the interactions between variables can be also identified by the ANOVA analysis. The significance of each variable and the interactions was evaluated by calculating p-value with 95% confidence where a variable was considered significant if the p-value is less than 0.05. Table 4-2 shows the ANOVA results for the ultimate flotation recovery. As seen in Table 4-2, the clay type and its concentration have a significant influence on the ultimate flotation recovery while the effects of other variables are not significant. The regression equations (Eqs (4-5) and (4-6)) indicate the influence of significant variables on ultimate flotation recovery. It can be observed that the calculated ultimate flotation recovery is substantially lower in the presence of bentonite than that in the presence of kaolin.

Table 4-2**.** ANOVA for the ultimate flotation recovery (R_∞) for the experimental design given in Table 4-1.

Source	DF	Adj SS	Adj MS	F-value	p-value
Clay type	1	249.75	249.75	39.46	0.0001
Clay conc	1	172.14	172.14	27.20	0.001
pH	1	2.51	2.51	0.40	0.55
Air rate	1	3.05	3.05	0.48	0.51
Dispersant conc	1	0.98	0.98	0.16	0.70
Clay type × Clay conc	1	249.75	249.75	39.46	0.0001
Clay type × pH	1	0.004	0.004	0.00	0.980
Clay type × Air rate	1	15.235	15.235	2.68	0.200
Clay type × Dispersant Conc	1	1.8310	1.8310	0.32	0.610
Clay conc × pH	1	0.657	0.657	0.12	0.756
Clay conc × Air rate	1	8.184	8.184	1.44	0.317
Clay conc × Dispersant Conc	1	21.353	21.353	3.75	0.148

(DF= Degree of freedom, Adj MS= Adjusted mean squares, Adj SS= The total sum of squares, F-value = Value obtained from statistical F-Test)

The variation of R_∞ with clay type may be quantified by the following regression equations:

For bentonite clays:

$$R_\infty = 96.96 - 2.852 \text{ Clay conc} \quad (4\text{-}5)$$

For kaolinite clays:

$$R_\infty = 96.96 + 0.134 \text{ Clay conc} \quad (4\text{-}6)$$

Table 4-3 shows the results of ANOVA on flotation rate constant k_{max} , performed to identify which variables are significantly affecting the flotation process. Clay concentration and pulp pH influenced k_{max} significantly. Interestingly, the differences in the clay type (kaolin or bentonite) did not indicate a significant effect on k_{max}.

Table 4-3. ANOVA for k_{max} for the experimental design given in Table 4-1..

Source	DF	Adj SS	Adj MS	F-value	p-value
Clay type	1	1.45	1.45	0.20	0.67
Clay conc	1	93.63	93.63	12.79	0.006
pH	1	53.92	53.92	7.37	0.02
Air rate	1	32.58	32.58	4.45	0.06
Dispersant conc	1	6.29	6.29	0.86	0.38
Clay conc × pH	1	29.54	29.54	4.04	0.08
Clay conc × Clay type	1	0.85	0.85	0.24	0.643
Clay conc × Air rate	1	6.75	6.75	1.90	0.217

The changes of k_{max} with clay concentration and pulp pH may be quantified by the following regression equation:

$$k_{max} = 7.46 - 3.21 \text{ Clay conc} + 0.62 \text{ pH} \quad (4\text{-}7)$$

The adhesion of clay particles onto the pyrite surfaces may have reduced the flotation rate constant. This decrease was exacerbated at low pH values because clay particle edges have a pH-dependent positive charge which becomes more positive at acidic or neutral pH values, making clay particles more susceptible to adhere on negatively charged pyrite surfaces (Swartzen-Allen and Matijevic, 1974).

More flotation experiments were designed to investigate the combined effects of Ca^{2+} ions and the bentonite and kaolin clays on pyrite flotation. The experiments were designed replacing dispersants with Ca^{2+} ions since lime is used in most of the industrial flotation operations to increase the pulp pH, especially in sulfide flotation. The flotation results are given in Table 4-4. ANOVA was also conducted on the model parameters to identify the significant flotation variables.

Table 4-4. Flotation performance in the presence of Ca^{2+} ions, $CuSO_4$ activator (40 g/t), PAX collector (40 g/t), and MIBC (10 g/ton).

Test	Clay type	Clay conc (%)	pH	Air rate (L/min)	C_{Ca2+} (g/ton)	R_∞ (%)	k_{max} (s^{-1})	r
1	1	0	7	5	0	98.58	13.71	0.99
2	1	10	7	5	1500	87.80	6.27	0.99
3	1	0	9	5	1500	83.68	8.98	0.99
4	1	10	9	5	0	98.09	7.27	0.99
5	1	0	7	10	1500	79.61	5.15	0.99
6	1	10	7	10	0	96.94	6.69	0.99
7	1	0	9	10	0	97.03	16.36	0.99
8	1	10	9	10	1500	86.26	12.53	0.99
9	2	0	7	5	0	98.58	13.71	0.99
10	2	10	7	5	1500	75.31	4.70	0.99
11	2	0	9	5	0	83.68	8.98	0.99
12	2	10	9	5	0	48.56	9.47	0.99
13	2	0	7	10	1500	79.61	5.15	0.99
14	2	10	7	10	0	38.32	7.59	0.99
15	2	0	9	10	0	97.03	16.36	0.99
16	2	10	9	10	1500	81.24	11.15	0.99

Table 4-5. ANOVA for the ultimate flotation recovery (R_∞) for the experimental design given in Table 4-4.

Source	DF	Adj SS	Adj MS	F-value	p-value
Clay conc	1	692.64	692.64	96.72	0.0001
pH	1	27.13	27.13	3.79	0.10
Air rate	1	20.78	20.78	2.90	0.14
C_{Ca2+}	1	15.93	15.93	2.22	0.19
Clay type	1	986.82	986.82	137.80	0.0001
Clay conc × C_{Ca2+}	1	803.17	803.17	112.15	0.0001
Clay conc × Clay type	1	986.82	986.82	137.80	0.0001
C_{Ca2+}× Clay type	1	513.48	513.481	71.70	0.0001
Clay × C_{Ca2+}× Clay type	1	513.48	513.481	71.70	0.0001

ANOVA analysis indicates that the clay type and the clay concentration are the significant variables affecting the ultimate recovery. Furthermore, the interactive effects of Ca^{2+} and the clay type and clay concentration are also shown as significant. Therefore, both significant individual variables and their interactions with Ca^{2+} on the ultimate flotation recovery need to be considered.

Table 4-6**.** Tukey pairwise comparison (Mason et al, 2003) of mean ultimate recovery (R_∞) for the experimental design given in Table 4-4.

.

(Clay con, $C_{Ca2+,}$ Clay type)	Number of experiments	Mean recovery
(0, 0, kaolinite)	2	97.81
(0, 0, bentonite)	2	97.81
(10, 0, kaolinite)	2	97.52
(10, 0.02, kaolinite)	2	87.04
(0, 0.02, kaolinite)	2	81.65
(0, 0.02, bentonite)	2	81.65
(10, 0.02, bentonite)	2	78.28
(10, 0, bentonite)	2	43.44

Significance of the variables and the interactions were quantified using Tukey mean analysis and the results are given in Table 4-6. It can be observed that the effect of Ca^{2+} on flotation performance is not consistent. Precisely, when the flotation slurry did not contain clay minerals, the mean ultimate recoveries reduced to 81.65% from 97.81% in the presence of Ca^{2+} (see Table 4-6). There was no substantial effect on the ultimate recovery by the addition of kaoline but a significant drop to 43.44% with the addition of bentonite. However, as seen from Table 4-6, ultimate recovery increased to 78.28% from 43.44% as a result of the addition of Ca^{2+} ions in the presence of

bentonite clay. Therefore, it is evident that Ca^{2+} ions reduce the adverse effects of bentonite clay on pyrite flotation. These results indicate that the effects of different clays have different effects on the flotation performance as well as the interaction with Ca^{2+} ions. These different effects could be attributed to the structural differences of the clays and their different swelling behaviours and thus their rheological characteristics.

Table 4-7 shows the results of the ANOVA analysis conducted for the flotation rate constant. Clay concentration, clay type, pulp pH, and Ca^{2+} concentration were the independent variables considered in the analysis. It was revealed that flotation rate constant was reduced substantially due to the presence of clay and Ca^{2+} ions and those effects can be quantified by the regression equation given below (Equation 4-8).

Table 4-7. ANOVA for k_{max} for the experimental design given in Table 4-4.
.

Source	DF	Adj SS	Adj MS	F-value	p-value
Clay conc	1	32.37	32.37	45.13	0.0001
pH	1	49.40	49.40	68.86	0.0001
Air rate	1	3.90	3.90	5.44	0.06
C_{Ca2+}	1	49.97	49.98	69.67	0.0001
Clay type	1	0.001	0.001	0.00	0.97
Clay conc × pH	1	0.31	0.30	0.43	0.54
Clay conc × C_{Ca2+}	1	78.84	78.84	109.91	0.0001
pH × C_{Ca2+}	1	9.92	9.92	13.82	0.01

The changes of k_∞ with clay concentration pulp pH and Ca^{2+} concentration may be quantified by the following regression equation:

$$k_{max} = 7.28 - 0.7284 \text{ Clay conc} + 0.970 \text{ pH} - 1029 \, C_{Ca2+} + 44.40 \text{ Clay conc} \times C_{Ca2+} + 78.7 \text{ pH} \times C_{Ca2+} \quad (4\text{-}8)$$

4.2.2 Effect of clays on rheology of flotation slurries

Figures 4-3 and 4-4 (a) (b) illustrate the rheograms of flotation slurries in a log-log plot, where Figure 4-3 shows the rheograms of the slurries without clay and Figure 4-3 (a) and (b) show the rheograms of flotation slurries with 10% (w/w) kaolin and 5%

(w/w) bentonite clays, respectively. As seen in Figures 4-3 and 4-4, straight line approximation can be given to the rheograms when plotted on a log-log plot.

Therefore, the rheograms can be approximated by the power law model given in eq 4-4. Flow index (*n)* and the consistency index (*K)* are the model parameters in the power law model. When n=1 slurry behaves as a Newtonian slurry. Similarly, slurry is pseudoplastic if n<1 and dilatant if n>1. *K* is an indicator of slurry viscosity. The higher the *K* values, the slurry is more viscous.

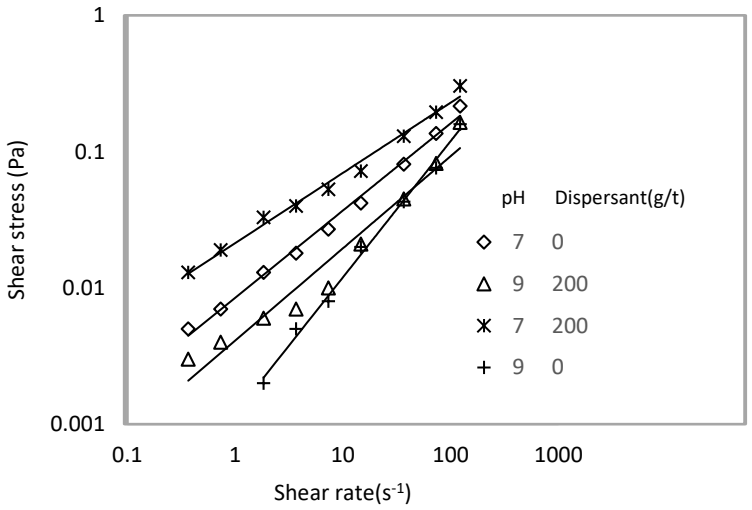

Figure 4-3. Rheogram of flotation slurries in the absence of clay minerals.

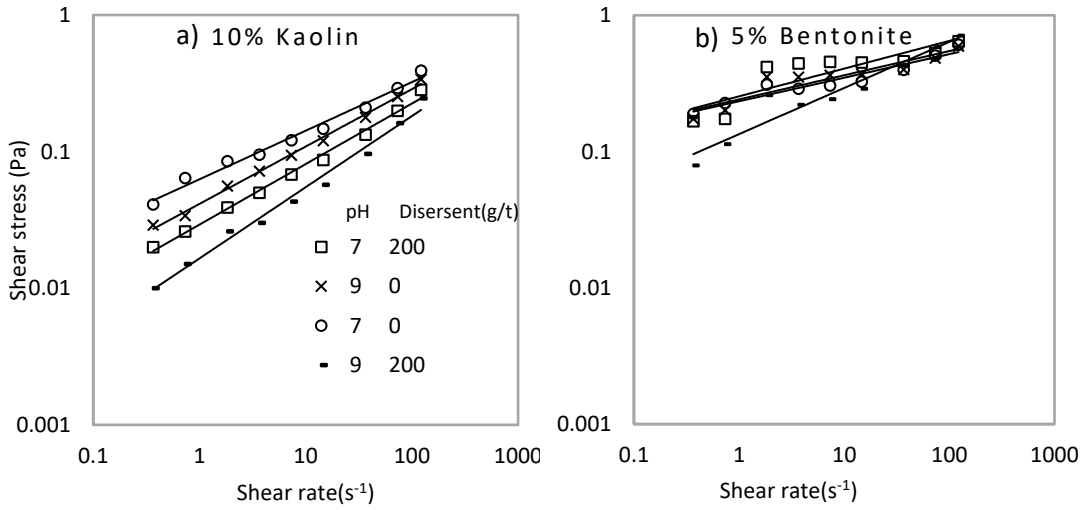

Figure 4-4**.** Rheograms of flotation slurries containing a) 10% kaolinite and b) 5% bentonite.

Table 4-8. Flow index and the consistency index of flotation slurries for the experimental design given in Table 4-1.

Test	Clay type	Clay conc. (%)	pH	Dispersant conc. (g/ton)	Flow index	Consistency index (Pas^n)
1	1	0	7	0	0.64	0.01
2	1	10	7	200	0.44	0.03
3	1	0	9	200	0.65	0.00
4	1	10	9	0	0.42	0.04
5	1	0	7	200	0.51	0.02
6	1	10	7	0	0.35	0.06
7	1	0	9	0	0.72	0.00
8	1	10	9	200	0.52	0.02
9	2	0	7	0	0.64	0.01
10	2	5	7	200	0.20	0.25
11	2	0	9	0	0.65	0.00
12	2	5	9	0	0.18	0.24
13	2	0	7	200	0.51	0.02
14	2	5	7	0	0.18	0.23
15	2	0	9	0	0.72	0.00
16	2	5	9	200	0.34	0.13

Flow index and the consistency index of flotation slurries in each experiment are given in Table 4-8. These model parameters were estimated by fitting power law model to the curves given in Figures 4-2 and 4-3. It can be observed that the flow indexes of all the slurries are less than unity and thus slurries behave as pseudo plastic slurries. Therefore, slurries exhibit higher apparent viscosities at low shear rates than that of higher shear rates. The consistency index varies from 0 to 0.25 Pas^n, which signifies the different rheological behaviour of the slurries. Precisely, slurry with higher consistency index has higher apparent viscosity under any shear rate with respect to the slurries with low consistency index. ANOVA was conducted on the flow index and consistency index values to identify the significantly affecting variables. ANOVA showed that the clay type and the clay concentration significantly affected both model parameters.

Table 4-9**.** ANOVA for a) flow index and b) consistency index

a)

Source	DF	Adj SS	Adj MS	F-value	p-value
Clay type	1	0.03	0.03	40.98	0.00
Clay conc.	1	0.05	0.05	71.10	0.00
pH	1	0.00	0.00	2.96	0.12
Air rate	1	0.00	0.00	0.74	0.41
Dispersant conc.	1	0.00	0.00	1.10	0.32
Clay type × Clay conc.	1	0.03	0.03	40.98	0.00
Clay conc × pH	1	0.00	0.00	1.24	0.30

b)

Source	DF	Adj SS	Adj MS	F-value	p-value
Clay type	1	0.04	0.04	6.95	0.03
Clay conc.	1	0.37	0.37	57.78	0.00
Air rate	1	0.00	0.00	0.57	0.48
pH	1	0.03	0.03	5.25	0.06
Dispersant conc.	1	0.00	0.00	0.00	0.96
Clay type × Clay conc.	1	0.04	0.04	6.95	0.03
Clay type × pH	1	0.00	0.00	0.00	0.97

Table 4-10. Tukey pairwise comparison of mean flow index and mean consistency index.

(Clay type, Clay conc)	Number of experiments	Mean flow index	Mean consistancy index (Pas^n)
(kaolinite, 0%)	4	0.63	0.01
(bentonite, 0%)	4	0.63	0.01
(kaolinite, 10%)	4	0.43	0.04
(bentonite, 5%)	4	0.22	0.21

As seen in Table 4-10 both clay types resulted in reducing the flow index, more specifically in the presence of bentonite clay. A similar trend could also be seen in the analysis for the consistency index, where the addition of clays increased the consistency index of the slurry, particularly in the case of bentonite. Hence, it may be concluded that the effect of clay is to increase the shear thinning properties of the flotation slurries while inducing higher apparent viscosities. It must be noted that bentonite clays showed the most extreme effects on the slurry rheology which may be attributed to the voluminous structures formed due to the hydration of bentonite particles. It has been observed that bentonite clay forms a gel-like structure due to

crystalline and osmotic swelling which enhances the slurry viscosity significantly even at low clay concentrations (Goh et al, 2011). Interlayer swelling of bentonite is a result of the penetration of water molecules into interlayer spacing of loosely bonded montmorillonite layers (Luckham and Rossi, 1999).

4.2.3 Effect of Ca^{2+} ions on the rheology of pure clay slurries

The rheograms of the pure clay slurries with different clay concentrations, in the presence and absence of Ca^{2+} ions are shown in Figure 4-5. The rheograms were fitted to the power law models and the model parameters are tabulated in Table 4-11.

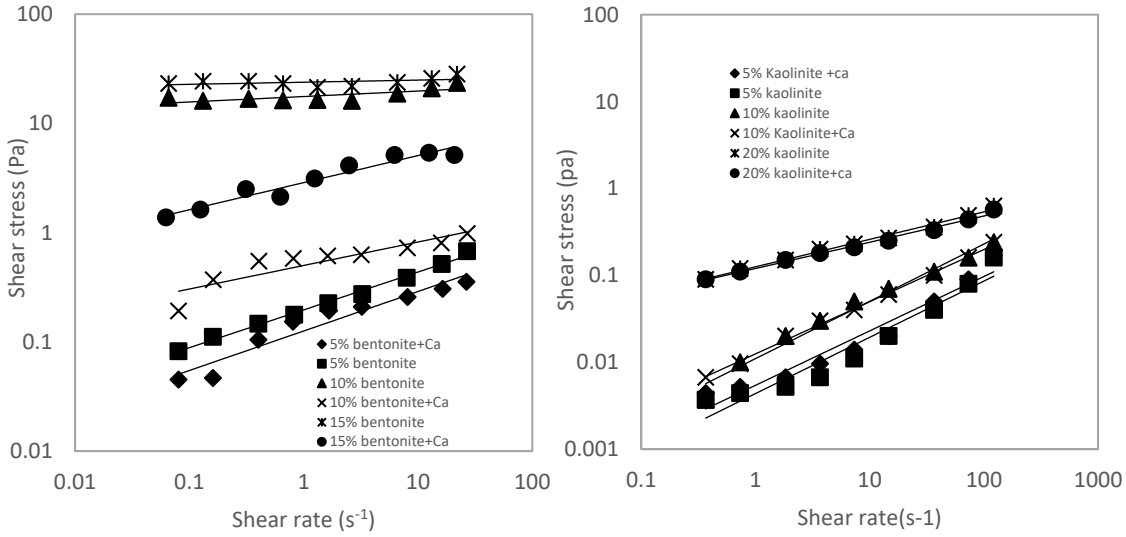

Figure 4-5. Rheograms of bentonite and kaolinite slurries.

The bentonite slurries were affected considerably by the pre-addition of the Ca^{2+} ions to the processed water, where the consistency index of bentonite slurries was decreased quite significantly. The consistency index of 15% bentonite slurry was reduced to 2.87 Pas^n from 23.82 Pas^n resulting in the addition of Ca^{2+} ions. It has been reported that the Ca^{2+} ions obstruct the interlayer swelling of bentonite particles by replacing the interlayer Na^+ ions and strengthening the interlayer bonding which prevents the penetration of water molecules into the interlayer region (Bradshaw et al., 2013). Therefore, the change in the swelling behaviour of bentonite results in altering the slurry rheology of the bentonite slurry. However, kaolin clay slurries were not affected by the addition of Ca^{2+} ions. These results were further clarified by the settling test results shown in Figure 4-6. It was observed that the addition of Ca^{2+} ions improved

the settling of bentonite particles which was attributed to the reduced swelling capacity. This is in agreement with the results obtained by other authors (Assemi et al., 2015; Cruz et al., 2015). The kaolin clay slurries were not significanttly affected by the addition of Ca^{2+} ions because its swelling properties are different to that of the bentonite, which also agrees well with the results obtained by Cruz et al. (2015). However, it should be noted that Ca^{2+} addition improved the settling of fine kaolin particles through agglomeration. However, the rheological measurements are performed in an agitated environment.

Table 4-11**.** Rheological properties of pure clay slurries

Clay (%)	Bentonite		Bentonite+Ca^{2+}		Kaolinite		Kaolinite+Ca^{2+}	
	Flow index	Consistency index (Pas^n)	Flow index	Consistency index (Pas^n)	Flow index	Consistency index (Pas^n)	Flow index	Consistency index (Pas^n)
5.00	0.35	0.20	0.36	0.13	0.64	0.0044	0.62	0.01
10.0	0.05	17.62	0.22	0.50	0.66	0.01	0.60	0.01
15.0	0.02	23.82	0.25	2.87	0.32	0.13	0.30	0.12

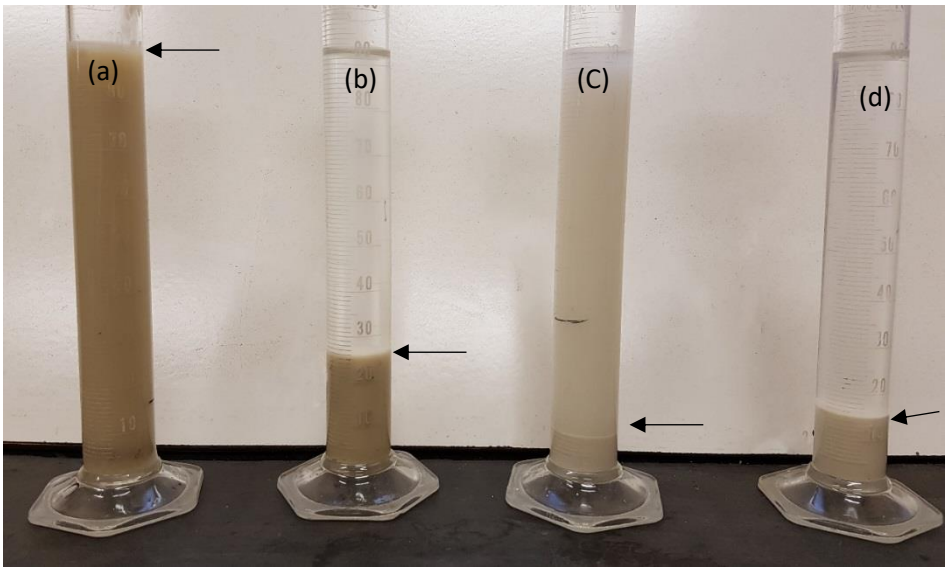

Figure 4-6. Settling tests results after 20 min for (a) 5% bentonite, (b) 5% bentonite + Ca^{2+}, (c) 5% kaolinite, (d) 5% kaolinite + Ca^{2+}.

4.2.4 Zeta potential measurements

The zeta potential measurement of pure pyrite, pyrite clay mixtures in the presence and absence of Ca^{2+} ions as a function of pH solution are shown in the Figure 4-7. These zeta potential measurements were implemented using aqueous solutions of purchased pure pyrite in the presence of kaolin, bentonite and Ca^{2+}, to better understand the flotation results and identification of the exiatance of clay coating on pyrite particles and its mechanism. It is evident that the isoelectic point for the tested pyrite particles exist around pH 4.5, therefore the pyrite surfaces have negative charge in the pH values where flotation experiments were conducted. Electrostatic attraction cannot be expected between clay and pyrite particles since both kaolin and bentonite particles have negative zeta potential. However, pyrite zeta potential becomes more negative with the addition of bentonite particles. It implies that bentonite particles have the potential to get adhered on the surfaces of pyrite particles at both acidic and alkaline pH values, possibly due to a coating effect of clay on pyrite particles. However, the addition of kaolin particles did not have any effect on the pyrite zeta potential.

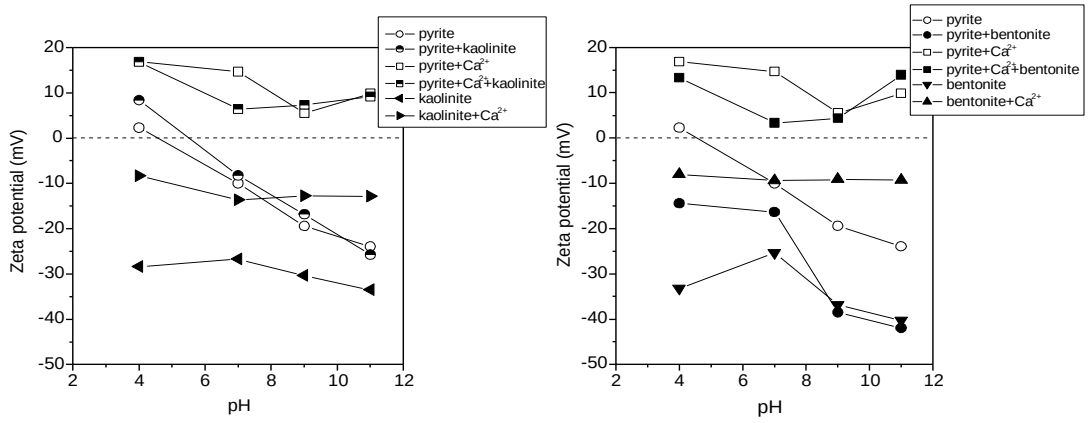

Figure 4-7. Zeta potential measurements versus pH solutions for pyrite, clay, and mixture of pyrite and clay with and without Ca^{2+}

Pyrite surfaces have become more positively charged owing to the addition of Ca^{2+} ions both in the presence and absence of clays. It implies that Ca^{2+} ions are more susceptible to adsorb on to the negatively charged pyrite surfaces. It has been reported that Ca^{2+} ions get adsorbed on to pyrite surfaces in the form of $CaOH^{+}$ ions (Li et al. 2012). Additionally, Li et al. (2012) stated that surface adsorption of $CaOH^{+}$ ions on to the pyrite surfaces impede the copper activation and thus reduce the adsorption of xanthate. However, this effect may be reduced by the addition of bentonite particles

which adsorbs some Ca^{2+} ions into the interlayer spacing of the bentonite particles, thereby decreasing the $CaOH^{+}$ adsorption on pyrite surfaces and thus increasing the pyrite recovery.

4.2.5 Effect of the rheology of slurries on flotation performance

According to the above observations, the presence of clay and Ca^{2+} significantly influenced the flotation performance and slurry rheology. The realtionships between ultimate flotation recoveries and the rheological model parameters (consistency index and flow index) are given in Figure 4-8.

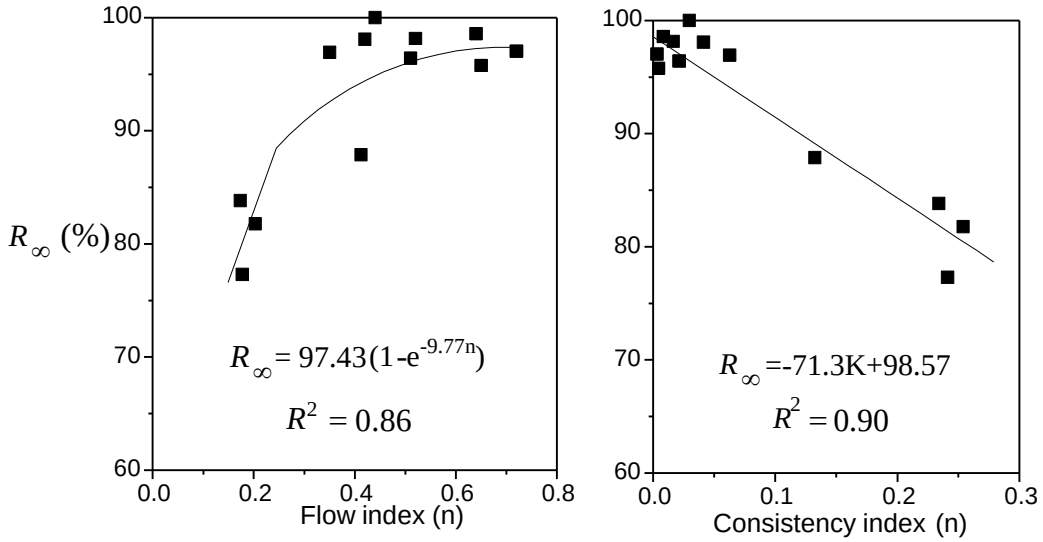

Figure 4-8**.** The relationships between the ultimate recovery, the flow index and the consistency index

It can be seen that the ultimate flotation recovery shows an increasing trend with increasing flow index but approaches a plateau at higher flow indexes. The slurries with low flow index values are the slurries with bentonite clay. It is evident that the increase in bentonite concentration reduces the flow index as seen in Table 4-1. The presence of bentonite clay increases the slurry apparent viscosity and thus inhibit the bubble-particle collisions and consequently poor flotation performance. Also, a negative linear relationship can be observed between the consistency index and the ultimate flotation recovery. It was reported that higher slurry viscosities impede the particle mobility and the dispersion of gas bubbles, hindering the bubble-particle collision and thus attachment adversely (Bakker et al. 2009; Shabalala and Harris, 2011). The availability of Ca^{2+} ions in the processed water decreased the adverse effects of the bentonite clays particles.

that the measurements of rheological parameters such as flow index and consistency index may be routinely used to monitor the flotation performance in operating plants.

The shear rate of the processed slurry at a particular point of an operational flotation cell depends on its relative position with respect to the impeller. Higher shear rates exist only around impeller (Bakker et al., 2009). Therefore, alterations to the hydrodynamics due to the increase in slurry viscosity may result in higher power requirement. “Cavern” like structure may build up around the impeller resulting in the higher apparent viscosity and yield stress which may cause poor dispersion of bubbles in the flotation cell (Bakker et al., 2009). Thus, it is evident that the addition of Ca^{2+} ions to the bentonite containing flotation slurries reduce the power requirement in a flotation cell.

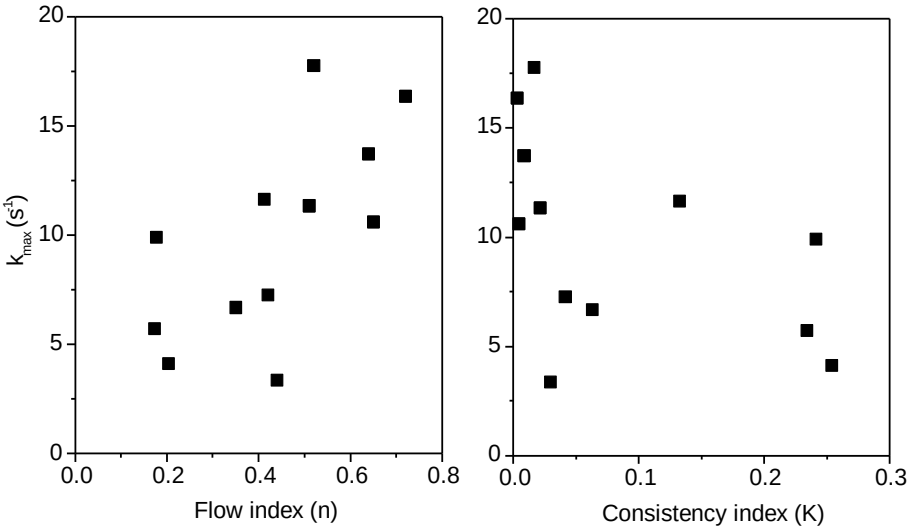

Figure 4-9. The relationships between the maximum rate constant, the flow index and the consistency index.

The relationships between the flow index and the consistency index with the maximum rate constant are shown in Figure 4-9. Within the experimental error, it shows an increase in k_{max} with increasing flow index. Increasing flow index implies that viscosity decreased, leading to higher k_{max} values as a result of improved mobility of particles and air bubbles. It should be noted that higher turbulence is not a solution because with higher turbulence, the particle-bubble detachment efficiency for coarser particles is high.

4.2.6 Effect of clays on froth stability

Froth stability experiments were conducted to evaluate the effect of bentonite and kaolin clays on the stability of the froth phase in flotation. Clay type, clay concentration, and the Ca^{2+} concentration were the independent variables considered in designing the experiments. All experiments were conducted using a froth column as explained in Chapter 3. Maximum froth height and the froth half-life were used to quantify the froth stability. Maximum froth height is the height of the froth phase at equilibrium and the froth half-life is the time it takes for the froth height to collapse into the half of the maximum froth height. The experimental results are given in Table 4-12.

Table 4-12. Experimental design for froth stability experiments.

Test	Clay type	Clay con (solid %)	Ca con(g/t)	Max froth height(cm)	Froth half-life(s)
1	Kaolin	0	0	29	8
2	Kaolin	10	0	16	6
3	Kaolin	15	0	17	7
4	Kaolin	20	0	17	5
5	Kaolin	0	1500	14	4
6	Kaolin	10	1500	19	6
7	Kaolin	15	1500	20	5
8	Kaolin	20	1500	18	6
9	Bentonite	0	0	29	8
10	Bentonite	10	0	13	5
11	Bentonite	15	0	17	9
12	Bentonite	20	0	13	8
13	Bentonite	0	1500	14	4
14	Bentonite	10	1500	19	10
15	Bentonite	15	1500	15	9
16	Bentonite	20	1500	17.5	10

ANOVA analysis was conducted on the maximum froth height and the froth half-life to identify which variables are significantly affecting the froth stability. ANOVA analysis results for maximum froth height and the froth half-life are given in Tables 4-13 and 4-14, respectively.

Table 4-13. ANOVA for maximum froth height

Source	DF	Adj SS	Adj MS	F-Value	p-Value
Model	5	183.73	36.746	13.67	0.001
Linear	3	80.03	26.677	9.93	0.005
Clay type	2	51.02	25.512	9.49	0.008
Ca^{2+}con	1	29.01	29.008	10.79	0.011
2-Way Interactions	2	132.69	66.345	24.69	0.000
Clay type* Ca^{2+} con	2	132.69	66.345	24.69	0.000
Error	8	21.50	2.687		
Total	13	205.23			

Table. 4-14. ANOVA for froth half life

Source	DF	Adj SS	Adj MS	F-Value	p-Value
Model	5	40.000	8.000	5.33	0.019
Linear	3	24.867	8.289	5.53	0.024
Clay type	2	23.667	11.833	7.89	0.013
Ca^{2+} con	1	1.200	1.200	0.80	0.397
2-Way Interactions	2	16.048	8.024	5.35	0.034
Clay type* Ca^{2+} con	2	16.048	8.024	5.35	0.034
Error	8	12.000	1.500		
Total	13	52.000			

According to the ANOVA analysis, clay type and Ca^{2+} ions concentration are the variables affecting significantly both maximum froth height and froth half-life. Moreover, the interactive effects of clay type and Ca^{2+} ions concentration have also been significant. In order to further quantify the effects of significant variables, Tukey pairwise mean comparison was conducted on both maximum froth height and froth half-life. The results are given in Tables 4-15 and 4-16, respectively

Table.4-15. Tukey mean analysis of froth height

(Clay type, Ca con(g/t))	Number of experiments	Mean froth height
(No clay,0)	1	29.00
(Kaolin, 1500)	3	19.00
(Bentonite, 1500)	3	17.16
(Kaolin, 0)	3	16.66
(Bentonite,0)	3	14.33
(No clay,1500)	1	14.00

Table.4-16. Tukey mean analysis of froth half-life

(Clay type, Ca con(g/t))	Number of experiments	Mean froth half-life (s)
(Bentonite, 1500)	3	9.66
(No clay, 0)	1	8.00
(Bentonite, 0)	3	7.33
(Kaolin, 0)	3	6.00
(Kaolin, 1500)	3	5.66
No clay, 1500)	1	4.00

According to the mean analysis, the presence of both clays reduced the maximum froth height significantly, however, the effect of bentonite clay is more pronounced. A small number of large bubbles might have resulted in low froth height; however, the bubble size distribution has not been studied in this thesis. Bentonite increases slurry viscosity significantly and this may restrict the generation of larger bubbles which reduces the maximum froth height (Wang et al, 2015b). The presence of kaolin clay also reduced the number of bigger bubbles, particularly if the slurry had more than 10% kaolin (Wang et al, 2015b; Farrokhpay et al, 2016).

Kaolin clay substantially reduced the froth half-life. Kaolin clay particles entrain into the froth phase due to their fine particle size (80 % less than 10 µm) (Cruz et al, 2015c). This might change the froth structure and reduce the froth half-life. Bentonite clays did not indicate a substantial influence on the froth half-life. Swelled bentonite particles do not entrain into the froth phase (Cruz et al, 2015c). Therefore, bentonite may not influence the froth structure and thus does not affect the froth half-life. The addition of calcium ions in the absence of clay significantly reduced the froth height and froth half-life. This effect may be attributed to the incorporation of Ca^{2+} ions into the frother monolayers, resulting in destabilizing bubbles (Zhang et al, 2004). As a result, the maximum froth height and the froth half-life were reduced.

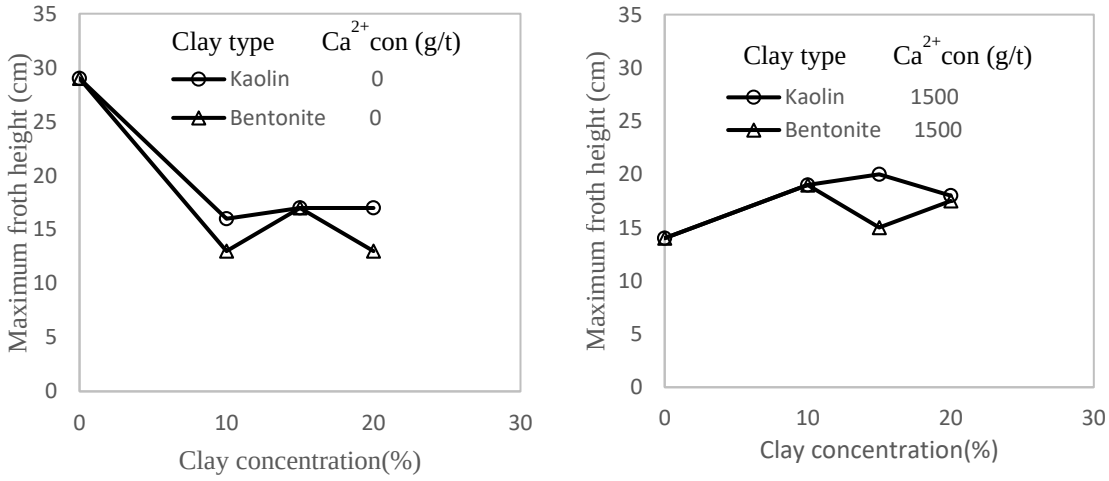

Figure 4-10. Effect of clay and Ca^{2+} on maximum froth height.

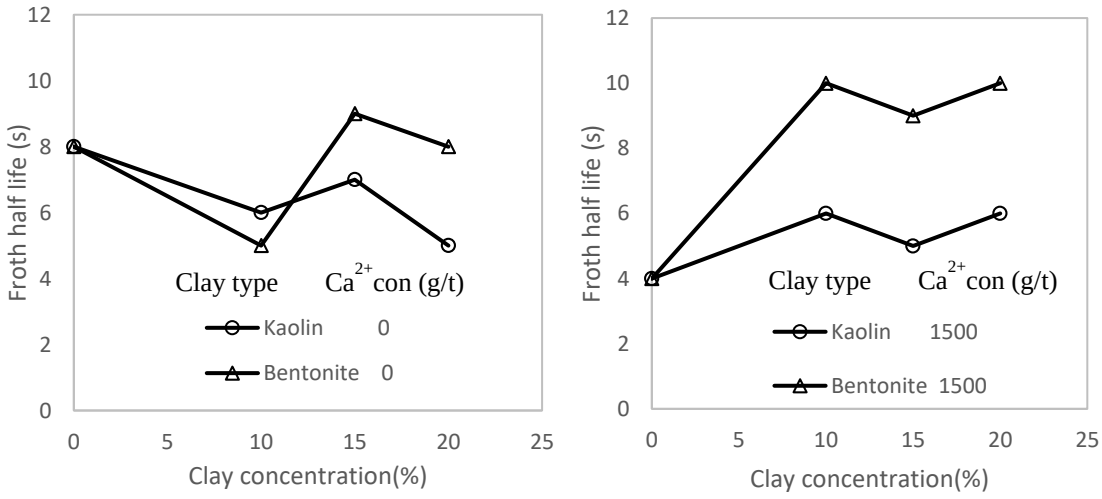

Figure 4-11. Effect of clay and Ca^{2+} on froth half-life.

Figures 4-10 shows that the addition of Ca^{2+} in the presence of kaolin increased the maximum froth height. It means that the presence of kaolin reduced the adverse effect of Ca^{2+}. The reason is that Ca^{2+} ions get adsorbed on kaolin basel surfaces because the basel planes of kaolin clay particles are negatively charged (Swartzen-Allen and Matijevic, 1974). In addition to that, the adsorption of Ca^{2+} ions to kaolin particle surfaces results in aggregation of fine kaolin particles to a voluminous structure which results in increasing clay entrainment into froth phase (Cruz et al, 2015c). Furthermore,

the stability of a froth phase could be higher when the froth phase contains higher percentage of solids (Farrokhpay, 2016).

It is evident that the presence of Ca^{2+} ions in the bentonite containing slurries reduced also the adverse effects on froth stability. Ca^{2+} ions get absorbed into the interlayers of bentonite particles, reducing the swelling of bentonite and thus decrease the slurry viscosity. The decrease in viscosity allows the formation of bigger bubbles which increases the maximum froth height (Farrokhpay, 2016). In addition to that, the adverse effects of Ca^{2+} ions on the froth stability was reduced because the concentration of freely available Ca^{2+} ions in the slurries decreased.

It must be noted that the changes in pulp pH and concentration of various electrolytes may also affect the behaviour of froth phases. Thus, a significant amount of future work is required for better understanding the influence of various factors on froth stability.

4.3. Summary

The results obtained from this study confirmed that the flotation performance of pyritic gold ore can be significantly affected by the available clay type and its concentration. More specifically, pyrite recovery was significantly reduced due to modification of slurry rheology in the presence of bentonite clay more than that kaolin clay. Addition of Ca^{2+} ions to the process water improved the flotation recovery of pyritic gold ore by mitigating the adverse effects of bentonite clay. More precisely, Ca^{2+} ions reduce the swelling capacity of bentonite clays thus minimizing the rheological influence. Flotation performance measures such as the ultimate recovery showed a strong correlation with the rheological parameters such as flow index and consistency index. Measurements of rheological properties and evaluating their correlations with flotation parameters may be used to routinely monitor the flotation performance in operating plants when processing ores with substantial amounts of clay. Furthermore, the influence of kaolin and bentonite on froth stability was similar to that on the flotation performance.

Chapter 5 Influence of clays on the performance of centrifugal gravity concentrators

5.0. Introduction

Gravity concentration devices utilize the differential movement of the particles in a slurry to separate valuable mineral from the gangue. The presence of clay in mineral slurries modify the hydrodynamics of the slurry by increasing the apparent viscosity and yield stress (Bakker et al., 2009; Shabalala et al, 2011). Therefore, the gravity separation efficiency could be reduced due to the presence of clay since the increased yield stress and viscosity obstruct the movement of particles (Wills and Napier-Munn, 2006). Nowadays, centrifugal gravity concentrators such as Knelson and Falcon are commonly used to recover minerals at finer particle sizes.

Knelson concentrator is a gravity concentration device which utilizes centrifugal forces and hydrodynamic forces for the beneficiation of dense material. Separation of minerals in a Knelson concentrator takes place due to the differences in particle density, size and shape (Coulter and Subasinghe, 2005; Laplante et al, 1996). Usage of gravity concentrators such as Knelson concentrators have low installation and operational costs. The most common application of Knelson concentrator is in gold processing industry since it has the ability to recover 96% of free liberated gold coarser than 30µm (Silva, 1986).

The influence of clay minerals on the performance of gravity concentrators have not been sufficiently investigated. Different clay types have distinct properties and swelling characteristics depending on the atomic structure of clay unit cells and the particle layer arrangement (Ndlovu et al, 2014; Bergaya and Lagaly, 2006). This chapter is focused on investigating the influence of kaolin and bentonite clays on the operation of the Knelson concentrator. The Knelson concentrator performance was evaluated based on the theory developed by Coulter and Subasinghe (2005).

5.1. Theory

A particle that enters into the Knelson concentrator bowl tends to traverse in a helical path attributing to the forces acting on the particle. A particle experiences centrifugal force (F_c) attributing to the rotation of the concentrator bowl. Required centripetal force is provided by the fluid drag force (F_d) resulted due to the flow of fluidizing water, and the Bagnold force (F_b). The Bagnold force is formed by the sheared dispersion and collision between particles (Bagnold, 1954). A schematic diagram of the Knelson concentrator is given in Figure 5-1.

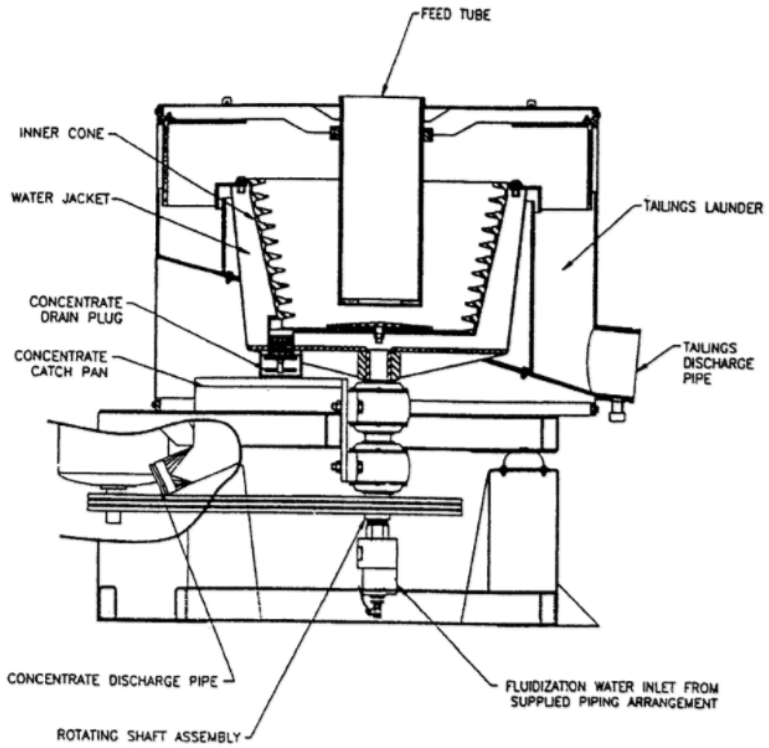

Figure 5-1. Schematic diagram of Knelson concentrator (Coulter and Subasinghe, 2005).

$$F_c = m_s r \omega^2 \tag{5-1}$$

$$F_d = \frac{1}{2} C_D A \rho_f V_f^{\ 2} \tag{5-2}$$

$$F_b \propto d^2, \rho_p, \lambda, \left(\frac{dV}{dy}\right)^2 \tag{5-3}$$

where F_c is the centrifugal force, F_d is the drag force, F_b is the Bagnold force, m_s is the submerged weight of the particle. r is the radius of the trajectory, ω is the angular velocity of the particle, C_D is the drag coefficient, A is the cross-sectional area of a particle. ρ_f and ρ_p are the densities of the fluid and the particle respectively, V_f is the fluid flow velocity of fluidization water, d is the particle diameter, λ is the linear concentration of particles, dV/dy is the velocity gradient.

$$F_c = F_d + F_b \tag{5-4}$$

The minimum requirement for a particle to remain in the concentrate bowl and traverse in a circular path is given in Eq (5-4). The disturbance to the equilibrium results in a net force, either towards the axis or periphery of the Knelson concentrator bowl. The direction of the resultant force of above forces determines the potential of a particle being reported to the concentrate. If the resultant force acting on a particle is directed outwards of the axis of the Knelson concentrator, the particle is more liable to report to the concentrate and if the resultant force is acting towards the axis of the Knelson concentrator particle tend to get fluidized and report to the tailings. Susceptibility of a particle being reported to the concentrate depends on the relative movement of particles due to the resultant force (Burt, 1999; Coulter and Subasinghe, 2005). Forces acting on a particle in an operational Knelson concentrator is given in Figure 5-2

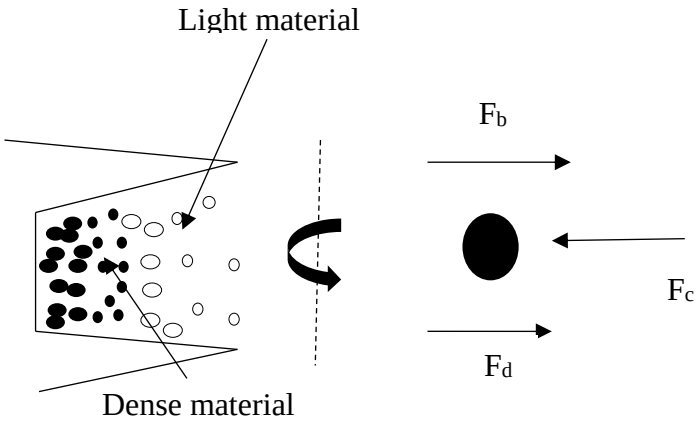

Figure 5-2. Force balance of a particle and accumulation of particles in a groove of a concentrate bowl (adapted from (Coulter and Subasinghe, 2005).

Coulter and Subasinghe (2005) developed a mechanistic model to evaluate the Knelson concentrator performance. In their work, a performance criterion(X) was proposed which is the ratio of the drag force and the resultant force of centrifugal and Bagnold forces. Calculation for X is given in Eqs 5-5 and 5-6.

$$F_c^* = F_c + F_b \tag{5-5}$$

$$X = \frac{F_d}{F_c^*} \tag{5-6}$$

It must be noted that higher X values indicate that forces acting outward from the ribs of the concentrate bowl are more dominant and particles are more susceptible to be transported to the tailings. In the case of low X values force acting towards the ribs of concentrate bowl are more dominant and particles tend to report to the concentrate. Coulter and Subasinghe (2005) quantified the performance of Knelson concentrator by plotting the recovered volume of material against X value. An example of a performance curve for a laboratory Knelson concentrator is given in Figure 5-3.

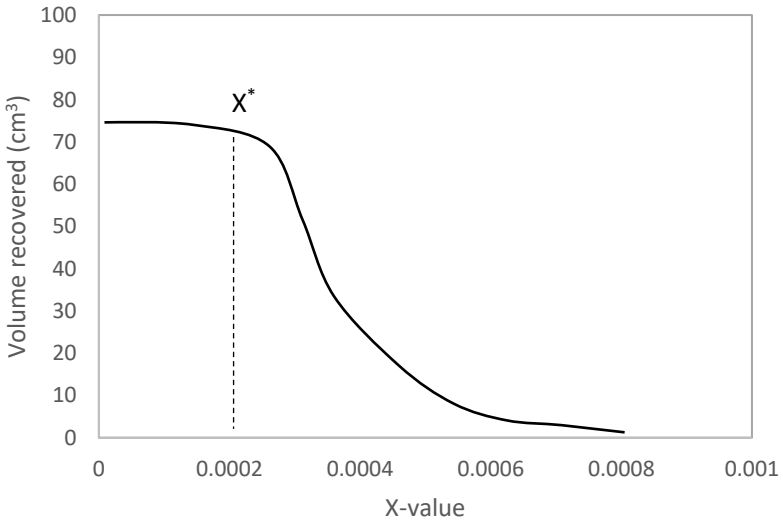

Figure 5-3. An example of a performance curve for a laboratory Knelson concentrator

Coulter and Subasinghe (2005) developed a mechanistic model to evaluate the Knelson concentrator performance. In their work, a performance criterion(X) was proposed which is the ratio of the drag force and the resultant force of centrifugal and Bagnold forces. Calculation for X is given in Eqs 5-5 and 5-6.

$$F_c^* = F_c + F_b \tag{5-5}$$

$$X = \frac{F_d}{F_c^*} \tag{5-6}$$

It must be noted that higher X values indicate that forces acting outward from the ribs of the concentrate bowl are more dominant and particles are more susceptible to be transported to the tailings. In the case of low X values force acting towards the ribs of concentrate bowl are more dominant and particles tend to report to the concentrate. Coulter and Subasinghe (2005) quantified the performance of Knelson concentrator by plotting the recovered volume of material against X value. An example of a performance curve for a laboratory Knelson concentrator is given in Figure 5-3.

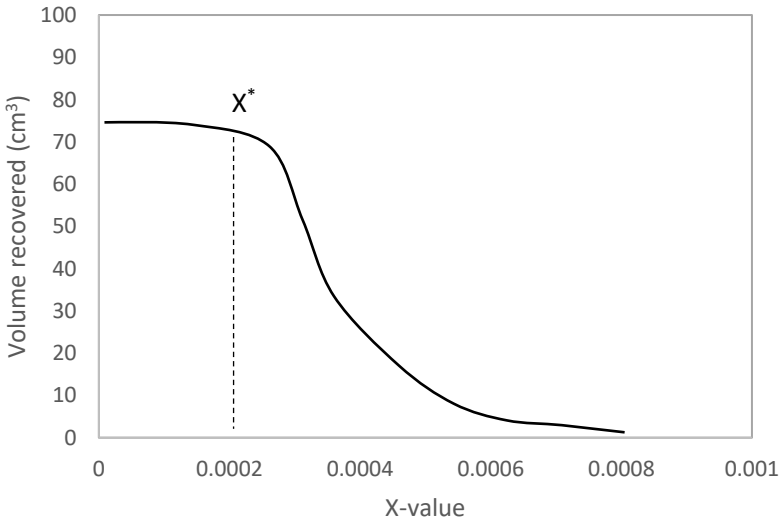

Figure 5-3. An example of a performance curve for a laboratory Knelson concentrator

As shown in Figure 5-3 maximum volume recovery can be obtained when the feed contains with particles with X values smaller than X^* value. In other words, particles

As shown in Figure 5-3 maximum volume recovery can be obtained when the feed contains with particles with X values smaller than X^* value. In other words, particles with X values less than X^* forms a packed bed resulting in higher volume recovery. If the feed contains particles with X values larger than X^* the bed formed inside the concentrator bowl become fluidized resulting in less volume recovery. It must be noted that particles become more susceptible to report to tailings as the X values increase above X^* due to more dominant drag force. X^* can be identified as the transitional X value which demarcates the transformation of bed in the concentrate bowl from packed bed to a fluidized bed (Coulter and Subasinghe, 2005).

5.2 Experimentation

Artificially mixed slurries of clay, magnetite and quartz (1 kg) were fed in to the Knelson concentrator at a solid rate of 200 g/min to evaluate the effect of clays (bentonite or kaolin) on the separation of magnetite. The experiments were conducted for 40% slurry density. The experiments were performed for two particle size ranges which are 0-100µm and 100-300µm and two fluidization water rates (3.5 l/min, 7.5 l/min). Moreover, all experiments were conducted at constant rotational speed (1250 rpm) of the concentrate bowl.

5.3. Results and discussion

5.3.1. Influence of clay on gravity separation using Knelson concentrator.

Gravity separation experiments were conducted to evaluate the influence of commonly encountered clay types (kaolin and bentonite) on the operation of Knelson concentrator. Artificially reconstituted feed slurries of magnetite and quartz with different concentrations of clay were used for the experiments. Clay concentration, feed particle size and the fluidization water flow rate were the operating variables considered. The volume of the recovered material and the magnetite recovery were considered as the response variables. Experimental design and the results are given in Table 5-1.

Table 5-1. Gravity experiments and results

Test No	Clay type	Clay con (%)	Fluidizing water flow rate(l/min)	Feed Particle size P80(μm)	Volume of concentrate(cm^3)	Magnetite recovery (%)
1	Bentonite	0	3.5	42.7	20.95	19.5
2	Bentonite	5	3.5	42.7	23.03	21.6
3	Bentonite	10	3.5	42.7	22.46	19.5
4	Bentonite	15	3.5	42.7	19.85	14.3
5	Bentonite	0	7.5	42.7	16.19	12.2
6	Bentonite	5	7.5	42.7	16.58	12.1
7	Bentonite	10	7.5	42.7	15.45	11.3
8	Bentonite	15	7.5	42.7	17.00	13.1
9	Bentonite	0	7.5	295	25.74	56.6
10	Bentonite	5	7.5	295	29.99	56.4
11	Bentonite	10	7.5	295	28.79	54.6
12	Bentonite	15	7.5	295	28.19	55.2
13	Bentonite	0	3.5	295	29.55	28.4
14	Bentonite	5	3.5	295	29.26	28
15	Bentonite	10	3.5	295	29.59	24
16	Bentonite	15	3.5	295	28.82	31.4
17	Kaolinite	0	3.5	42.7	20.95	19.5
18	Kaolinite	10	3.5	42.7	21.06	23
19	Kaolinite	15	3.5	42.7	29.36	23.6
20	Kaolinite	0	3.5	295	29.55	28.4
21	Kaolinite	10	3.5	295	31.10	29.2
22	Kaolinite	15	3.5	295	37.32	25.8
23	Kaolinite	0	7.5	42.7	16.19	12.2
24	Kaolinite	10	7.5	42.7	6.89	12.2
25	Kaolinite	15	7.5	42.7	10.78	13
26	Kaolinite	0	7.5	295	25.74	56.6
27	Kaolinite	10	7.5	295	27.65	64.8
28	Kaolinite	15	7.5	295	27.15	68

ANOVA analysis was performed on the response variables to identify the operating variables that influence significantly on the operation of Knelson concentrator. ANOVA tables for the recovered volume of solids and magnetite recovery are given in Table 5-2 and Table 5-3. A variable is considered significant if the p-value is less than 0.05

Table 5-2. ANOVA analysis of recovered solid volume

Source	DF	Adj SS	Adj MS	F-Value	P-Value
Clay con (%)	3	21.94	7.314	1.02	0.407
Fluidizing water flow rate	1	261.79	261.793	36.63	0.000
feed Particle size	1	831.08	831.080	116.27	0.000
Clay type	1	0.05	0.054	0.01	0.932
Fluidizing water flow rate*feed Particle size	1	50.21	50.205	7.02	0.017
Error	20	121.51	7.148		
Total	27	1318.99			

Table 5-3. ANOVA analysis of magnetite recovery

Source	DF	Adj SS	Adj MS	F-Value	p-Value
Clay con (%)	3	11.77	3.92	0.32	0.809
Fluidizing water flow rate	1	800.41	800.41	65.80	0.000
feed Particle size	1	4414.59	4414.59	362.92	0.000
Clay type	1	54.60	54.60	4.49	0.067
Fluidizing water flow rate*feed Particle size	1	2424.06	2424.06	199.28	0.000
Error	8	97.31	12.16		
Total	27	9004.59			

ANOVA analysis, given in Tables 5-2 and 5-3 indicate that fluidizing water rate and the feed particle size have affected quite significantly on both volumes of the concentrate and the magnetite recovery. In contrast, analysis confirmed that both clay concentration and clay type to be insignificant to the concentrate volume and the magnetite recovery. Influence of significant variables can be quantified by the mean analysis given in Table 5-4.

Table 5-4. Grouping Information Using the Tukey Method and 95% Confidence.

(Fluidization water flow rate, P_{80})	N	Mean volume of concentrate (cm^3)	Mean magnetite recovery (%)
(7.5, 295.0)	7	27.7378	59.5333
(3.5, 295.0)	7	30.8761	27.8833
(3.5, 42.7)	7	22.6541	20.8583
(7.5, 42.7)	7	14.2864	12.3083

Table 5-4 shows that higher fluidization water flowrate (F.W.R) resulted in increased magnetite recovery in the case of coarse particles (P_{80}=295µm) due the higher drag forces on coarse quartz (gangue) particles which reduce the quartz recovery. However, low fluidization water rate resulted in decreasing the magnetite recovery of coarse particles while increasing the total volume of concentrate. This observation was attributed due to the increased Bagnold force on denser material in comparison to their centrifugal forces. It must be noted that coarse quartz particles are subjected to low drag forces under low fluidization water flow rate that enhances their probability to percolate into the concentrate. In other words, coarse quartz particles are subjected to a resultant force acting towards the concentrate bowl (Coulter and Subasinghe, 2005). Also, coarse quartz particles might have got compacted and thus preventing the capture of magnetite particles. Therefore, the transportation of magnetite particles was inhibited due to the filling of grooves of the concentrate bowl with quartz particles.

It is evident that the experimental results of feed slurries comprising fine particles were quite opposite from the results with coarse particles. Lower fluidization water rate resulted in increasing the recovery of fine magnetite particles. In contrast, higher fluidization water rate decreased the fine magnetite recovery due to the high fluid drag that acts outwards the concentrate bowl. It is eminent that selecting optimum operating conditions in the Knelson concentrator to maximise the recovery is challenging since factors such as feed particle distribution, particle density and machine characteristics have to be accounted for.

5.3.2 Performance curve analysis

5.3.2.1. Performance curve for fine particles

Figure 5-5 shows the relationship between mean X-parameter and the recovered magnetite volume under different operating conditions. It is evident that the presence of clay or differences in clay type did not affect the performance curves. Also, it can be seen that (P_{80}= 42.7 µm) the performance curves tend to follow a similar trend regardless of the differences in the fluidizing water rate (F.W.R). The trends of the performance curves have two distinct regimes, the regime at which the volume recovery rapidly increased and the regime at which the volume recovery remain fairly constant with decreasing X value. The transitional points between these regimes can be denoted as X^*as seen in Figure.5-5. Coulter and Subasinghe (2005) described X^* as the boundary X value in which particles transit to packed bed state from fluidized state. In other words, if the feed has X values less than X^*, the maximum recovery of magnetite can be obtained. However, if the feed has X values larger than X^*, the recovered volume decreased. It can be observed that X^* is about 0.00001 for fine magnetite particles. It should be noted that the values showing the minimum in curves are very small values and could be an experimental error.

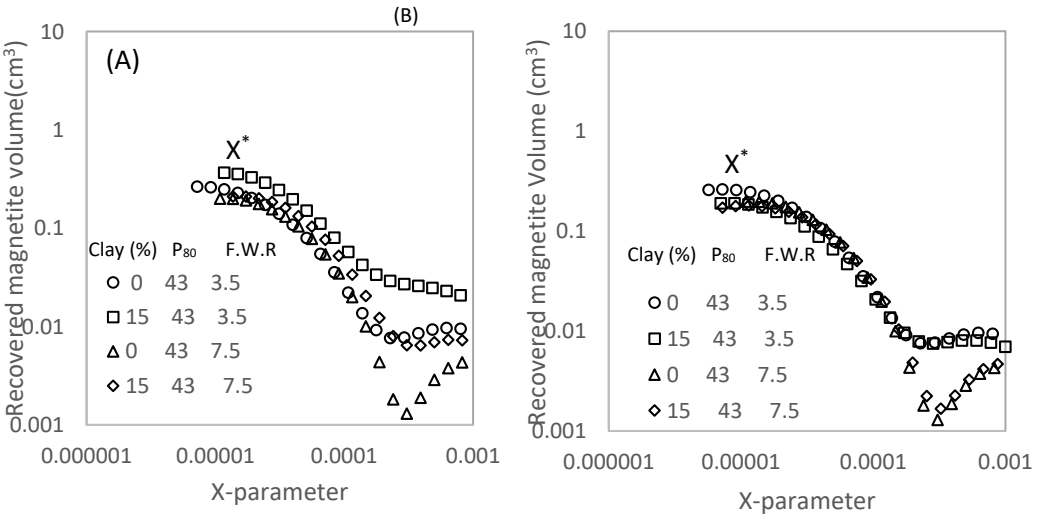

Figure 5-4. Plot of magnetite volume recovered vs X- parameter for mixtures of quartz and magnetite (fine sizes 0-100µm) as a function of percentage of, (A) kaolin (B) bentonite and fluidizing water rate (F.W.R).

Figure.5-5 shows the relationship between the recovered volume of quartz and the X-Parameter for fine particles. It is evident that the three regimes observed in the performance curves of fine magnetite particles can also be identified with fine quartz as seen in Figure 5-5. The X^* is similar to the values observed with fine magnetite particles. Therefore, it can be postulated that X^* is independent of the particle density for fine particles.

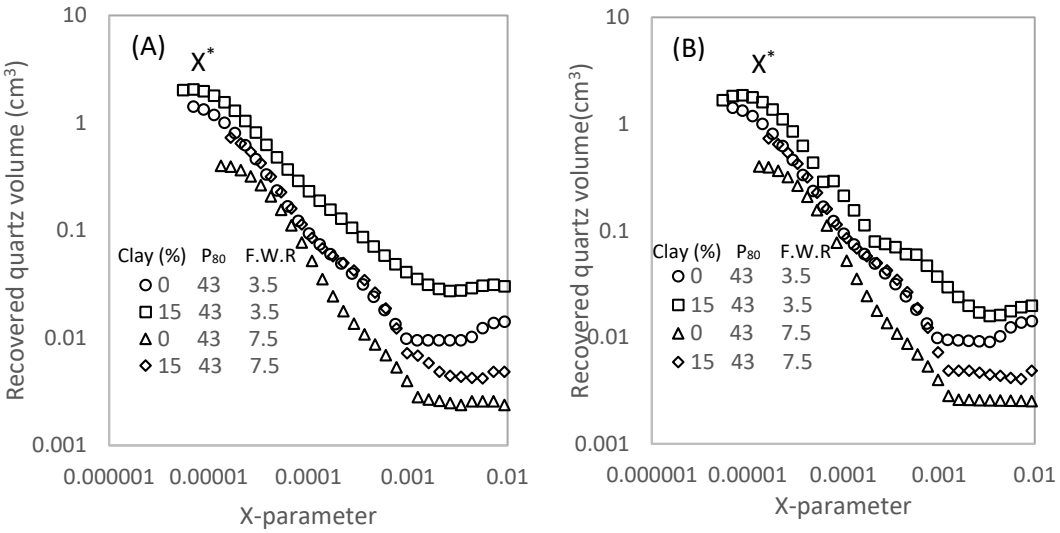

Figure 5-5. Plot of quartz volume recovered vs X- parameter for mixtures of quartz and magnetite (fine sizes 0-100µm) As a function of percentage of, (A) kaolin (B) bentonite and fluidizing water rate (F.W.R).

5.3.2.2 Performance curve of coarse particles

According to the performance curves, X^* for the coarse magnetite particles was about 0.000002 (see Fig.5-6) while that for fine particles was about 0.00001 (see Fig.5-4). Therefore, it can be postulated that the size distribution of the feed influences X^* value. Finer particles are unable to compete with larger particles to enter into the concentrate and thus the increase in particle size resulted in lower X^*. However, the presence of both kaolin and bentonite clays did not affect X^* or the magnetite recovery. The decrease in the fluidization water rate resulted in lower magnetite recovery. This observation could be attributed to the compaction of the bed with coarse quartz particles at low fluidization water rate which might have prevented the transportation of coarse magnetite particles to the concentrate.

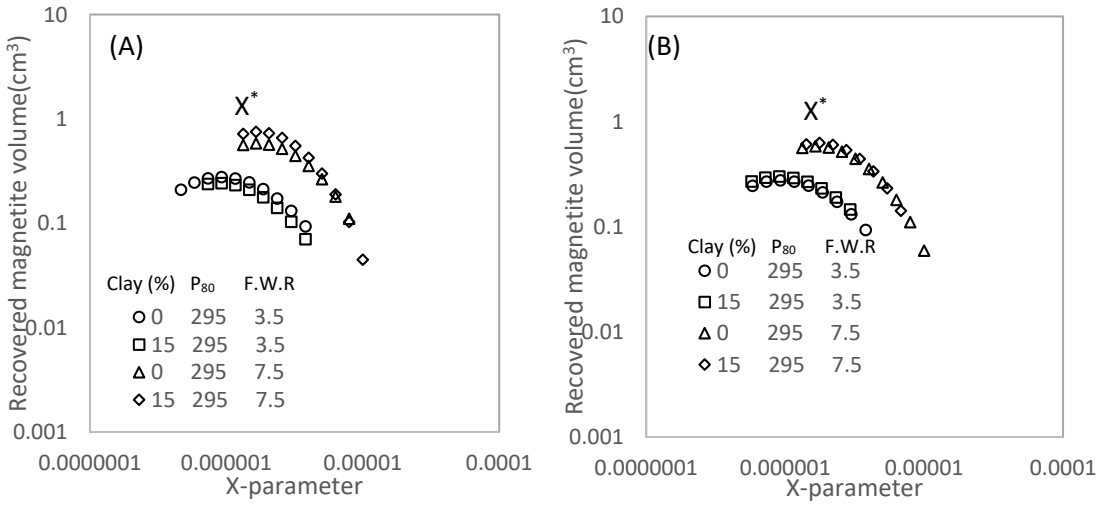

Figure 5-6. Plot of magnetite volume recovered vs X- parameter for mixtures of quartz and magnetite (coarse sizes 100-300µm) as a function of percentage of, (A) kaolin (B) bentonite and fluidizing water rate (F.W.R).

Figure.5-7 shows the relationship between recovered coarse quartz volume and the X-values. Considering that quartz has low density when compared to magnetite, performance curves can be plotted for higher X values. The two regimes discussed in section 5.2.2.1 can also be identified in the performance curves with coarse quartz. As seen in Figure 5-7, X^* is similar to that of coarse magnetite particle.

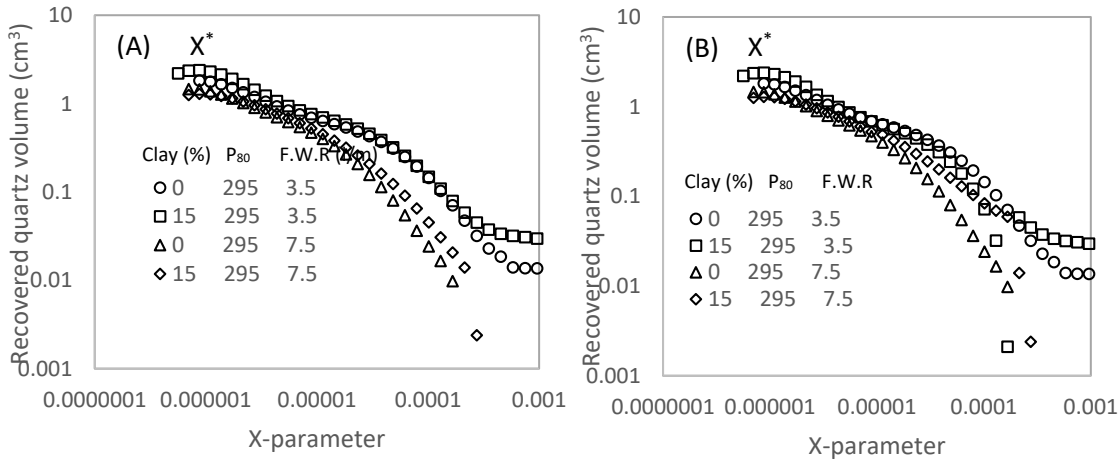

Figure 5-7. Plot of quartz volume recovered vs X- Parameter for mixtures of quartz and magnetite (coarse sizes 100-300µm) As a function of persantage of, (A) kaolin (B) bentonite and fluidizing water rate (F.W.R).

5.3.3 Rheological aspects and the influence of clay in the processing environment

The presence of clay alters the rheological behaviour of processed slurries and adversely affect downstream processes such as flotation, filtration and other processes (Connelly, 2011). However, the statistical analysis indicated that effect of clay on the operation of the Knelson concentrator is negligible. The rheological measurements of the feed slurries are given in Figure 5.8.

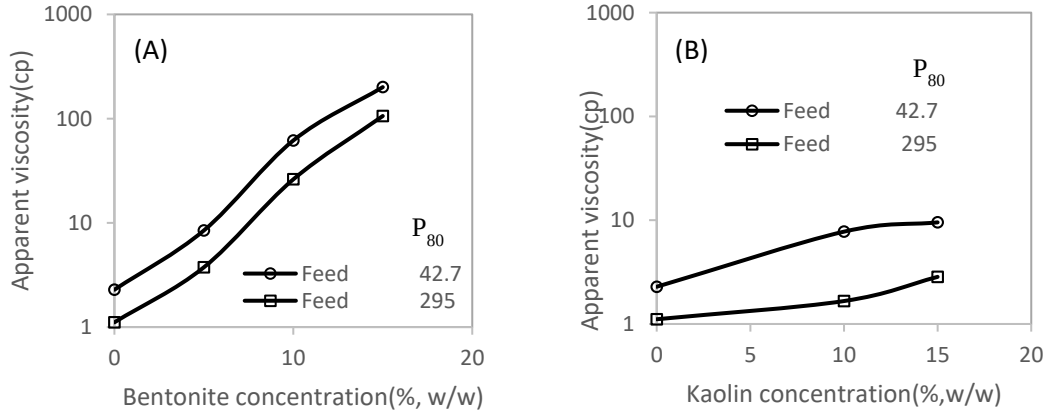

Figure 5-8. Apparent viscosities of feed and processed slurries (A) bentonite (B) kaolin.

Figure 5-8 shows the apparent viscosities of the feed slurry with increasing clay concentrations. As shown in Figure 5-8, the increase in the concentration of both clays resulted in increasing the apparent viscosity of feed slurries in which the effect of bentonite is significantly more dominant. However, the statistical analysis, given in the section 5.3.1, confirmed that both clays did not have a significant influence on the magnetite recovery even in the presence of clays in the feed at concentrations that affect rheological characteristics. That observation can be further justified with the performance curves given in Figure 5-9. It is evident that performance curves were not affected by the addition of both clay types. Considering that clay particles have low density and the high shear environment inside the concentrate bowl, clay particles might get transported to the tailing without entering the concentrated bed inside the concentrate bowl.

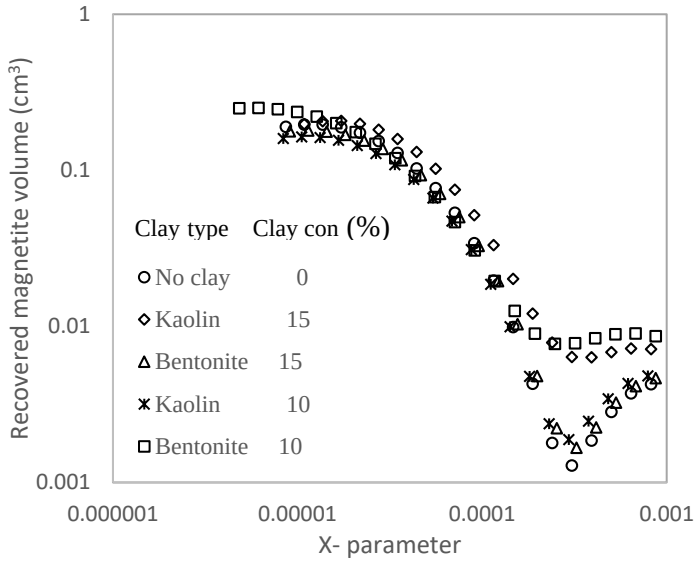

Figure 5-9. The relationship between recovered magnetite volume and X parameter for the experiments with different clay concentrations.

5.4 Summary

This study confirms that the effect of clays on the operation of the Knelson concentrator is not significant at concentrations commonly encountered in the industrial practice. Although the addition of clays increased the apparent viscosity, hydrodynamics in the concentrator bowl was not affected. It must be noted that the feed size distribution and the fluidization water rate influenced significantly the performance of the Knelson concentrator. Selection of the optimum fluidization water rate is of significant importance to enhance the performance of the Knelson concentrator. Identification of the transitional X-values in which packed bed transform to a fluidised bed, can be used to optimise the magnetite mineral recovery of specific Knelson concentrator by varying operating conditions.

Chapter 6 Influence of hydrophobicity and clays on the fine particle filtration

6.0 Introduction

Filtration is commonly used in the mineral processing industry as a separation technique to remove water from the solid material. While the higher rate of filtration is of large importance, it is also beneficial to reduce the moisture content of the resulting cake to reduce the cost of transportation and storage of solids. Moreover, the improved filtration performance is quite important in recycling water for various unit operations due to the scarcity of water. Filtration performance is generally evaluated by the filtration rate and the moisture content of filter cake which are reliant on the specific cake resistance which in turn depend on numerous factors such as mineralogy, particle size, size distribution, particle shape and chemical environment (Besra et al, 1999).

The presence of fine particles significantly reduces the filtration efficiency because fine particles reduce the effective capillary diameter of flow channels formed during the formation of the filter cake. It has been observed that in the presence of a high percentage of fine particles, the moisture content of filter cake increases while the filtration rate decreases. Studies have shown that changing the chemical environment by the addition of flocculants and surfactants can improve the filtration performance of fine particles (Sastry et al, 1983). However, the mechanisms by which this improvement occurs has not been identified or explained in the context of fluid flow dynamics.

It has been observed that the filtration rate can be improved by making the flow channels of the filter cake less resistant to the liquid flow. Studies have revealed that hydrophobicity of the solid surfaces significantly affect the liquid flow profile and the more hydrophobic the solid surface is the lower the resistance to the fluid flow. Measurements made of the slip at the solid surface has been shown to depend on the nature of the flow (laminar or turbulent) and the shear experienced at the superhydrophobic surfaces at the micro and nanometer scale (Maali and Bhushan, 2012). Pan et al et al. (2016) measured the slip in capillary flow due to changes in surface hydrophobicity and incorporated it in modelling filtration of clay suspensions.

The reduction of filtration rates particularly can be exacerbated by the presence of even small quantities of various clays in the slurries. It is well known that the presence of clays increases viscosity of slurries which in turn affect the rheological characteristics and adversely affect various ore preparation and downstream separation processes such as flotation, crushing (Connelly, 2011), dewatering (Kozicki et al, 1968; Mpofu et al, 2005) and etc. Therefore, this chapter is mainly focused on investigating the effects of kaolin and bentonite clays on the filtration of pyritic gold ore and how to improve the filtration performance of clay containing ore mitigating the adverse effects of clay. Furthermore, the influence of hydrophobicity on filtration was quantified in the presence and absence of clays.

6.1 Filtration Modelling

A filtration model can be developed using first principles by modelling of liquid flow through a filter cake (Pan et al, 2016). It has been reported (Pan et al, 2016; Tretheway and Meinhart, 2001) that the flow rate of filtrate may be affected by the hydrophobicity of the particle surfaces and enhanced with increasing hydrophobicity. It may be postulated that when the surface of particles is covered partially by adsorbed molecules of hydrocarbon chains, the resistance to the flow of water is less than when the surface is wetted by water. This situation may be construed to be equivalent to the existence of a slip velocity at or near the walls of flow channels (Churaev et al, 1984). In this work, a comparison is made of the filtration models with and without the existence of a slip velocity.

The flow of filtrate takes place through the void spaces between the solid particles in contact with each other. While the flow takes place through capillaries of tortuous nature with varying cross-sections, it may be simplified to take place through a collection of capillaries of uniform cross-sections with effective radius R and length L. The model also assumes that the capillary length is equal to the filter cake thickness.

The simplified Navier-Stokes equation in cylindrical coordinates is used to describe the liquid flow through a single capillary:

$$\frac{\Delta P}{\mu L} = \frac{d^2 v}{dr^2} + \frac{1}{r}\frac{dv}{dr} \qquad (6\text{-}1)$$

where ΔP is the pressure drop, v is the flow velocity of the liquid, μ is the dynamic viscosity of the liquid and r is the radial distance from the centre of the capillary.

The integrations of Eq 6-1 gives:

$$v = \frac{\Delta P r^2}{4\mu L} - C_1 \ln r + C_2 \qquad (6\text{-}2)$$

where C_1 and C_2 are the constants of integration that can be determined from boundary conditions. Figure 6-1 shows the velocity profiles under non-slip and slip boundary conditions.

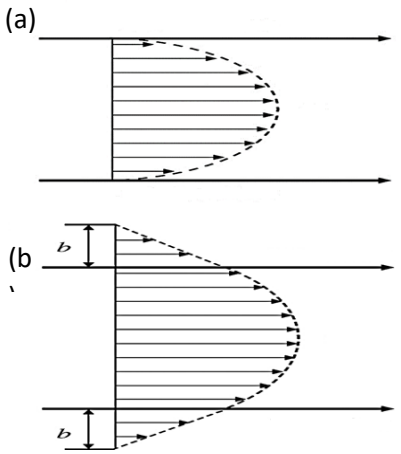

Figure 6- 1. Flow velocity profiles (a) under non-slip boundary conditions (b) under slip boundary conditions

Under non-slip boundary conditions, where the flow velocity at the particle surface is zero, parabolic flow velocity profile may be described by the Eq.6-3.

$$v = \frac{\Delta P(R^2 - r^2)}{4\mu L} \qquad (6\text{-}3)$$

Under the slip boundary conditions, Mooney (1931) has shown that a non-zero velocity exists at the walls of a flow channel. The slip velocity may be quantified by assuming that the velocity profile extends beyond the surface of the solid to a distance *b* known as the *slip length* as shown in Figure 6-1b (Neto et al, 2005). It is also

assumed that the velocity gradient at the surface extends linearly up to the slip length. Thus, the slip velocity may be calculated by multiplying the velocity gradient at the wall with the slip length.

Thus, the slip velocity may be calculated by multiplying the velocity gradient at the wall with the slip length:

$$v_{slip} = \frac{\Delta P R b}{2\mu L} \tag{6-4}$$

where b is the slip length.

Combining Eqs (6-3) and (6-4), the velocity profile in the presence of slip can be:

$$v = \frac{\Delta P(R^2 - r^2)}{4\mu L} + \frac{\Delta P}{\mu L}\left(\frac{Rb}{2}\right) \text{(Pan et al, 2016)} \tag{6-5}$$

Integration of Eq (6-5) across the cross-sectional area of the capillary gives the volume flow rate of liquid through the capillary:

$$Q = \frac{dV}{dt} = \frac{\pi \Delta P}{\mu L}\left[\frac{R^4}{8} + \frac{bR^3}{2}\right] \tag{6-6}$$

where Q is the volume flow rate of the filtrate, V is the filtrate volume.
The thickness of the filter cake (L) can be determined using the mass balance on the solids deposited:

$$L = \frac{wV}{A(1-\varepsilon)} \tag{6-7}$$

A is the cross-sectional area of the filter cake, w is the volume of solids deposited by the passage of a unit volume of filtrate, ε is the filter cake porosity.

Combining Eqs (6-6) and (6-7) to determine ΔP_c i.e. the pressure drop across the filter cake:

$$\Delta P = \frac{8\mu w V}{R^2 A^2 \varepsilon (1-\varepsilon)(1+4b/R)} \frac{dV}{dt} = \Delta P_c \tag{6-8}$$

The pressure drop across the filter medium can be determined using Darcy's law (Ruth, 1935):

$$\Delta P_m = \mu r_m \frac{1}{A}\frac{dV}{dt} \tag{6-9}$$

where the filter medium resistance is r_m. The overall pressure drop can be determined by summing the pressure drop across the filter cake and the pressure drop across the filter medium:

$$\Delta P = \left[\frac{8\mu w V}{R^2 A^2 \varepsilon(1-\varepsilon)(1+4b/R)} + \frac{\mu r_m}{A} \right] \frac{dV}{dt} \tag{6-10}$$

Eq 6-10 can be rearranged to determine the filtration rate.

$$\frac{dV}{dt} = \frac{\Delta P A^2}{\mu\left(\frac{8wV}{R^2 \varepsilon(1-\varepsilon)(1+4b/R)} + A r_m \right)} \tag{6-11}$$

Eq.6-11 shows that the higher the slip length, the higher is the filtration rate. The slip length can be improved by adding the hydrophobic reagent which results in increasing the filtration rate. It should be noted the slip length is zero in the absence of hydrophobic reagents because the slippage does not occur at the liquid-solid interface encountered in the case of hydrophilic solids (Joseph and Tabeling, 2005; Pan et al, 2016).

Eq. 6-11 may be transformed to the well-known filtration model (McCabe et al., 2004) in terms of specific cake resistance, r_c:

$$\frac{dV}{dt} = \frac{\Delta P A^2}{\mu\left(r_c w V + A r_m\right)} \tag{6-12}$$

where $r_c = 8/(R^2 \varepsilon(1-\varepsilon)(1+4b/R))$ (6-13)

which reduces to $r_c = 8/(R^2 \varepsilon(1-\varepsilon))$ in the absence of slip. (6-14)

The differential equation, given in Eq. 6-12 can be solved in the following manner

$$\int \frac{\mu r_c w V}{A^2} dV + \int \frac{\mu r_m}{A} dV = \int \Delta P dt$$

$$\frac{\mu r_c w V^2}{2A^2} + \frac{\mu r_m V}{A} = \Delta P t$$

$$\frac{t}{V/A} = \frac{\mu r_c w V}{2\Delta P A} + \frac{\mu r_m}{\Delta P} \qquad (6\text{-}15)$$

Plot of t/ (V/A) versus (V/A) yields a linear relationship from which r_c (specific cake resistance) and r_m (Filter medium resistance) may be calculated from the slope and the intercept, respectively. The slip length may then be calculated from Eq.6-13 based on porosity (ε) and capillary radius (R).

6.2 Experimentation

The pressure filtration experiments were conducted on the artificially mixed slurries of pyritic gold ore and one of the clays (kaolin or bentonite) in order to identify the effects of bentonite and kaolin clays on filtration. The experiments were performed using a 20 cm diameter cylindrical pressure filter. The slurries were filtered at a constant pressure of 500 kPa and the volume of the filtrate was measured with time for each experiment.

The vacuum filtration experiments were conducted to identify the effects of hydrophobic reagents (DAH) on the filtration of pyritic gold ore in the absence and presence of bentonite and kaolin. The experiments were performed using a constant vacuum pressure of 71 kPa. All the filtration experiments were conducted using Whatman grade 3 qualitative filter papers with a pore size of 6 μm.

6.3 Results and discussion

6.3.1 Influence of clays on fine particle filtration

Batch filtration experiments were conducted using a 500kPa pressure filter to evaluate the influence of clay on the filtration performance. Some representative results of the filtration experiments are shown in Fig. 6-2. As seen in Fig. 6-2, there is a good agreement between the experimental and calculated data using the model given in Eq. 6-15 because R^2 was around 0.98.

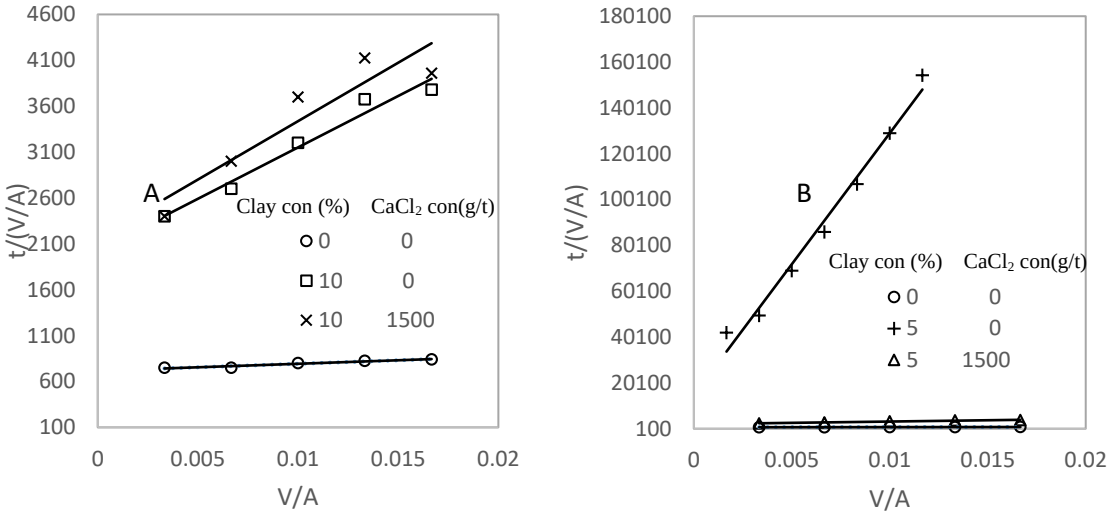

Figure 6-2. Fitting of filtration data to Eq 6-15 for experiments with (A) kaolin and (B) bentonite.

Clay type, clay concentration, particle size, slurry density and the calcium concentration were the independent variables considered in designing the experimental program as seen in Table 6-1. Specific cake resistance (r_c) and the filter medium resistance (r_m) were computed using the filtration equation given in Eq.6-15. The final moisture content of the cakes was also measured after conducting filtration experiment for five minutes. Table 1 also shows the porosity data for the filter cakes; the porosities of the filter cakes (ε) were calculated using the filtration data:

$$\varepsilon = 1 - \frac{M}{AL\rho_{solid}} \tag{6-16}$$

where M is the mass of the dry filter cake. As seen in Table 6-1, the porosity ranged between 0.34 and 0.42 even though the mean particle size varied from 75 to 300 μm. It means that the particle size did not affect significantly the porosity within the particle 75 to 300 μm size range. This range of porosity is in agreement with the range obtained by Aksu et al (2015) for spherical glass beads.

Table 6-1. Pressure filtration experiments result with the addition of bentonite and kaolin clays

Clay type	Clay con (%)	P_{80}	Ca^{2+} con (g/t)	Slurry density (%)	Specific cake resistance×10^{13} (m^{-2})	Filter cake porosity	Filter medium resistance×10^{13} (m^{-1})	Final moisture content (%)
Kaolin	0	150	0	40	0.93	0.37	0.03	15.74
Kaolin	10	150	0	60	4.34	0.38	0.27	12.58
Kaolin	0	300	0	60	1.62	0.38	0.02	13.19
Kaolin	10	300	0	40	40.21	0.38	0.12	18.28
Kaolin	0	150	1500	60	1.64	0.39	0.04	13.15
Kaolin	10	150	1500	40	45.74	0.36	0.09	17.41
Kaolin	0	300	1500	40	1.87	0.35	0.02	10.79
Kaolin	10	300	1500	60	9.54	0.39	0.29	14.70
Kaolin	0	75	0	40	0.89	0.37	0.02	10.96
Kaolin	10	75	0	40	12.27	0.37	0.07	22.15
Kaolin	0	75	0	60	1.86	0.38	0.03	13.32
Kaolin	10	75	0	60	4.69	0.42	1.87	25.00
Kaolin	0	75	1500	40	1.47	0.36	0.00	11.07
Kaolin	10	75	1500	40	13.65	0.34	0.07	24.50
Kaolin	0	75	1500	60	1.68	0.38	0.03	10.89
Kaolin	10	75	1500	60	22.77	0.41	0.18	26.14
Bentonite	0	150	0	40	0.93	0.37	0.03	15.74
Bentonite	5	150	0	60	268.00	0.41	11.90	41.40
Bentonite	0	300	0	60	1.62	0.38	0.02	13.19
Bentonite	5	300	0	40	2270.00	0.39	8.40	76.70
Bentonite	0	150	1500	60	1.64	0.39	0.04	13.15
Bentonite	5	150	1500	40	18.60	0.36	0.04	19.60
Bentonite	0	300	1500	40	1.87	0.35	0.02	10.79
Bentonite	5	300	1500	60	16.50	0.40	0.19	15.25
Bentonite	0	75	0	40	0.89	0.37	0.02	10.96
Bentonite	5	75	0	40	824.00	0.38	0.57	64.24
Bentonite	0	75	0	60	1.86	0.38	0.03	13.32
Bentonite	5	75	0	60	697.00	0.42	0.91	44.35
Bentonite	0	75	1500	40	1.47	0.36	0.00	11.07
Bentonite	5	75	1500	40	14.00	0.35	0.08	24.08
Bentonite	0	75	1500	60	1.68	0.38	0.03	10.89
Bentonite	5	75	1500	60	8.32	0.40	0.19	15.74

ANOVA analysis were performed to identify the significance of operating variables on the filtration performance. A variable can be considered significant if the p-value is less than 0.05. The significance of the variables was further quantified by the mean analysis. ANOVA analysis of the specific cake resistance is given in Table 6-2.

Table 6-2**.** ANOVA analysis for specific cake resistance

Source	DF	Adj SS	Adj MS	F-value	p-value
Clay type	1	1397163	1397163	15.67	0.001
Clay con (%)	1	845698	845698	9.49	0.005
P_{80} size	1	165559	165559	1.86	0.187
Ca^{2+} Con(g/t)	1	1364632	1364632	15.31	0.001
Slurry density (%)	1	120583	120583	1.35	0.257
2-Way Interactions	3	2282928	760976	8.54	0.001
Clay type×Clay con (%)	1	839208	839208	9.41	0.006
Clay type×Ca^{2+} Con (g/t)	1	1302141	1302141	14.61	0.001
Clay con(%)×Ca^{2+} Con (g/t)	1	820772	820772	9.21	0.006
3-Way Interactions	1	782133	782133	8.77	0.007
Clay type×Clay con(%)×Ca^{2+} Con(g/t)	1	782133	782133	8.77	0.007
Error	22	1961441	89156		
Total	31	5833443			

According to the ANOVA analysis given in Table.6-2, specific cake resistance is significantly affected by the clay type, clay concentration and Ca^{2+} concentration while other operating variables were insignificant. Furthermore, the analysis illustrated that two and three-way interaction terms of the significant variables are also significant. The significance of operating variables can be quantified by the mean analysis given in Table 6-3. It must be noted that both clay types resulted in increasing the specific cake resistance while bentonite clay was more prominent. Observed results are in agreement with the results obtained by Benna et al (2001) where the permeability of filter cake was substantially reduced in the presence of 3% sodium bentonite. The presence of 5% bentonite clay resulted in increasing the filter cake resistance by approximately 100 times than that without clay.

It can be assumed that the presence of bentonite clay interrupts the fluid flow through the pores in the filter cake due to the swelling of bentonite particles. Bentonite particles interlayer spacing have the capacity to swell by twenty times of its original size due to crystalline and osmotic swelling (Luckham and Rossi, 1999). The addition of calcium ions into the processed water prevented specific cake resistance from being increased significantly due to the presence of bentonite clay. Ca^{2+} ions replace the monovalent ions in the interlayer regions of montmorillonite particles thus strengthen the interlayer bonding which prevents the osmotic swelling of clay particles (Cruz et al, 2015c; Luckham and Rossi, 1999). The swelled bentonite particles happened to aggregate to a network structure which is not observed when swelling was suppressed with Ca^{2+} ions (Mcfarlane et al, 2006).

Table 6-3. Tukey mean analysis of specific cake resistance

(Clay type, Clay con(%),Ca^{2+} Con(g/t))	Mean specific cake resistance$\times 10^{-13}$ (m^{-2})
(Kaolin, 0, 0)	11.32
(Bentonite,0,0)	11.32
(Kaolin,10,0)	25.37
(Bentonite,05,0)	1025.65
(Kaolin,0,1500)	11.66
(Bentonite,0,1500)	11.66
(Kaolin,10,1500)	22.92
(Bentonite,05,1500)	24.34

Even though the kaolin clay was observed to be not detrimental as bentonite it should be noted that kaolin clay increased the filter cake resistance slightly from 11.32×10^{13} to 25.37×10^{13} m^{-2}. The increase in specific cake resistance may be attributed to the decreased effective capillary radius of flow channels due to deposition of fine kaolin particles. Kaolin clay particles have the potential to be closely packed because of the platy morphology, anisotropic structure and surface charges of particles which results in increasing the resistance to the fluid flow (Besra et al, 1999). However, the Ca^{2+} ions did not indicate a considerable influence on kaolin-containing ore. ANOVA analysis was also performed on filter medium resistance and the ANOVA analysis is given in Table 6-4.

Table 6-4**.** ANOVA analysis of filter medium resistance

Source	DF	Adj SS	Adj MS	F-value	p-value
Clay type	1	34.871	34.871	8.38	0.008
Clay con (%)	1	28.099	28.099	6.75	0.016
P_{80} size	1	4.654	4.654	1.12	0.302
Ca^{2+} Con(g/t)	1	40.010	40.010	9.61	0.005
Slurry density (%)	1	1.786	1.786	0.43	0.519
2-Way Interactions	3	61.170	20.390	4.90	0.009
Clay type×Clay con (%)	1	20.945	20.945	5.03	0.035
Clay type×Ca^{2+} Con (g/t)	1	35.608	35.608	8.55	0.008
Clay con(%)×Ca^{2+} Con (g/t)	1	23.969	23.969	5.76	0.025
3-Way Interactions	1	21.388	21.388	5.14	0.034
Clay type×Clay con(%)×Ca^{2+} Con(g/t)	1	21.388	21.388	5.14	0.034
Error	22	91.576	4.163		
Total	31	197.377			

According to the ANOVA analysis, given in Table 6-4, clay concentration and the Ca^{2+} concentration are the significantly affecting operating variables on the filter medium resistance. Furthermore, the interaction between significant variables can also be identified as significant. Influence of significant variables is quantified in the mean analysis given in Table 6-5.

Table 6-5. Mean analysis of filter medium resistance

(Clay type, Clay con (%),Ca^{2+} Con(g/t))	Mean filter medium resistance$\times 10^{-13}$(m^{-2})
(Kaolin, 0, 0)	0.18
(Bentonite,0,0)	0.18
(Kaolin,10,0)	0.74
(Bentonite,05,0)	5.61
(Kaolin,0,1500)	0.18
(Bentonite,0,1500)	0.18
(Kaolin,10,1500)	0.63
(Bentonite,05,1500)	0.28

The analysis showed that the presence of 5% bentonite clay resulted in significantly increasing the filter medium resistance. This observation may be attributed to the blinding of apertures of the filter medium by the gelatinous sludge formed by the swelling of bentonite particles due to hydration, similar to that occurred within the filter cake. The addition of Ca^{2+} ions significantly reduced the adverse effects of bentonite clay on filter medium resistance since Ca^{2+} disrupts the formation of gelatinous sludge which blocks the filter medium pores. Also, the effect of kaolin clay on filter medium resistance needs to be considered because the filer medium resistance increased approximately by four times than that without clay. The increase in filter medium resistance in the presence of kaolin occurred because the filter medium pores get blinded with fine kaolin clay particles. Therefore, it may be concluded that the filter medium resistance increased due to the blinding of pores in the presence of clays.

ANOVA analysis was also conducted on the moisture content of the resulting filter cake to identify the significance of operating variables. The analysis revealed that clay type, clay concentration and the Ca^{2+} concentration are significantly affecting the cake moisture content. The significance of the variables can be quantified by the mean analysis given in Table 6-6.

Table 6-6. Mean analysis of filter cake moisture content

(Clay type, Clay con(%),Ca^{2+} Con(g/t))	Mean final filter cake moisture content (%)
(Kaolin,0,0)	13.18
(Bentonite,0,0)	13.18
(Kaolin,10,0)	19.38
(Bentonite,05,0)	56.55
(Kaolin,0,1500)	11.36
(Bentonite,0,1500)	11.36
(Kaolin,10,1500)	19.86
(Bentonite,05,1500)	21.78

The presence of 5% bentonite clay increased the moisture content of the filter cake up to 56.55% from 13.18 % as a result of the retention of water in the interlayers of the bentonite clay particles without being drained. However, the addition of the calcium ions decreased the moisture content of bentonite-containing ore from 56.63% to 21.78%. Ca^{2+} ions replace the interlayer monovalent ions and strengthen the bonding between interlayer cations and clay basal surfaces thus preventing the penetration of water molecules (Assemi et al, 2015). Also, it can be seen that the presence of kaolin clay increased the filter cake moisture content by about 8%. The obtained results confirmed that the presence of clay minerals adversely influenced the filtration performance of pyritic gold ore. In particular, bentonite has the most detrimental effects on the filtration performance. The differences in particle structure and the swelling capacity caused two clay types to influence the filtration performance differently.

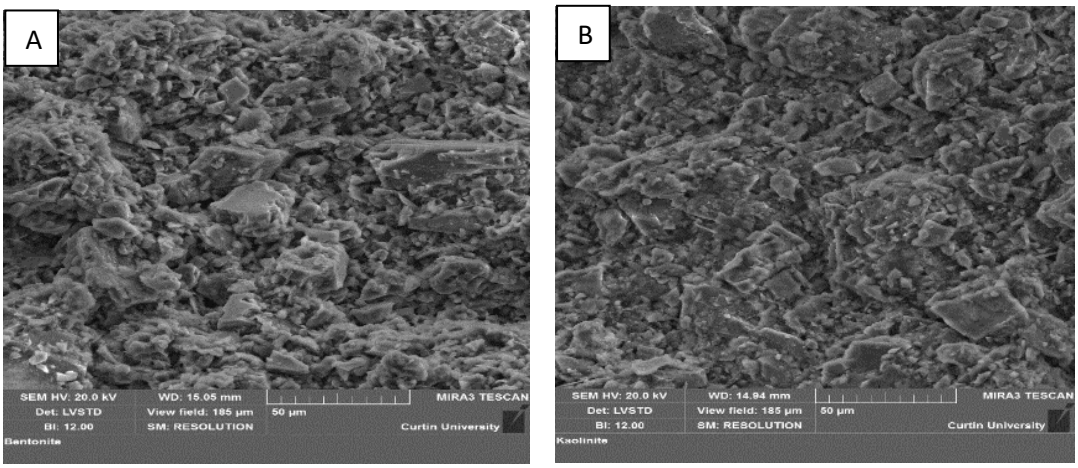

Figure 6-3. SEM images of filter cake surface containing (A) 5 % (w/w) bentonite clay (B) 10%(w/w) kaolin clay.

Figure 6-3 shows the microstructure of the filter cake surfaces containing 5% bentonite and 10% kaolin. It is evident that the packing structure was affected differently by the presence of two clay types. It can be observed that bentonite containing filter cake surface is more uneven than that of kaolin containing filter cake which could be attributed to the swelling of bentonite particles. This observation can be justified by the results obtained in Benna et al (2001), where it was concluded that microstructure of the filter cake changes significantly because of the differences in particle aggregation due to the swelling of sodium bentonite.

6.3.2 Influence of hydrophobicity and particle morphology on the fine particle filtration

Vacuum filtration experiments were conducted on different particle size fractions applying DAH (dodecyl amine hydrochloride) as a hydrophobic reagent. Figure 6-4 shows the measured data of filtration experiments conducted at varying particle size fractions and the DAH concentrations, and the linear trends when plotted according to Eq.6-15. Specific cake resistance can be calculated using the slope and the filter medium resistance from the intercept of the resulting straight lines. Calculated filter cake and filter medium resistances for the factorial experiments at four particle sizes and four DAH concentrations are given in Table 6-7.

Furthermore, Figure 6-4 indicates that the slope of the curves decreases with increasing particle size and it implies that specific cake resistance decreases with increasing particle size. Also, it can be seen that the effect of adding DAH is reflected in changes to the slope and the intercept, particularly in finer particle size fractions. These effects are further discussed and quantified in Section 6.3.2.1.

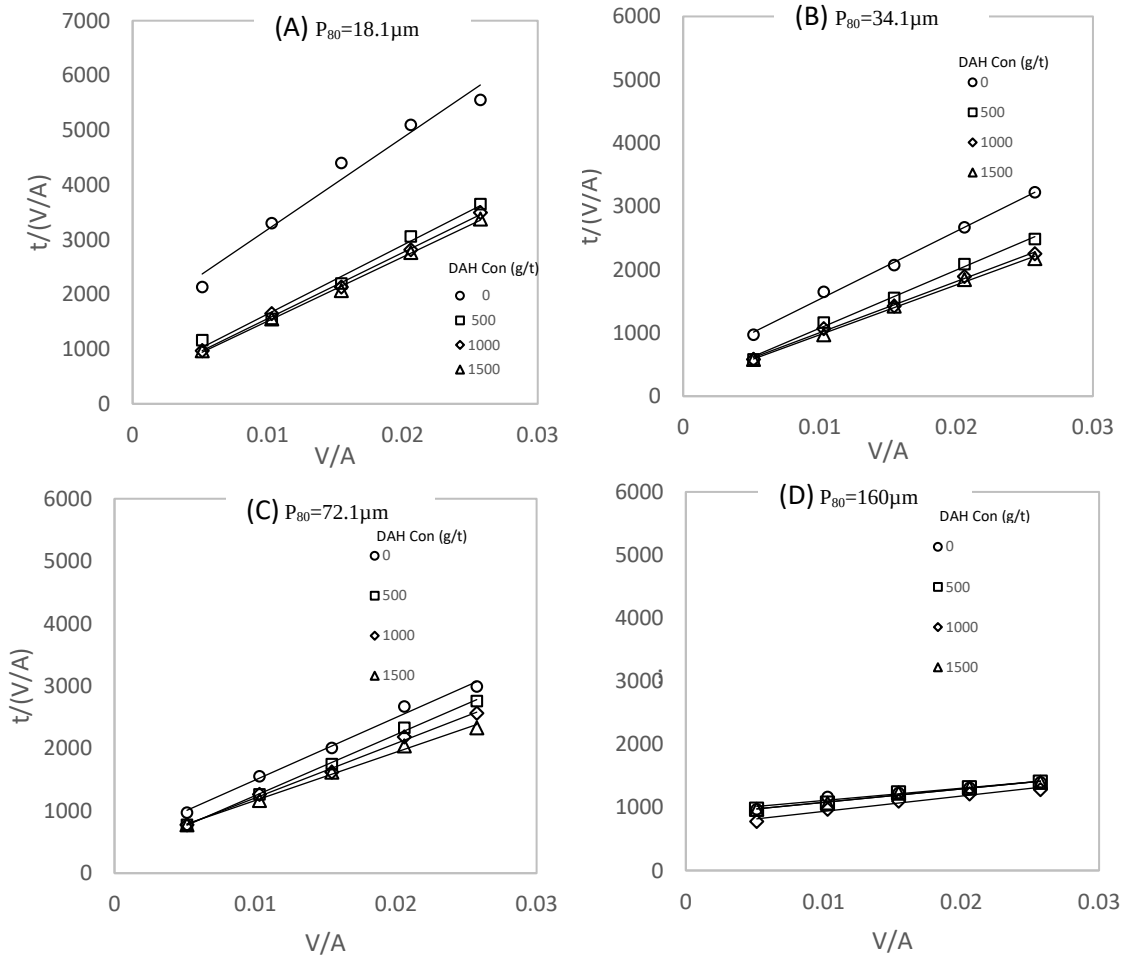

Figure 6-4. The plot of t/ (V/A) versus V/A for different concentrations of DAH

Table 6-7. Vacuum filtration tests with addition of DAH

Test No	P_{80} (μm)	DAH con(g/t)	Specific cake resistance × 10^{-13} (m^{-2})	Filter medium resistance×10^{-10} (m^{-1})	Filter cake porosity	Slip length (nm)	Moisture content (%)
1	18.1	0	6.73	8.25	0.36	0	40.43
2	18.1	500	4.86	1.87	0.34	73.28	39.83
3	18.1	1000	4.65	1.91	0.34	84.48	40.60
4	18.1	1500	4.60	1.86	0.34	86.60	41.50
5	34.1	0	4.16	2.52	0.35	0	34.46
6	34.1	500	3.61	0.85	0.34	36.51	34.10
7	34.1	1000	3.12	1.06	0.34	78.26	35.16
8	34.1	1500	3.07	0.99	0.34	82.26	35.07
9	72.1	0	3.98	2.69	0.35	0	29.74
10	72.1	500	3.87	1.46	0.35	6.56	14.45
11	72.1	1000	3.53	1.82	0.34	31.71	12.67
12	72.1	1500	3.15	2.14	0.35	63.17	12.23
13	160	0	0.77	5.01	0.36	0	25.63
14	160	500	0.83	4.74	0.36	0	12.50
15	160	1000	1.04	3.79	0.36	0	12.00
16	160	1500	0.89	4.74	0.35	0	11.55

6.3.2.1 Influence of particle size on filtration

Figure 6-5 shows the behaviour of the specific cake resistance with different particle size fractions without the addition of any hydrophobic reagent. It is evident that resistance of the filter cake decreased with increasing particle size and the observations may be attributed to the increase in the effective capillary radius with the increasing particle size. The presence of fine particles, particularly those less than about 50 μm substantially increases the specific cake resistance which results in low filtration efficiencies. In processing complex ores, fine feed sizes are common due to small liberation sizes and would benefit from the methods to reduce cake resistance (Wills and Napier-Munn, 2006).

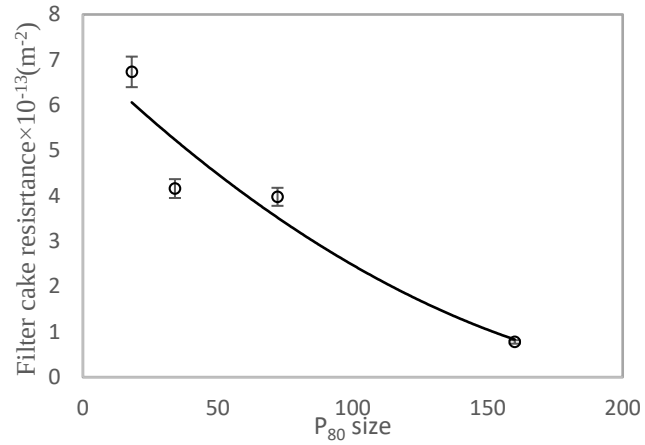

Figure 6-5. Influence of particle size on specific cake resistance

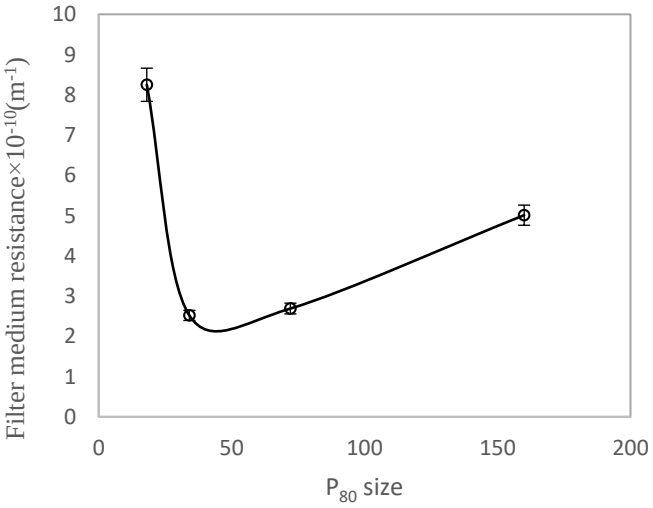

Figure 6-6**.** Influence of particle size on filter medium resistance

Although the medium resistance is expected to be independent of the size of particles being filtered, Figure 6-6 shows that the filter medium resistance initially decreases with decreasing particle size but increases at finer sizes. This could be attributed to the degree of blinding of the medium apertures with particles. Therefore, specific pattern between the particle size and the filter medium resistance is difficult to be established.

6.3.2.2 Influence of hydrophobicity on the filtration of gold pyritic ore

DAH (dodecyl amine hydrochloride) was used to induce hydrophobicity on the particle surfaces in order to study the effect of increasing the hydrophobicity on the surface of particles which would result in reducing the wettability of particle surfaces. It is well known that the contact angle between a silica particle and an air bubble increases with the increase in DAH concentration in flotation studies, demonstrating that the addition of DAH increases the hydrophobicity of silica (Fuerstenau and Jia, 2004).

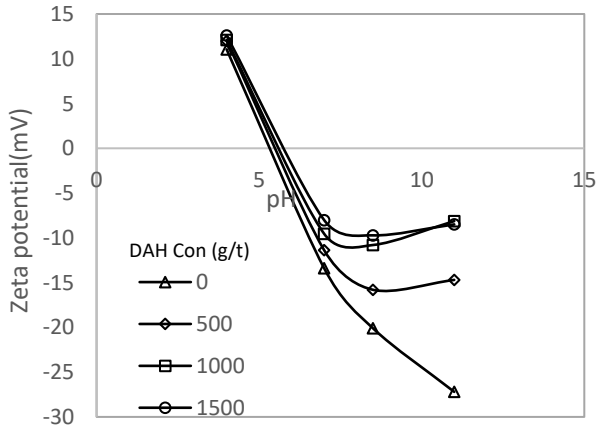

Figure 6-7. Zeta potential of pyritic gold ore particles at different DAH concentrations

Figure 6-7 indicates the changes in zeta potential of fine pyritic gold ore particles at four different concentrations of DAH. It is evident that the zeta potential of the particles become less negative with increasing DAH concentration in the tested pH range (8-8.5). This implies that the positively charged DAH molecules (pKa=-2.08) have been adsorbed on the ore particles and thus induces hydrophobicity on the particle surfaces.

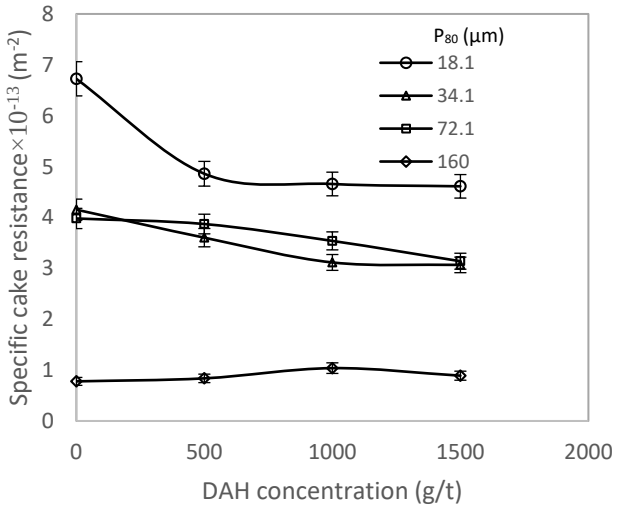

Figure 6-8. The relationship between DAH concentration and the specific cake resistance.

Figure 6-8 shows the influence of the concentration of DAH on the specific cake resistance. It must be noted that specific cake resistance shows a decreasing trend with increasing DAH concentration for all particle sizes tested. It may be construed that there is a considerable effect of reducing the resistance to flow with fine particles where the effective capillaries are small. With larger capillaries this effect is less pronounced as the flow velocities through them are much higher at similar applied pressure differences.

The results of the ANOVA analysis conducted on the filter cake resistance are given in Table 6-8. It shows that the filter cake resistance was more affected by particle size than DAH concentration within the range of concentrations tested. However, Figure 6-8 shows that for fine particles (less than about 30µm) there is a considerable decrease in specific cake resistance due to the addition of DAH.

Table 6-8. ANOVA analysis on filter cake resistance

Source	DF	Adj SS	Adj MS×10^{-27}	F-value	p-value
Particle size (P80)	3	3.852	1.284	54.92	0.000
DAH concentration(g/t)	3	0.220	0.073	3.14	0.080
Error	9	0.210	0.023		
Total	15	4.280			

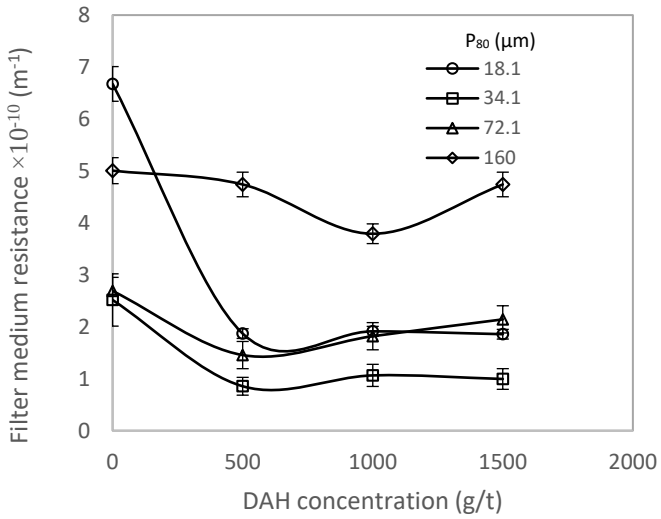

Figure 6-9**.** The relationship between DAH concentration and the filter medium resistance.

Figure 6-9 indicates the behaviour of filter medium resistance with the DAH concentration. A significant decrease in filter medium resistance is observed with the introduction of DAH in the finest particle size fraction (P_{80}=18.1 µm). This observation could be attributed to the aggregation of very fine particles due to the presence of DAH which minimizes the blinding of pores in the filter medium (Hu et al, 2013).

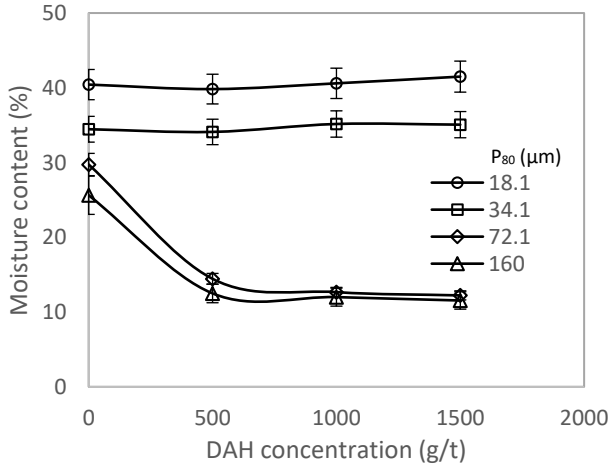

Figure 6-10. The relationship between DAH concentration and moisture content

Figure 6-10 shows the effect of DAH concentration on the final moisture content of the filter cake. It is evident that the increase in DAH concentration resulted in reducing the filter cake moisture content particularly for the particles larger than 34.1 µm (P_{80}>34.1) possibly due to the reduction in surface tension and the capillary pressure.

The surface tension affects more fines than large particles because the capillary diameter of fine particles was much smaller than that of large particles. As a result, the capillary wall effect was more dominant in the case of fine particles. This is important to the mineral industry as large tonnages of concentrates are shipped over long distances and having less water implies increased capacities. ANOVA was also conducted on the filter cake moisture content, and the results are given in Table 6-9. The results showed that the moisture content was more influenced by particle size than DAH concentration since the retention of water in filter cake reduced with increasing particle size due to decreased capillary pressure and surface tension.

Table 6-9**.** ANOVA analysis on filter cake moisture content

Source	DF	Adj SS	Adj MS	F-value	p-value
Particle size (P80)	3	1738.8	579.60	31.02	0.000
DAH Concentration(g/t)	3	140.8	46.93	2.51	0.124
Error	9	168.2	18.69		
Total	15	2047.8			

6.2.2.3 Existence of slip on hydrophobic surfaces

It is evident from Section 3.3 that the presence of hydrophobic reagents decreased the specific cake resistance and increased the fluid flow velocity through capillaries of the filter cake. This phenomenon has been described (Pan et al., 2016) by the existence of slip at the particle surface. Filtration rate incorporating slip may be described by Eq 6-11 in terms of a slip length (b). The slip lengths have been calculated by using the observed filtration data and the methods are described in section 6.3.2.3.1.

6.3.2.3.1 Estimation of slip length

The method used in estimating the slip lengths occurring in the presence of hydrophobic agents using the model given in Eq. 6-11, is described below. It involves the estimation of four parameters: r_c , r_m , ε and R . Filter medium resistance (r_m) and the specific cake resistance (r_c) were determined by plotting filtration experimental data according to Eq. 6-15 using the slope and the intercepts of the linear plots, respectively.

Estimation of mean porosity: Generally, the porosity of filter cakes does not vary considerably as they are fairly densely packed. Researchers have estimated the porosity (ε) of the filter cake by methods based on either a) flow properties such as filtration rate, permeability and cake resistance or b) difference between the wet and dry mass of cake under saturated conditions (Tien et al, 2013). In this work, as the degree of saturation of the cake is unknown at the end of a filtration cycle, the porosity (ε) has been estimated using measured quantities according to the Eq 6-16.

It has been reported that the porosity is slightly higher at the surface of the filter cake and decreases with the depth of the filter cake (Lin and Miller, 2000), particularly with feeds containing a wide particle size distribution. The histogram in Figure 6-11 shows that the measured porosity values vary within a narrow range (0.34 - 0.36) regardless of the differences in particle size with a mean of 0.347 and a standard deviation of 0.006. It is similar to a mean value of 0.35 observed for similarly ground quartz slurry (Aksu et al, 2015). As the porosity is not affected by the presence of a hydrophobic regent the calculations were based on all observations, with and without such a reagent.

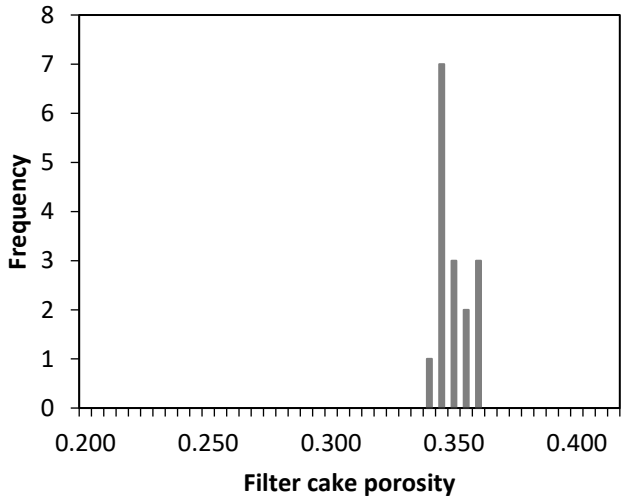

Figure 6-11**.** Histogram of filter cake porosity

Estimation of effective capillary radius: Even though the flow channels in the capillary filtration model are assumed to be rectilinear with an average capillary radius of R , actual flow channels in a packed bed are interconnected pores of tortuous nature (Tien et al, 2013; Neesse et al, 2009). The packing structure of the filter cake depends on the morphology and the size distribution of the particles (Lin and Miller, 2000b). While the

addition of hydrophobic reagents does not have any influence on the packing structure of the filter cake it affects the flow through the cake and in turn the cake resistance. Thus, Eq (6-14) was used to estimate the mean capillary radius based on the measured cake resistances in experiments without the addition of hydrophobic reagents.

Figure 6-11 shows the variation of the calculated average capillary radius with particle size. As expected, it can be seen that the average capillary radius increases with the particle size.

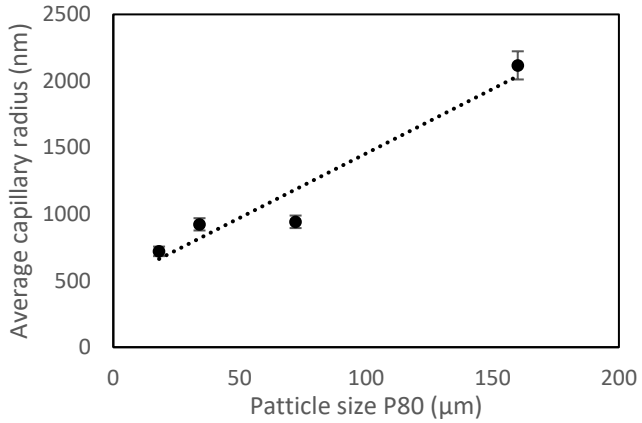

Figure 6-12**.** The relationship between the average capillary radius and particle size

Having estimated the above parameters *R*, ε and r_c, the slip length, *b*, can be estimated using Eq (6-13).

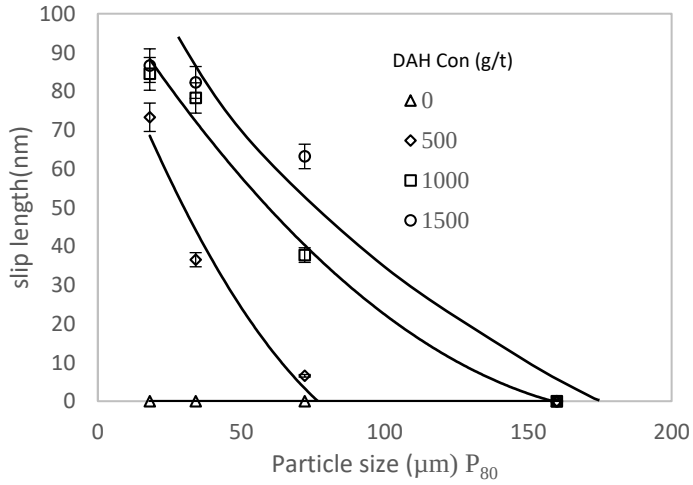

Figure 6-13**.** The relationship between slip length, particle size and the DAH concentration.

Figure 6-13 shows the influence of DAH concentration on the slip length in cakes of different particle size fractions. It can be seen that the increase in the DAH concentration resulted in higher slip length. This suggests that the presence of hydrophobic reagent makes particle surfaces less wettable thereby reducing the resistance to the flow of liquid. Figure 6-19 also shows that the slip length increased more in cakes with finer particle sizes. The influence of particle size on the slip length was the most dominant in the case of the finest size fractions compared to those with larger particles in which the capillary radius is larger and the flow is higher.

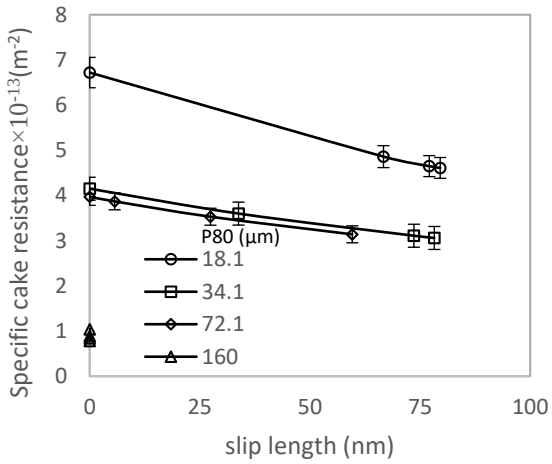

Figure 6-14**.** The relationship between slip length and specific cake resistance.

Figure 6-14 shows that the specific cake resistance decreased linearly with increasing the slip length. This effect is particularly pronounced in the case of the finest size fractions. This implies that the filtration rate of fine particles can be increased by adding hydrophobic reagents to reduce specific cake resistance, particularly in the fine particle filtration.

6.3.3 Influence of hydrophobicity on the filtration of clay containing ore

Previous studies (Pan et al, 2016; Tretheway and Meinhart, 2001) have revealed that the increased hydrophobicity at the boundary surfaces of fluid flow channels has the potential to increase the fluid flow velocity due to the existence of slip at the liquid/solid interface. Also, it can be construed that the fine particle filtration can be improved by increasing the hydrophobicity of particle surfaces according to the results given in the section 6.3.2. Therefore, vacuum filtration experiments were conducted

adding DAH (dodecyl amine hydrochloride) as a hydrophobic reagent to identify the influence of the hydrophobicity on filtration of clay-containing ore.

6.3.3.1. Bentonite-containing ore

Vacuum filtration experiments were performed on artificially mixed slurries of bentonite clay and pyritic gold ore. Table 6-10 shows the used factorial design where the Ca^{2+} concentration and the DAH concentration were the operational variables. Table 6-11 shows the results of the associated ANOVA analysis, performed on specific cake resistance.

Table 6-10**.** Filtration experiments with bentonite and DAH.

Run	Clay con (%)	Ca^{2+}con(g/t)	DAH con (g/t)	Specific cake resistance$\times 10^{-13}$ (m^{-2})	Final Moisture content (%)
1	0	0	0	4.69	35.95
2	10	0	0	539	61.36
3	0	1500	0	4.51	34.14
4	10	1500	0	32	30.90
5	0	0	1000	3.44	20.46
6	10	0	1000	766	50.10
7	0	1500	1000	4.08	21.87
8	10	1500	1000	44	35.35

Table 6-11**.** ANOVA Analysis for specific cake resistance in the bentonite-containing ore.

Source	DF	Adj SS$\times 10^{-30}$	Adj MS$\times 10^{-30}$	F-value	p-value
Clay con	1	23.30	23.30	40.11	0.02
Ca^{2+} conc	1	18.90	18.90	32.53	0.02
DAH con	1	0.70	0.70	1.22	0.38
Error	2	0.73	0.73		
Total	7	63.61			

The ANOVA analysis indicates that the bentonite concentration and the Ca^{2+} concentration significantly affected the specific cake resistance as was observed in section 6.3.1. However, the effect of DAH on specific cake resistance was insignificant. The changes of specific cake resistance with clay concentration and Ca^{2+}

concentration may be quantified by the following regression equation Eq 6-17 with a correlation coefficient of 0.66.

Specific cake resistance= $1.58\times10^{15}+ 3.41\times10^{14}$ Clay con– 2.05×10^{12} Ca^{2+} con (6-17)

(For measurement units refer to Table 6-10.)

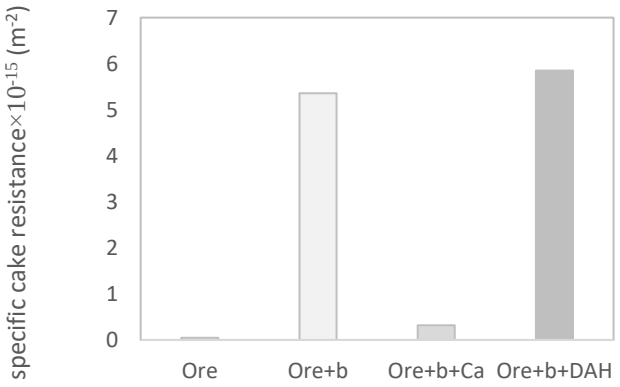

Figure 6-15**.** Influence of bentonite (b), DAH and Ca^{2+} on specific cake resistance.

Figure 6-15 clearly indicates the influence of bentonite, Ca^{2+} concentration and DAH on the specific cake resistance of bentonite-containing ore. The presence of bentonite in gold bearing pyritic ore increased the specific cake resistance quite significantly. The addition of Ca^{2+} ions to the process water of bentonite-containing ore resulted in reducing the increased specific cake resistance due to the presence of bentonite clay, thereby improving the filtration performance. However, the addition of DAH did not affect the specific cake resistance.

Table 6-12**.** ANOVA table for filter cake moisture content of the bentonite-containing ore

Source	DF	Adj SS	Adj MS	F-value	p-value
Clay con	1	516.65	516.65	24.77	0.03
Ca^{2+} con	1	372.78	372.78	17.88	0.05
DAH con	1	158.15	158.15	7.58	0.11
Error	2	41.71	20.85		
Total	7	1369.46			

Table 6-12 shows the results of ANOVA analysis for the moisture content of the filter cake executed to identify which variables are affecting significantly. The analysis revealed that the bentonite concentration and the Ca^{2+} concentration significantly affected the moisture content which agrees with the results in section 6.3.1. The changes of the moisture content with bentonite concentration and Ca^{2+} concentration can be described by the following regression equation with correlation coefficient of 0.65.

$$\text{Moisture content (\%)} = 33.93 + 1.607\ \text{Clay con} - 0.00910\ Ca^{2+}\ \text{con} \quad (6\text{-}18)$$

(For measurement units refer to Table 6-10.)

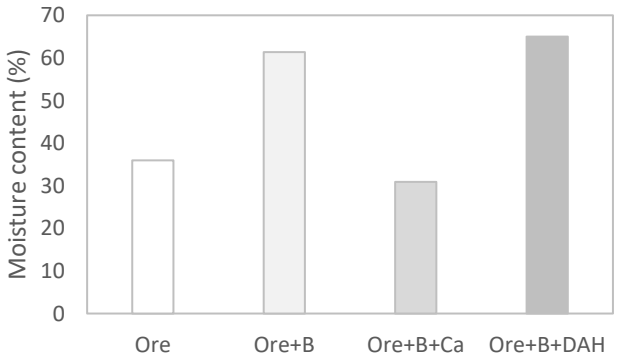

Figure 6-16**.** Influence of bentonite, Ca^{2+} concentration and DAH on moisture content.

Figure 6-16 compares the influence of bentonite, Ca^{2+} concentration and the DAH on the moisture content. The presence of bentonite resulted in increasing the moisture content substantially. The addition of Ca^{2+} ions to bentonite-containing ore reduced the detrimental effect of bentonite on the moisture content. This can be attributed to the reduced swelling capacity of the bentonite particles. Ca^{2+} ions replace the interlayer Na^{+} ions of bentonite particles, creating strong interlayer bonding which restrict the interlayer swelling due to hydration (Assemi et al., 2015; Basnayaka et al., 2017). However, DAH did not indicate any influence to the cake moisture content of the bentonite-containing ore. Furthermore, the ANOVA analysis conducted on the filter

medium resistance showed that the influence of DAH on filter medium resistance was also insignificant.

Figure 6-17 shows the results of the zeta potential measurements at various pH values. The zeta potentials of pure bentonite followed the same trend as those obtained by Mekhamer (2011). As seen in Figure 6-17, DAH may have slightly adsorbed on bentonite because the zeta potential of bentonite in the presence of DAH was slightly lower than that of bentonite in distilled water at the same pH values. On the contrary, Ca^{2+} ions significantly affected the zeta potential of bentonite particles, indicating that Ca^{2+} ions were adsorbed on bentonite particles. It is true that the zeta potential become more positive with increasing in Ca^{2+} concentration. For example, the zeta potential of pure bentonite at pH 10 was -48 mV while that of pure bentonite with Ca^{2+} at the same pH value was -10 mV. The reason is due to the adsorption of Ca^{2+} ions on the bentonite surfaces, reducing its zeta potential.

These results showed that the addition of Ca^{2+} decreased both specific cake resistance and the cake moisture content of the bentonite-containing ore. The results are in agreement with the rheological measurements of pure bentonite slurries shown in Figure 8 and also reveal that the bentonite increases the yield stress of the slurry and thus reduce the flow characteristics. Figure 6-18 also shows that the addition of Ca^{2+} significantly reduced the shear stress of the bentonite slurry due to the reduced swelling properties of bentonite particles. As a result, the specific cake resistance decreased in the case of bentonite-containing ores.

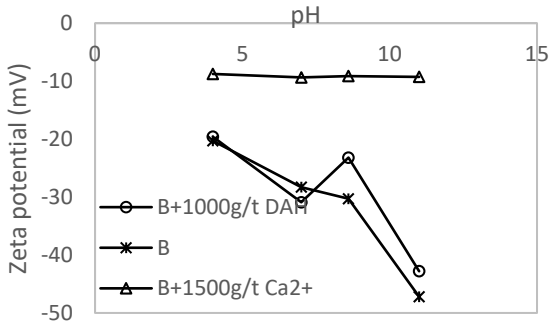

Figure 6-17**.** Zeta-potential measurements of 10% pure bentonite (B) slurry with Ca^{2+} and DAH.

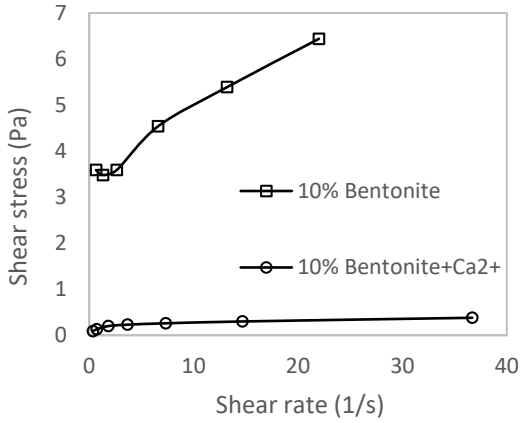

Figure 6-18**.** Rheograms of 10% pure bentonite clay slurries with and without Ca^{2+} ions.

6.3.3.2 Kaolin-containing ores

Similar to the experiments with bentonite, vacuum filtration experiments were performed on the artificially mixed slurries of pyritic gold ore and kaolin clay. Table 6-13 shows the factorial design and the responses of the filtration experiments conducted on ore containing kaolin with DAH.

Table 6-13**.** Filtration experiments with kaolin clay and DAH

Run	Clay con. (%)	Ca^{2+} con. (g/t)	DAH con. (g/t)	Specific cake resistance×10^{-13} (m^{-2})	Final moisture content (%)
1	0	0	0	4.68	30.95
2	10	0	0	8.27	35.70
3	0	1500	0	4.50	30.14
4	10	1500	0	8.16	34.76
5	0	0	1000	3.43	20.46
6	10	0	1000	7.54	22.70
7	0	1500	1000	4.08	21.87
8	10	1500	1000	6.26	22.25

Table 6-14**.** ANOVA analysis for specific cake resistance in kaolin-containing ore

Source	DF	Adj SS×10^{-22}	Adj MS×10^{-22}	F-value	p-value
Clay con	1	228000	228000	88.59	0.00
Ca^{2+} con	1	1000	1000	0.39	0.56
DAH con	1	23000	23000	8.94	0.04
Error	4	0.002	0.0004		
Total	7	0.04			

Table 6-14 shows the results of ANOVA analysis on specific cake resistance to identify which variables affected it significantly. It shows that the kaolin concentration and the DAH concentration significantly affected the specific cake resistance. The changes of specific cake resistance with clay concentration and DAH concentration may be quantified by the following regression equation with a correlation coefficient of 0.95.

$$\text{Specific cake resistance} = 4.71\times10^{13} + 3.38\times10^{12}\text{Clay con} - 1.07\times10^{10}\text{DAH con} \quad (6\text{-}19)$$

(For measurement units refer to Table 6-13.)

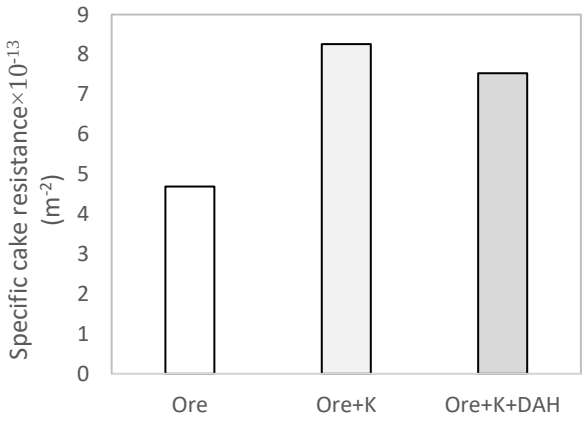

Figure 6-19**.** Influence of kaolin (K) and DAH on specific cake resistance

Figure 6-19 clearly indicates the influence of kaolin and DAH on the specific cake resistance. The presence of 10% kaolin in gold bearing pyritic ore increased the specific cake resistance from 4.68×10^{13} to 8.27×10^{13} m^{-2} and this is in agreement with the observations in section 6.3.1. The addition of DAH to kaolin-containing ore resulted in decreasing the specific cake resistance from 8.27×10^{13} to 7.54×10^{13} m^{-2}.

Table 6-15**.** ANOVA analysis for filter cake moisture content of kaolin-containing ore

Source	DF	Adj SS	Adj MS	F-Value	p-value
Clay con	1	17.970	17.970	9.61	0.036
Ca^{2+} con g/t	1	0.078	0.078	0.04	0.848
Amine con	1	244.979	244.979	130.96	0.000
Error	4	7.482	1.871		
Total	7	270.510			

Table 6-15 shows the results of ANOVA analysis for the moisture content of the resulting filter cakes to identify the important variables that affect significantly. The analysis revealed that the DAH concentration significantly affected the filter cake moisture content. Ca^{2+} ions did not have significant influence on filter cake moisture content in the presence of kaolin clay. The reason is that Ca^{2+} reduces the swelling of bentonite; however, kaolin is non-swelling clay and thus Ca^{2+} did not have any effect on filtration of kaolin-containing ore. The changes of cake moisture content with DAH concentration and kaolin concentration may be quantified by the following regression equation with a correlation coefficient of 0.97.

Moisture content (%) = 31.389 - 0.01107 DAH con + 0.2997 Kaolin con (6-20)

(For measurement units refer to Table 6-13.)

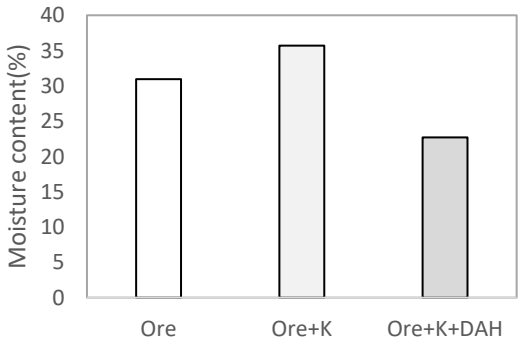

Figure 6-20**.** Influence of kaolin (K) and DAH on moisture content

Figure 6-20 shows the influence of kaolin and DAH on the moisture content. As seen in Figure 6-20, the addition of DAH reduced the cake moisture content of kaolin-containing ore considerably from 33.7 to 22.7 %. The moisture content was reduced in the presence of DAH probably because the addition of DAH makes surfaces of kaolin particles hydrophobic (Pan et al, 2016) and thus repels water from kaolin surfaces. A similar statistical analysis was conducted on filter medium resistance and it revealed that DAH concentration does not have a considerable influence on filter medium resistance.

These results show that the addition of DAH decreased both specific cake resistance and the moisture content of kaolin-containing ore. This may be attributed to either an increase of flow velocity due to lowering of the slurry viscosity or the existence of slip at the particle surface due to adsorption of hydrophobic reagent. In order to better understand the underlying mechanism, the zeta potential of pure kaolin slurries was studied under similar chemical environments. Figure 6-21 shows that the zeta potential of kaolin particles became less negative in the presence of DAH, demonstrating that DAH molecules were adsorbed on kaolin particle surfaces thereby making the surface charge of particles less negative even at higher pH values. Thus, the increased filtration rates could be attributed to the existence of slip at the particle/water interphase due to the adsorption of DAH molecules. Adsorption of DAH on kaolin was more prominent than in bentonite due to the larger aspect ratio and the non swelling proprty of kaolin particles. The addition of DAH did not alter the rheological properties of kaolin slurry, particularly at low shear rates as seen in Figure 6-22. The difference observed in the rheograms at the high shear rate is insignificant when compared with the differences observed with bentonite slurries.

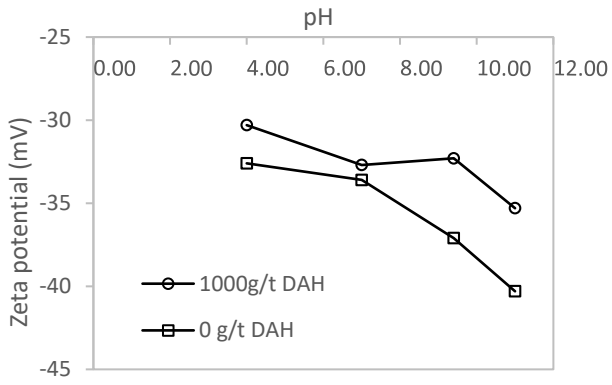

Figure 6-21**.** Zeta potential measurement of kaolin at different pH values with out and with DAH

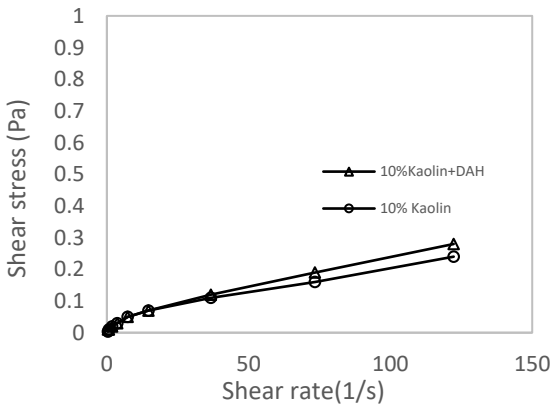

Figure 6-22**.** Rheograms of 10% kaolin slurries with and without DAH

6.4 Summary

The results of this study confirmed that the presence of clay minerals inhibit the filtration performance by reducing the rate of filtration particularly in the case of swelling bentonite clay. Bentonite clays reduced the filtration performance by both increasing the specific cake resistance and the final moisture content of filter cake quite significantly while the effect of kaolin clay on specific cake resistance and final was less pronounced. The addition of Ca^{2+} ions decreased both filter cake resistance and the moisture content of the bentonite containing filter cake due to lowered swelling capacity. However, kaolin containing ore was not affected by the addition of Ca^{2+} ions.

Also, this study was focused on investigating the influence of hydrophobicity on filtration performance. Filtration performance was quantified using a capillary

filtration model both in presence and absence of a hydrophobic reagents. It was revealed that the filtration efficiency of fine particles can be improved by the addition of an adequate hydrophobic reagent (DAH). Walls of the flow channels became hydrophobic due to the adsorption of the hydrophobic reagents (DAH) on the particle surfaces thereby imposing slip velocity to the fluid flow. This results in increasing the rate of filtration particularly in fine particles. Furthermore, the addition of a hydrophobic reagent improved the filtration performance of kaolin clay containing ore. However, bentonite containing ore was not affected by the addition of the hydrophobic reagent (DAH).

Chapter 7 Conclusions and recommendations

This chapter summarises the conclusions and the recommendations for the future work.

7.0 Conclusions

In this study, the effects of clays were investigated on three important techniques used in mineral beneficiation, namely, froth flotation, enhanced gravity separation and filtration. It was aimed at verifying, quantifying and investigating possible mechanisms of the adverse effects known to occur due to presence of clay and identify methods of mitigating such effects.

Flotation: Investigated the influence of kaolin and bentonite clay on flotation performance of a typical pyritic gold ore. The results obtained in this work indicated that the flotation performance can be significantly affected by the available clay type and its concentration. More specifically, the sulphide mineral recovery was significantly reduced due to the modification of slurry rheology in the presence of bentonite clay more than that of kaolin clay. Therefore, it can be concluded that swelling type clays are more detrimental to the flotation performance. The addition of Ca^{2+} ions to the processed water improved the flotation recovery of pyritic gold ore by reducing the adverse effects of bentonite clay. More precisely, Ca^{2+} ions reduced the swelling capacity of bentonite clays and thus minimizing the rheological influence. It is evident that the changing chemical environment can reduce the adverse effects of clay minerals on flotation. Flotation performance characteristics such as the ultimate recovery showed a strong correlation with the rheological parameters such as flow index and consistency index. The presence of both clay types reduced the maximum froth height which may be resulted due to the reduced number of larger bubbles. However, a direct relation to the flotation recoveries and the froth stability was not observed in the presence of clay. Measurements of rheological properties and evaluating their correlations with flotation parameters can be applied to routinely monitor the flotation performance in operating plants when processing ores with substantial amounts of clay. It should be noted that apart from rheology, other effects such as slime coating and entrainment might have also influenced flotation; however, these effects were not studied in this thesis.

Enhanced gravity concentration: The influence of kaolin and bentonite clays on the centrifugal separation of magnetite from quartz using was investigated. It was found that the addition of both clays did not have significant influence on the separation efficiencies. Although the addition of bentonite clay enhanced the apparent viscosity of the feed slurry quite significantly, the hydrodynamics in the concentrator bowl was not affected due to the dilution of feed slurry by the fluidizing water. It must be noted that feed size distribution and the fluidization water rate influenced significantly the performance of the centrifugal separator. The optimum fluidization water rate is very important for enhancing the performance of the centrifugal separator. Identification of the transitional X-values (X^*) where bed inside the concentrator bowl transforms from packed bed state to fluidized bed , can be used to optimise the gold recovery of specific Knelson concentrator by varying operating conditions.

Filtration: The influence of kaolin and bentonite clays on the filtration performance was investigated. The addition of both kaolin and bentonite clays reduced the filtration performance by decreasing the rate of filtration and increasing the final moisture content of the filter cake, where bentonite showed the most detrimental effects. Therefore, it can be stated that bentonite clay inhibited the filtration more than kaolin clay. Bentonite clay particles adsorbs the water molecules into the interlayers and thus increasing the particle volume quite significantly. This phenomenon results in blocking the flow channels of the filter cake, resulting in high filter cake resistance as well as higher retained moisture. The addition of Ca^{2+} ions decreased both filter cake resistance and the moisture content of the bentonite containing filter cake due to the decrease in bentonite swelling capacity. However, kaolin-containing ore was not affected by the addition of Ca^{2+} ions. Also, this PhD project was focused on investigating the influence of hydrophobicity on the filtration performance.

Furthermore, the influence of the surface hydrophobicity on the filtration performance was also investigated. It was revealed that the filtration efficiency of fine particles can be improved by the addition of adequate amount of a hydrophobic reagent. The resulting decrease in flow resistance and increase in the filtration rates can be modelled using a capillary filtration model that incorporates a slip velocity at the particle surfaces within the bed due to the enhanced hydrophobicity. This results in increasing the rate of filtration particularly in the case of fine particles. Furthermore, the addition

of hydrophobic reagents improved the filtration performance of kaolin clay containing ore. However, bentonite-containing ore was not affected by the addition of hydrophobic reagents since the hydrophobic reagents did not have any effect on the swelling mechanism of bentonite particles.

It is evident that the presence of clay minerals can adversely affect the efficiency of mineral processing techniques discussed above. The extent of the adverse effects of clays depend on the available clay type and its concentration. Adverse effects of clays on mineral processing techniques may also be controlled by changing the chemical environments.

7.1 Recommendations for future research

- This study is focused on effects of kaolin and bentonite clays only. The influence of other clay types such as talc, muscovite, and vermiculite are recommended to be investigated because those clays may have different chemical and physical properties.
- It was observed that the addition of Ca^{2+} ions reduced the adverse effects of bentonite clay on flotation and filtration. In future work, the interaction between clay particles and other cations (eg : Mg^{2+}, Al^{3+}) can be investigated.
- In the gravity separation experiments with Knelson concentrator, both kaolin and bentonite did not have any significant influence on the separation efficiency due to the flow dynamics within the separation zone at the particles encountered. It may be useful to investigate the effect of different particle sizes in the feed.
- The addition of the hydrophobic reagents improved the filtration rates. In this work, all the experiments were conducted under the same pressure difference. It is recommended to investigate the filtration performance under different pressure differences.
- In the filtration study, amine was the hydrophobic reagent. It is recommended to investigate the influence of other hydrophobic reagents with different carbon chains on the filtration performance.

Appendix 1

Attribution tables for the published papers included in this thesis

1. Basnayaka, L., Subasinghe, N., Albijanic, B., 2017. Influence of clays on the slurry rheology and flotation of a pyritic gold ore. Appl. Clay Sci. 136, 230–238.

	Conception and design	Acquisition of data and method	Data conditioning and manipulation	Analysis and statistical method	Interpretation and discussion	Final Approval
Mr. Lahiru Basnayaka	85 %	95 %	85 %	85 %	85 %	60 %
I acknowledge that these represent my contribution to above research output Signed:- Lahiru Basnayaka						
A/Prof. Dr Nimal Subasinghe	10 %	0 %	10 %	10 %	10 %	20 %
I acknowledge that these represent my contribution to above research output Signed:-						
Dr Boris Albijanic	5%	5%	5%	5%	5%	20%
I acknowledge that these represent my contribution to above research output Signed:-						

2. Basnayaka, L., Subasinghe, N., Albijanic, B., 2018. Influence of clays on fine particle filtration. Appl. Clay Sci. 136, 230–238.

	Conception and design	Acquisition of data and method	Data conditioning and manipulation	Analysis and statistical method	Interpretation and discussion	Final Approval
Mr. Lahiru Basnayaka	85 %	95 %	85 %	85 %	85 %	60 %
I acknowledge that these represent my contribution to above research output Signed:- Lahiru Basnayaka						
A/Prof. Dr Nimal Subasinghe	10 %	0 %	10 %	10 %	10 %	20 %
I acknowledge that these represent my contribution to above research output Signed:-						
Dr Boris Albijanic	5%	5%	5%	5%	5%	20%
I acknowledge that these represent my contribution to above research output Signed:-						

Appendix 2

Example ANOVA analysis

This example ANOVA analysis is performed manually for readers to understand the basic principles of ANOVA. The results from Table 4-12 were used for the ANOVA. The maximum froth height was the dependent variable, while Ca^{2+} concentration and the clay type were the independent variables. Table 1 shows the results from Table 4-12.

Table 1 Maximum froth height recorded under different clay types and Ca^{2+} concentrations

Ca^{2+} Concentration	**Clay type**		
	No clay	Kaolin	Bentonite
0 (g/t)	29	16	13
	29	17	17
	29	17	13
1500 (g/t)	14	19	19
	14	20	15
	14	18	17.5

As seen in Table 1, there are two factors: clay type (kaolin, bentonite and no clay) and Ca^{2+} concentration (0 and 1500 g/t). The steps considered in ANOVA analysis are given below:

- Define null and alternative hypotheses.
- State *alpha.*
- Calculate degree of freedoms.
- State decision rule.
- Calculate test statistics.
- State results.
- State conclusions.

The following hypotheses were defined:

1. H_o; $\bar{X}_{0(g/t)\ Ca^{2+}} = \bar{X}_{1500(g/t)\ Ca^{2+}}$

   H_1; $\bar{X}_{0(g/t)\ Ca^{2+}} \neq \bar{X}_{1500(g/t)\ Ca^{2+}}$

2. $H_{o;}$ $\bar{X}_{No\ clay} = \bar{X}_{Kaolin} = \bar{X}_{Bentonite}$

   H_1; Not all clay type means are equal

3. H_o; an interaction is absent

   H_1; an interaction is present

$\alpha = 0.05$ is considered as the level of significance.

Calculation of degrees of freedom

$DF_{Ca^{2+}Con} = a-1 = 2-1=1$

$DF_{clay\ type} = b-1 = 3-1 = 2$

$DF_{Ca^{2+}Con \times clay\ type} = (a-1)(b-1) = 2\times1=2$

$DF_{Error} = N-ab = 18-(2\times3) = 12$

$DF_{total} = N-1 = 18-1 = 17$

Where a, is the number of conditions in the Ca^{2+} concentration and b, is the number of clay types and N is the total number of the experimental data.

Next step in ANOVA analysis is to state the decision rule. Critical F value for each factor and the interaction of the factors is determined using F distribution table:

$F_{critical}$ (Ca^{2+} Con) = 4.75

$F_{critical}$ (Clay type) = 3.88

$F_{critical}$ (Ca^{2+} Con × Clay type) = 4.75

Next step is to calculate the test statistics. Ultimate goal of statistical calculation is to calculate the F value for the each factor and the interactions. If the calculated F value is greater than the critical F value, the considered factor or the interaction is statistically significant.

In the ANOVA analysis, the following statistical values need to be calculated:

$SS_{Ca^{2+}Con}$ (Sum of squares of different Ca^{2+}Concentrations)

$SS_{clay\ type}$ (Sum of squares of different Clay types)

$SS_{Ca^{2+}Con \times clay\ type}$ (Sum of squares of interactions)

SS_{error} (Sum of squares of error)

SS_{Total} (Sum of squares of total)

$MS_{Ca^{2+}Con}$ (Mean squares of different Ca^{2+}Concentrations)

$MS_{clay\ type}$ (Mean of squares of different Clay types)

$MS_{Ca^{2+}Con \times clay\ type}$ (Mean of squares of interactions)

MS_{error} (Mean of squares of error)

$$SS_{Ca^{2+}Con} = \frac{\sum(\sum a_i)^2}{b \times n} - \frac{T^2}{N}$$

(Here *T* is the total sum of the results and *n* is the number of results for interaction bewteen variables)

$$SS_{Ca^{2+}Con} = \frac{180^2 + 150.5^2}{3 \times 3} - \frac{330.5^2}{18}$$

$$SS_{Ca^{2+}Con} = 48.347$$

$$SS_{clay\ type} = \frac{\sum(\sum b_i)^2}{a \times n} - \frac{T^2}{N}$$

$$SS_{clay\ type} = \frac{129^2 + 107^2 + 94.5^2}{2 \times 3} - \frac{330.5^2}{18}$$

$$SS_{clay\ type} = 101.7$$

$$SS_{Ca^{2+}Con \times clay\ type} = \frac{\sum(\sum a_i b_i)^2}{n} - \frac{\sum(\sum b_i)^2}{a \times n} - \frac{\sum(\sum a_i)^2}{b \times n} + \frac{T^2}{N}$$

$$SS_{Ca^{2+}Con \times clay\ type} = \frac{87^2+50^2+43^2+42^2+57^2+51.5^2}{3} - \frac{180^2+150.5^2}{3 \times 3} - \frac{129^2+107^2+94.5^2}{2 \times 3} + \frac{330.5^2}{18}$$

$$SS_{Ca^{2+}Con \times clay\ type} = 309.36$$

$$SS_{Total} = \sum y^2 - \frac{T^2}{N}$$

$$SS_{Total} = 480.9$$

$$SS_{Total} = SS_{Ca^{2+}Con} + SS_{clay\ type} + SS_{Ca^{2+}Con \times clay\ type} + SS_{error}$$

$$SS_{error} = 21.49$$

Since squares of the sums and the degrees of freedom are known, the means of squares and the F values can be calculated:

$$\text{Mean of Squares} = \frac{SS}{DF}$$

$$\text{F value} = \frac{MS}{MS_{error}}$$

The ANOVA table can be created using the calculated mean of squares and above given equations:

Table 2 ANOVA analysis for maximum froth height data

Source	DF	SS	MS	F- Value	P- Value
Ca^{2+} Con	1	48.35	48.35	27.00	0.00022336
Clay type	2	101.7	50.85	28.39	2.81816E-05
Ca^{2+} con× Clay type	2	309.36	154.68	86.37	7.50986E-08
Error	12	21.49	1.79		
Total	17	480.9			

According to the ANOVA analysis, "Ca^{2+} con", "Clay type" and their interactions have significant influence on the maximum froth height since the F values are greater than the critical F values.

Furthermore, the P-values were determined for the calculated F statistics using the "Fdist" function in excel. It can be seen that P-values are less than 0.05 for both factors and the interaction. Therefore, it supports the claim made with F statistics.

Appendix 3

The flotation curves and fitting of the Klimpal flotation model for the flotation experiments are given in Table 4-1.

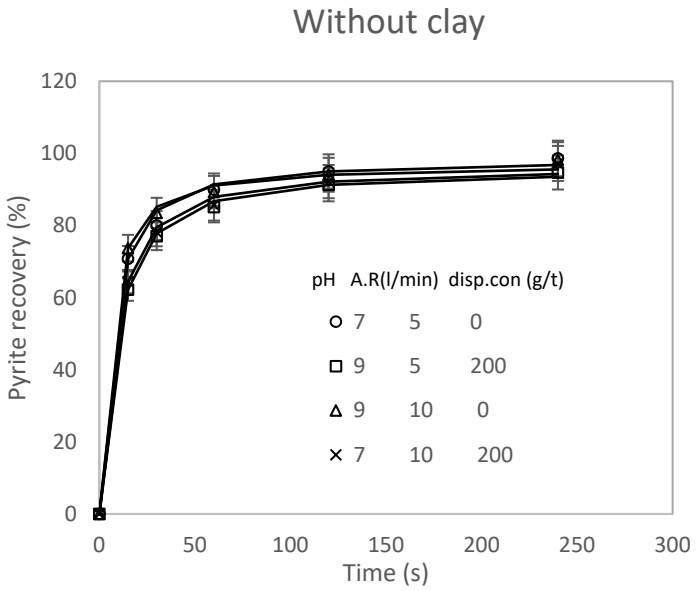

Figure 1 Flotation curves and model fitting for experiments without clay.

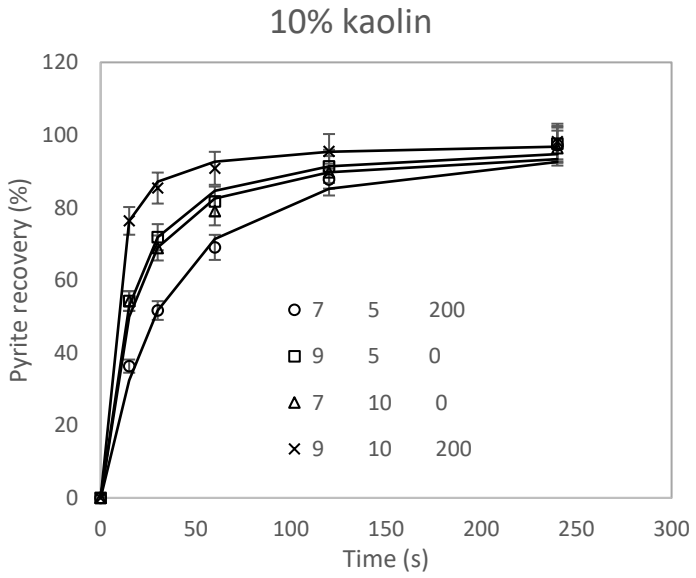

Figure 2 Flotation curves and model fitting for experiments with 10% kaolin clay.

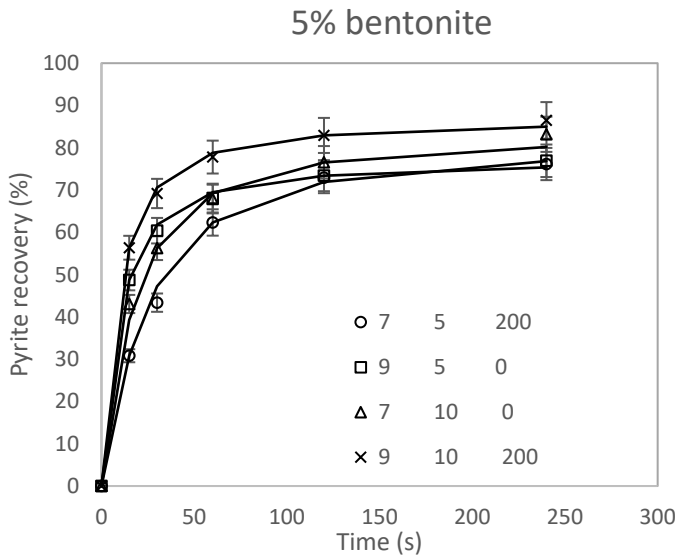

Figure 3 Flotation curves and model fitting for experiments with 5% bentonite clay.

References

Addai-Mensah, J., 2007. Enhanced flocculation and dewatering of clay mineral dispersions. Powder Technol. 179, 73–78.

Aksu, I., Bazilevskay, E., Karpyn, Z.T., 2015. Swelling of clay minerals in unconsolidated porous media and its impact on permeability. Geo Res. J. 7, 1–13.

Aktas, Z., Cilliers, J.J., Banford, A.W., 2008. Dynamic froth stability: particle size, airflow rate and conditioning time effects. Int. J. Miner. Process. 87, 65–71.

Amarante, S.C., Araujo, A.C., Valadao, G.E.S., Peres, A.E.C., 2002. Cake dewatering of some iron ore industrial products. Miner. Metall. Process 19 (3), 161.

Arnold, B.J., Aplan, F.F., 1986a. The effect of clay slimes on coal flotation, part 2: the role of water quality. Int. J. Miner. Process. 17, 243–260

Assemi, S., Sharma, S., Tadjiki, S., Prisbrey, K., Ranville, J., Jan D., Miller. 2015. Effect of Surface Charge and Elemental Composition on the Swelling and Delamination of Montmorillonite Nanoclays Using Sedimentation Field-flow Fractionation and Mass Spectroscopy. Clays. Clay. Miner. 63(6), 457-468.

Bagnold, R., 1954. Experiments on gravity-free dispersion of large solid spheres in a Newtonian fluid under shear. Proc. Royal soc. London, Ser. A. 225, 49-63

Bakker, C.W., Meyer, C.J., Deglon, D.A., 2009. Numerical modelling of Non-Newtonian slurry in a mechanical flotation cell. Miner. Eng. 22 (11), 944–950.

Benna, M., Ariguib, N.K., Clinard, C., Bergaya, F., 2001. Static filtration of purified sodium bentoite clay suspensions. Effect of clay content. Appl. Clay. Sci.19,103-120.

Bergaya, F., Lagaly, G., 2006. Handbook of Clay Science: General Introduction Clays, Clay Minerals, and Clay Science, 1-18.

Besra, L., Sengupta, D.K., Roy, S.K., 1999. Particle characteristics and their influence on dewatering of kaolin, calcite and quartz suspensions. Int. J. Miner. Process. 59, 89–112.

Bradshaw, S.L., Benson, C.H., Scalia, J., 2013. Hydration and Cation Exchange during Subgrade Hydration and Effect on Hydraulic Conductivity of Geosynthetic Clay Liners. J. Geotech. Geoenviron. Eng. 139(4), 526–538.

Brigatti, M. F., Galán, E., and Theng, B. K. G., 2013, Chapter 2 – structure and mineralogy of clay minerals, In Developments in Clay Science, (B. Faïza and L. Gerhard, Ed.), Amsterdam, Netherlands: Elsevier, Vol. 5,pp. 21–81.

Brindley, G.W., Brown, G., 1980. Crystal structures of clay minerals and their X-ray Identification. (London) In: Brindley, G.W., Brown, G. (Eds.), Mineralogical Society, pp. 98–104 (pp. 210–212).

Bulatovic, S.M., 2007. Handbook of Flotation Reagents: Chemistry, Theory and Practice: Flotation of Sulphide Ores Boston. Elsevier, Oxford.

Celik, M. S., Hancer, M., and Miller, J. D., 2002. Flotation chemistry of boron minerals. J. Colloid. interf. Sci, 256(1), pp. 121–131.

Chen, T., Zhao, Y., Li, H., Song, S., 2017a, Effects of colloidal montmorillonite particles on froth flotation of graphite, galena and fluorite. Physicochem. Probl. Mi. 53(2), pp. 699–713.

Chen, X., Peng, Y., 2018. Managing clay minerals in froth flotation—A critical review. Min Proc Ext Met. Rev 39:5, 289-307

Churaev, N. V., Sobolev, V. D., Somov, A. N., 1984. Slippage of liquids over lyophobic solid surfaces. J. Colloid Interf. Sci. 97, 574–581.

Connelly, D., 2011. High clay ores: a mineral processing nightmare. Aust. J. Min. 28–29.

Coulter, T., Subasinghe, G.K.N., 2004. A mechanistic apporch to modelling Knelson concentrators. Miner. Eng. 18, 9-17.

Cruz, N., Peng, Y., Wightman, E., and Xu, N., 2015b. The interaction of pH modifiers with kaolinite in copper–gold flotation. Miner. Eng, 84. pp. 27–33.

Cruz, N., Peng, Y., Wightman, E., and Xu, N., 2015c. The interaction of clay minerals with gypsum and its effects on copper-gold flotation. Miner. Eng, 77. pp. 121–130.

De Kretser, R.G., Boger, D.V., 1992. The compression, dewatering and rheology of slurried coal mine tailings. Proceedings 5th Australian Coal Science Conference, Newcastle, Australia, pp. 422–429

Deer, W.A., Howie, R.A., Zussman, J., 1992. An Introduction to Rock Forming Minerals. Longman Scientific & Technical, Essex.

Dippenaar, A., 1988. The Effect of Particles on the Stability of Flotation Froth. (Report No. 81) IMM, South Africa.

Dixon, J.B., Weed, S.B., 1989. Minerals in soil environments. Second ed., In: Dixon, J.B.,Weed, S.B. (Eds.), Soil Science Society of America, Madison, Wisconsin, USA.

Dowling, E.C., Klimpel, R.R., Aplan, F.F., 1985. Model discrimination in the flotation of a porphyry copper ore. Miner. Metall. May, pp. 87-1-01.

Farrokhpay, S., Bradshaw, D., 2012. The effect of clay minerals on froth stability in mineral flotation. Proceedings of the 26th International Mineral Processing Congress, New Delhi.

Farrokhpay, S., 2011. The significance of froth stability in mineral flotation- a review Adv. Colloid Interface Sci. 166, 1–7.

Farrokhpay, S., 2012. The importance of rheology in mineral flotation: a review. Miner.Eng. 36, 272–278.

Farrokhpay, S., Ndlovu, B., Bradshaw, D., 2016.Behaviour of swelling clays versus non-swelling clays in flotation. Miner. Eng, 96-97, pp. 59-66.

Fuerstenau, M.C., 1985. Chemistry of Flotation, AIMME, New York.

Fuerstenau, D.W., Jia, R., 2004. The adsorption of alkylpyridinium chlorides and their effect on the interfacial behavior of quartz. Colloids Surf. A: Physicochem. Eng. Aspects. 250 (1–3), 223–231.

Gaudin, A. M., 1957, Flotation, New York: McGraw-Hill.

Glembotskii, V.A., Klassen, V.I., and Plaksin, I.N., 1972. Flotation, Primary Sources, New York.

Goh, R., Leong, Y.-K., and Lehane, B., 2011, "Bentonite slurries—zeta potential, yield stress, adsorbed additive and time-dependent behaviour." Rheologica Acta, 50(1), pp. 29–38.

Grafe, M., Klauber, C., McFarlane, A., & Robinson, D. (Eds.). (2017). Clays in the Minerals Processing Value Chain. Cambridge: Cambridge University Press. doi:10.1017/9781316661888

Harris, A., Nosrati, A., Addai-Mensah, J., 2018. The influence of pulp and interfacial chemistry and mode of electrical power input on electroosmotic dewatering of Na-exchanged smectite dispersions. Appl Clay Sci. 162, 214-222.

Harris, C.C., Chakravarti, A., 1970. Semi-batch flotation kinetics: species distribution analysis. Trans. AIME. 247, 162–172.

He, M., Wang, Y., Forssberg, E., 2004. Slurry rheology in wet ultrafine grinding of industrial minerals: a review. Power Technol. 147, 94–112.

Hocine, T., Benhabib, K., Bouras, B., 2017. Comparative study between new polyacrylamide-based copolymer poly(AM-4VP) and a cationic commercial flocculant: application in turbidity removal on semi-industrial pilot. J. Polym. Environ

Hung, K., Pan, L., Yoon, R.H., 2017. A capillary flow model for filtration. Min. Eng. 115,88–96.

Hunter, R.J., 2001. Foundations of Colloids Science, second ed. Oxford University Press, Oxford.

He, M., Forssberg, E., 2007. Influence of slurry rheology on stirred media milling of quartzite. Int. J. Miner. Process. 84 (1–4), 240–251.

Hurlbut, C.S., Sharp, W.E., 1998. Dana's Minerals and How to Study Them (After Edward Salisbury Dana), fourth ed. John Wiley & Sons, Inc., New York, pp. 248–257.

Hu, Y., Liu, L., Min, F., Zhang, M., Song, S., 2013. Hydrophobic agglomeration of colloidal kaolinite in aqueous suspensions with dodecyl amine. Colloids Surf. A. 434, 281-286.

Ives, K.J. (ed.) (1984). The Scientific Basis of Flotation, Martinus Nijoff Publishers, The Hague.

Inoue, A., Bouchet, A., Velde, B., Meunier, A., 1989. A convenient technique for estimating smectite layer percentage in randomly interstratified illite/smectite minerals. Clay Clay Miner. 37, 227–234.

Jaireth, S., Huston, D., 2010. Metal endowment of cratons, terranes and districts: insights from a quantitative analysis of regions with giant and super-giant deposits. Ore Geology Reviews. 38, 288–303.

Jaques, A.L., Jaireth, S., Walshe, J.L., 2002. Mineral systems of Australia: An overview of resources, settings and processes. Aust. J. Earth. Sci, 49(4), 623-660.

Johnson, S.B., Franks, G.V., Scales, P.J., Boger, D.V., Healy, T.W., 2000. Surface chemistry–rheology relationships in concentrated mineral suspensions. Int. J. Miner. Process.267–304.

Jones, M.H., Woodcock, J.T., 1983. Decomposition of alkyl dixanthogens in aqueous solutions, Int. J. Min. Proc., 10, 1.

Joseph, P., Tabeling, P., 2005. Direct measurement of the apparent slip length. Phys Rev E. 71(3 Pt 2A): 035303.

Jorjani, E., Barkhordar, H.R., Tayebi Khormani, M., Fazeli, A., 2011. Effects of aluminosilicate minerals on copper–molybdenum flotation from Sarcheshmeh porphyry ores. Miner. Eng. 24, 754–759.

Kelly, E.G., Carlson, C.E., 1991. Two flotation models: resolution of a conflict. Miner. Eng. 4 (12), 1333–1338.

King, R.P., 1982. The Principles of Flotation, S. fr. I.M.M.

King, R.P., 2002. Introduction to Practical Fluid Flow. First ed. Butterworth-Heinemann, Oxford.

Klimpel, R.R., 1999.The selection of wet grinding chemical additives based on slurry rheology control. Powder Technol. 105 430–435.

Kozicki, W.,Tiu, C., Rao, A.R.K,. 1968. Filtration of non-Newtonian fluid. Can. J. Chem. Eng.46, 313-321.

Konta, J., 2000. Clay science at the threshold of the new millennium: a look at the history and present trends. Acta Univ. Carol. Geol. 44, 11–48.

Krekeler, M.P., 2004. Improved constraints on sedimentary environments of palygorskite deposits of the Hawthorne formation, Southern Georgia, from a detailed study of a core. Clays Clay Miner. 52, 253–262.

Laird, D.A., 2006. Influence of layer charge on swelling of smectites. Appl. Clay Sci. 34,74–87.

Laplante, A. R., Woodcock, F. C. and Huang, L. 2000. A laboratory procedure to characterise gravity recoverable gold, Trans. Soc. Min. Metall. Explor. 308, 53–59.

Lauten, R.A., Sitanggang, H., Pongkor, A., Pratomo, A., Pongkor, A., Ramdani, D., 2014. Biopolymer Addition to Boost Recovery and Throughput in Gold Leaching

Processes. A Case Study from Antam Pongkor, Indonesia. CIM Hydrometallurgy June 2014.

Leja, J., 1982. Surface Chemistry of Froth Flotation, Plenum Press, New York.

Lin, C.L., Miller, J.D., 2000b. Pore structure and network analysis of filter cake. Chem. Eng. J. 80, 221–231

Liu, D., Peng, Y., 2014. Reducing the entrainment of clay minerals in flotation using tap and saline water. Powder Technol. 253, pp. 216–222.

Liu, D., Peng, Y., 2015, Understanding different roles of lignosulfonate in dispersing clay minerals in coal flotation using deionised water and saline water. Fuel, 142, pp. 235–242.

Liu, D., Edraki, M., Berry, L., 2018. Investigating the settling behaviour of saline tailing suspensions using kaolinite, bentonite, and illite clay minerals. Powder Technol. 386, 228-236

Luckham, P.F., Rossi, S., 1999. The colloidal and rheological properties of bentonite suspensions.Adv. Colloid Interf. Sci. 82 (1–3), 43–92.

Lyubomir; K., Luis, B., Metodi, M., 1993. Sulphides and gold recovery from slime by gravity methods at the Asarel refining factory. Godishnik na Minno-Geolozhkiya Universiteta = Annual of the University of Mining and Geology 39, Part 2(Pages 123-128.

Maali, A., Bhushan, B., 2012. Measurement of slip length on super hydrophobic surfaces. Phil. Trans. R. Soc. 370(1967), 2304-2320.

Malkin, A.Y., Isayev, A.I., 2006. Rheology: Concepts, Methods and Applications. Chem Tec Publishing, Toronto.

Mason., Robert, L., Gunst., Richard, F., Hess., James, L., 2003. Statistical Design and Analysis of Experiments - With Applications to Engineering and Science (2nd Edition). John Wiley & Sons

McCabe, W., Smith, J., Harriott, P., 2004. Unit Operations of Chemical Engineering. McGraw Hill Chemical EngineeringSeries, New York.

McFarlane, A., Bremmell, K., Addai-Mensah, J., 2006. Improved dewatering behavior of clay minerals dispersions via interfacial chemistry and particle interactions optimization. J. Colloid Interface Sci. 293, 116–127.

Mekhamer, W. K., 2011. Stability changes of Saudi bentonite suspension due to mechanical grinding. J. Saudi Chem. Soc. 15, 361–366.

Miller, J.D., Lin, C.L., Chang, S.S., 1983. MIBC adsorption at the coal/water interface. Colloids Surf. 7 (4), 351–355.

Mooney, M., 1931. Explicit formulas for slip and fluidity. J. Rheol. 2,210

Mpofu, P., Mensah, J.A., Ralston, J., 2005. Interfacial chemistry, particle interactions and improved dewatering behaviour of smectite clay dispersions. Int. J. Miner. Process. 75,155–171.

Mueller, S., Llewellin, E.W., Mader, H.M., 2010. The rheology of suspensions of solid particles. Proc. Roy. Soc. A 466, 1201–1228.

Neto, C., Evans, D. R., Bonaccurso, E., Butt, H. J., Craig, V. S. J., 2005. Boundary slip in Newtonian liquids: a review of experimental studies. Rep. Prog. Phys. 68, 2859.

Ndlovu, B., Farrokhpay, S., Bradshaw, D., 2013. The effect of phyllosilicate minerals on mineral processing industry. Int. J. Miner. Process. 125, 149–156.

Ndlovu, B., Forbes, E., Farrokhpay, S., Becker, M., Bradshaw, D., Deglon, D., 2014. A preliminary rheological classification of phyllosilicate group minerals. Miner. Eng. 55, 190–200.

Oats, W. J., Ozdemir, O., and Nguyen, A. V., 2010., Effect of mechanical and chemical clay removals by hydrocyclone and dispersants on coal flotation. Miner. Eng. 23(5), pp. 413–419.

Pan, L., Hung, K., Yoon, R.H., 2016. A capillary flow model for filtration. XXVIII International Mineral Processing Congress proceedings, Quebec, September (11-15).

Papo, A., Piani, L., and Ricceri, R., 2002., Sodium tripolyphosphate and polyphosphate as dispersing agents for kaolin suspensions: rheological characterization. Colloids and Surfaces A: Physicochemical and Engineering Aspects, 201(1), pp. 219–230.

Patra, P., Bhambhani, T., Nagaraj, D.R., Somasundaran, P., 2010. Effect of morphology of altered silicate minerals on metallurgical performance: transport of Mg silicates to the froth phase. In: Pawlik, M. (Ed.), Proceedings 8th UBC-McGill-UA International Symposium on the Fundamentals of Mineral Processing: Rheology and Processing of fine Particles. The Canadian Institute of Mining, Metallurgy and Petroleum,Vancouver, British Columbia, Canada, pp. 31–42.

Peng, Y., and Zhao, S., 2011, The effect of surface oxidation of copper sulfide minerals on clay slime coating in flotation. Miner. Eng. 24(15), pp. 1687–1693.

Polat, M., Chander, S., 2000. First-order flotation kinetics models and methods for estimation of true distribution of flotation rate constants. Int. J. Miner. Process. 58, 145–166.

Quast, K, Ding, L, Ralston, J and Fornasiero, D, 2008. Effect of slime clay particles on coal flotation, in Proceedings of the Chemeca 2008: Towards a Sustainable Australasia, Newcastle.

Rand, B., Melton, I.E., 1977. Particle interactions in aqueous kaolinite suspensions: I. Effect of pH and electrolyte upon the mode of particle interaction in homoionic sodium kaolinite suspensions. J. Colloid Interface Sci. 60 (2), 308–320.

Rastogi, R.C., Aplan, F.F., 1985. Coal flotation as a rate process. Min. Metall. Proc. Aug. 137–145.

Ruth, B.F., 1935. Studies in filtration III. Derivation of general filtration equation. Ind. Eng. Chem.27 (6):708.

Sastry, K.V.S., Kawulok-Englund, H.Y., Hosten, C., 1983. Comparative Study of Vacuum Filtration Behaviour of Iron Ore Concentrate Slurries. Min.Eng. 35 (10), p.1432-1436

Savassi, O. N., Alexander, D. J., Franzidis, J. P., and Manlapig, E. V., 1998. An empirical model for entrainment in industrial flotation plants. Miner.Eng. 11(3), pp. 243–256.

Schoonheydt, R., Johnston, C., 2006. Chapter 3 surface and interface chemistry of clay minerals. In: Bergaya, F., Theng, B.K.G., Lagaly, G. (Eds.), Handbook of Clay Science, first ed. Elsevier Science, Amsterdam, The Netherlands, pp. 87–113.

Schulze, H.J. 1984. Physio-chemical Elementary Processes in Flotation, Elsevier Science Publishing Co., Amsterdam.

Shabalala, N.Z.P., Harris, M., Filho, L.S.L., Deglon, D.A., 2011. Effect of slurry rheology on gas dispersion in a pilot-scale mechanical flotation cell. Miner. Eng. 2 (13), 1448–1453.

Shi, F.N., Napier-Munn, T.J., 2002. Effects of slurry rheology on industrial grinding performance. Int. J. Miner. Process. 65, 125–140.

Silva, M.A., 1986. Placer gold recovery methods, Special publication.

Smith, P. G., and Warren, L. J., 1989, Entrainment of particles into flotation froths. Min. Proc. Ext. Met. Rev. 5(1–4), pp. 123–145.

Somasundaran, P., Brij, M., Moudgil, (Eds.)., 1988. Grinding aids based on slurry rheology control, Reagents in Mineral Technology. Surfactant Science Series, New York, vol. 27, pp. 179– 193

Sutherland, K.L. and Wark, I.W. 1955. Principles of Flotation, Australian IMM.

Swartzen-Allen, S.L., Matijevic, E., 1974. Surface and colloid chemistry of clays. Chem. Rev.74 (3), 385–400.

Tangsathitkulchai, C., 2003. The effect of slurry rheology on fine grinding in a laboratory ball mill. Int. J. Miner. Process. 69, 29–47.

Tao, D., Dopico, P.G., Hines, J., Kennedy, D., 2010. An experimental study of clay binders in fine coal froth flotation. Proceedings of the International Coal Preparation Congress, Lexington, USA, pp. 478–487.

Tien, C., Ramarao, V., 2013. Can filter cake porosity be estimated based on the Kozeny-Carman equation. Powder Technol. 237, 233–240.

Tomlinson, H.S., Fleming, M.G., 1965. Flotation rate studies. In: Roberts, A. _Ed.., Proc. VI Int. Miner. Proc.Cong., Pergamon, pp. 563–579.

Tremolada, J., Dzioba, R., Bernardo-Sanchez, A., Menendez-Aguado, J.M., 2010. The preg-robbing of gold and silver by clays during cyanidation under agitation and heap leaching conditions. Int. J. Miner. Process. 94, 67–71.

Tretheway, D.C., Meinhart, C.D., 2002. Apparent fluid slip at hydrophobic microchannel walls. Phys, Fluids. 14(3), L9-L12.

Vasudevan, M., Nagaraj, D.R., Patra, P., Somasundaran, P., 2010. Effect of altered silicates in flotation performance: role of changes in pulp rheology. In: Pawlik, M. (Ed.), Proceedings 8th UBC-McGill-UA International Symposium on the Fundamentals of Mineral Processing: Rheology and Processing of Fine Particles. The Canadian Institute of Mining, Metallurgy and Petroleum, Vancouver, British Columbia, Canada,pp. 21–30

Wang, L., Peng, Y., Runge, K., and Bradshaw, D., 2015a. A review of entrainment: mechanisms, contributing factors and modelling in flotation." Miner. Eng. 70. pp. 77–91.

Wang, Y., Peng, Y., Nicholson, T., Lauten, R.A., 2015b. The different effects of bentonite and kaolin on copper flotation. Appl. Clay Sci. 114, 48–52.

Wang, Y., Forssberg, E., 1995. Dispersants in stirred ball mill grinding. KONA 13, 67–77.

Wei, R., Peng, Y., and Seaman, D., 2013, The interaction of lignosulfonate dispersants and grinding media in copper–gold flotation from a high clay ore. Miner. Eng. 50–51. pp. 93–98.

Wills, B. A., & Napier-Munn, T. (2006). Wills' mineral processing technology: an introduction to the practical aspects of ore treatment and mineral recovery. Retrieved from https://ebookcentral.proquest.com

Yu, Y., Cheng, G., Ma, L., Huang, G., Wu, L., and Xu, H., 2017a. Effect of agitation on the interaction of coal and kaolinite in flotation. Powder Technol. 313(Supplement C), pp. 122–128.

Yu, Y., Ma, L., Wu, L., Ye, G., and Sun, X., 2017b. The role of surface cleaning in high intensity conditioning. Powder Technol. 319 (Supplement C), pp. 26–33.

Zhang, H., Miller, C.A., Garrett, P.R., Raney, K.H., 2004. Defoaming effect of calcium soap. J. Colloid Interface Sci. 279 (2), 539–547

Zhang, M., Peng, Y., 2015a. Effect of clay minerals on pulp rheology and the flotation of copperand gold minerals. Miner. Eng. 70, 8–13.

Zhang, M., Peng, Y., and Xu, N., 2015b, The effect of sea water on copper and gold flotation in the presence of bentonite. Miner. Eng. 77. pp. 93–98.

Zhao, S., Peng. Y, 2014. Effect of electrolytes on the flotation of copper minerals in the presence of clay minerals. Miner. Eng. 66–68. pp. 152–156.

Zhang, M., Xu, N., Peng, Y., 2015c, “The entrainment of kaolinite particles in copper and gold flotation using fresh water and sea water.” Powder Technol. 286. pp. 431–437.